UNIVERSITY OF LATVIA

FACULTY OF COMPUTING

KASPARS SUDARS

DATA ACQUISITION FROM REAL WORLD OBJECTS

DOCTORAL THESIS

FIELD:	COMPUTER SCIENCE
SUB-FIELD:	DATA PROCESSING SYSTEMS AND COMPUTER NETWORKING
SCIENTIFIC SUPERVISOR:	DR.HABIL. IVARS BIĻINSKIS

RIGA - 2011

This work has been supported by the European Social Fund within the project «Support for Doctoral Studies at University of Latvia».

Anotācija

Datu ieguve no apkārtējās vides ir un būs būtiska daudzos pielietojumos. Tagad pasaulē ar to izstrādi nodarbojās daudzas firmas, bet pamata principi palikuši nemainīgi ilgus gadus. Darbā veikti pētījumi, kā uzlabot datu ieguvi, lietojot pieeju, kad signāli tiek reprezentēti ciparu formā netradicionāli: pieņemtās periodiskās diskretizācijas vietā lietojot neregulāro signālu diskretizāciju un kvantēšanu. Konkrēti, darbā pētītas un analizētas: (1) asimetriskās datu saspiešanas/atjaunošanas metodes; (2) GHz signālu diskretizācija, lietojot divus atšķirīgus ACP paralēli; (3) uzlabota bioimpedances signālu datu ieguves metode; (4) uz signāla-references funkciju krustošanās noteikšanas balstīta datu ieguves pieeja un tās realizācijas īpatnības. Izstrādāta un testēta ātrdarbīga F-DFT procesora FPGA implementācija.

Atslēgas vārdi: datu ieguve, neregulārā diskretizācija, bioimpedances mērīšana, DASP

Annotation

Work is focused on methods and algorithms for data acquisition from real world objects, and it is based on the theory of non-traditional Digital Signal Processing, including non-uniform sampling and pseudo-randomized quantizing. That leads to obtaining data simultaneously from an increased number of data sources, to widening the frequency range and to significant complexity reductions. In particular, research has been done in the directions of: (1) asymmetric data compression/reconstruction; (2) data acquisition from sources in the GHz frequency range; (3) rational acquisition of bioimpedance data; (4) data acquisition based on signal and sine wave reference function crossings. Microelectronic implementation of the research results is considered. In particular, FPGA implementation of a Fast-DFT processor has been developed and tested.

Keywords: data acquisition, nonuniform sampling, bioimpedance measurements, DASP

Acknowledgements

I would like to express my sincere gratitude to my supervisor Dr. Ivars Biļinskis for introduction to the world of science and his tremendous support during the elaboration of the doctoral Thesis.

The doctoral Thesis is carried out with help of the University of Latvia, Computing Faculty and the Institute of Electronics and Computer Science, including material help.

I would like to thank my family, especially my mom, and friends for their support.

Content

Abbreviations

ADC	Analog to Digital Converter
CI	Cross-Interference (coefficients, effect)
CS	Compressive Sensing (Sampling)
DAC	Digital to Analog Converter
DAQ	Data Acquisition
DAS	Data Acquisition System
DASP	Digital Alias-free Signal Processing
DFT	Discrete Fourier Transform
DQ	Deterministic Quantizing
DSP	Digital Signal Processing
FFT	Fast Fourier Transform
FPGA	Field Programmable Gate Array
LPF	Low-pass Filter (filtering)
LSB	Least Significant Bit
MAF	Moving Average Filter (filtering)
MCU	Microcontroller Unit
MUX	Multiplexer
NU	Nonuniform (sampling)
OSI	Open Systems Interconnection
PC	Personal Computer
PRQ	Pseudo-randomized Quantizing
R&D	Research and Development
RQ	Randomized Quantizing
S&H	Sample and Hold (scheme)
SECOEX	Sequential Component Extraction (recovery method for nonuniformly sampled signals)
SN	Sensor Network
SNR	Signal-to-Noise Ratio
SRC	Signal and Reference Crossing (sampling)
SWC	Signal and Sine-wave Crossing (sampling)
VHDL	Hardware Description Language

1. Introduction

1.1 Motivation for research in the area of data acquisition for computer systems

Massive data acquisition from real life objects and supplying computers with this information in an effective way evidently is vital to realizing full potential of computer system applications in many areas. Various types of sensors are used for obtaining information from objects of natural or technical origin. Most of them convert the primary information into continuous-time or analog signals. Data acquisition (DAQ) from only this type of sensors is considered in this work. As the acquired data are to be given as discrete quantities, the analog sensor signals have to be digitized to obtain their representations in the digital domain. Usually the classic Digital Signal Processing (DSP) technology is used for this.

This approach, based on the assumption that digitizing is based on the classical sampling and quantizing concepts, leads to significant narrowing of the digital domain, to using of more expensive analog signal processing methods and technical means for performing signal processing in the high and ultra high frequency range. It means that this approach negatively impact data acquisition technologies and limits their application range. The research described in this summary is motivated by the importance of achieving progress in the direction of computer system applications in the wide area of Information Technologies related to computer system interaction with real world biological and industrial objects.

1.2 Research goal and the basic problems that have to be resolved

Research activities of this work target reaching the goal of discovering innovative methods for massive data acquisition from real life objects and effective supplying computers with this information. That evidently is vital for realizing full potential of computer system applications in many areas. The research is focused on resolution of the following basic problems that have been indicated at the beginning of this work as the most essential:

- Too high DAQ system complexity;
- Relatively small quantity of sensors that typically can be connected to inputs of a single DAQ system;
- Limited number of channels for simultaneous data acquisition in parallel;

- Power consumption of DAQ systems, often limiting the duration of their autonomous performance time.

Basic tasks

To achieve progress in these directions, the following tasks are to be addressed:

1. Research focused on development of innovative methods and algorithms for complexity-reduced DAQ paying attention, in particular, on the following:
   - Combining data acquisition with signal specific digital pre-processing;
   - Reduction of power consumption;
   - Increasing the number of sensors that can be connected to a single DAQ system at least up to 100;
   - Compression of acquired data.
2. Development of algorithms and computer programs for sensor data transfer to computers.
3. Experimental investigations of the developed problem solutions, mostly by computer simulations in MATLAB environment.
4. Description of the developed DAQ structures in VHDL.

Approach to resolution of the considered problems

To reach the goal of this work a flexible approach to complexity-reduced multi-channel data acquisition from a large quantity of sensors has been used. The developed methods, systems and algorithms for data acquisition from wideband, event timing and large distributed clusters of signal sources are discussed with emphasis on data gathering from a large quantity of signal sources. Special signal digitizing techniques, including pseudo-randomized multiplexing, time-to-digital conversions and signal sample value taking at time instants when the input signal crosses a sinusoidal reference function, are used for that. Development of the discussed massive data acquisition systems is based on the knowledge accumulated over a long period of time in the area of Digital Alias-free Signal Processing.

1.3 Outline of Thesis

Thesis consists of 4 main Chapters (from 2. to 5.) excluding Introduction and Conclusions.

2. Chapter – *DAQ Systems for Gathering and Supplying Information to Computers*

In this Chapter a brief overview about current level of development in the field of DAQ is given. Relatively many various DAQ systems are currently produced and offered by many companies. Most of them actually are operating on the basis of a few basic DAQ principles that might be considered as classic: *Shannon sampling theorem* and *Nyquist frequency limitation.*

Uniform sampling is still leading and the most used sampling technique. Therefore performance of the existing DAQ systems mainly depends on the currently achieved perfection of the involved microelectronic elements.

3. Chapter – *Data Acquisition Based on NU Sampling: Achievable Advantages and Involved Problems*

This Chapter shows applicability of NU sampling and quantizing approaches in various dimensions of DAQ: widening frequency range of DAQ, fault-tolerant DAQ, asymmetric 2D data compression/reconstruction, simplify DAQ system hardware etc. The basics of cross-interference CI effect also is described and explained in this Chapter.

The method for DAQ system widening frequency range (using 2 ADCs in parallel) and improve acquired signal quality (in terms of signal resolution, dynamic range etc.) is developed and described in this Chapter.

4. Chapter – *Methods for Data Acquisition Exploiting Advantages of Pseudo-randomized Quantizing*

Signal quantizing methods – deterministic, randomized and pseudo-randomized quantizing – are considered in this Chapter. Special attention is drawn on one particular case of DAQ – biomedical data acquisition. The bioimpedance signal demodulation is essential in this DAQ case. The method for bioimpedance signal acquisition is suggested and described in this Chapter.

5. Chapter – *Data Acquisition Based on Gathering Timing Information*

In this Chapter the signal representation by timing information is considered. In such a way the DAQ systems can be significantly improved (simplified their hardware structure, reduced energy consumption etc.). The signal sampling based on detection the signal and sine-wave crossing instants (SWC sampling) is suggested and considered for this reason in this Chapter. The conditions of SWC sampling applicability in DAQ are studied and described.

6. Chapter – *FPGA based implementation of the considered DAQ methods*

In this Chapter the description of experimental activities and obtained research results is given. The novel logical structure for DFT coefficients estimation without massive multiplication has been implemented into FPGA and its performance evaluated. The comparison with equal purpose FIR digital filter reveals that considered F-DFT processor structure requires approximately 2 times less count of logical elements. The development of F-DFT processor has to continue.

7. Chapter – *Obtained research results*

The obtained research results are summarized in this Chapter, followed by Conclusions in Chapter 8.

1.4 Dissemination of the research results

The main results of scientific work are approved in 11 scientific publications:

1. Bilinskis I., Sudars K. *Processing of signals sampled at sine-wave crossing instants.* Proceedings of the “2007 Workshop on Digital Alias-free Signal Processing” (WDASP’07), London, UK, 17 April 2007, pp. 45-50.
2. Sudars K., Ziemelis Z., *Expected performance of the sine-wave crossing data acquisition systems,* Proceedings of DASP Workshop, London, UK, 17 April 2007.
3. Bilinskis I., Sudars K. *Digital representation of analog signals by timed sequences of events*, “Electronics and Electrical Engineering”, No. 3(83), March, 2008, Presented in International Conference “Electronics 2008”, Kauna, Lithuania, 20-22 May 2008.
4. Bilinskis I., Sudars K. *Specifics of constant envelope digital signals*, “Electronics and Electrical Engineering”, No. 4(84), April, 2008, Presented in International Conference “Electronics 2008”, Kauna, Lithuania, 20-22 May 2008.
5. Artyukh Yu., Bilinskis I., Sudars K., Vedin V., *Multi-channel data acquisition from sensor systems.* Proceedings of the 10th International Conference “Digital Signal Processing and its Applications” (DSPA'2008), Moscow, Russia, 2008, Vol.X-1, pp.117-119.
6. Artyukh Y., Bilinskis I., Sudars K., European Patent Application No. EP2075912 A1, *Method for complexity-reduced digital filtering and parameter estimation of analog signals*, Assignee: Institute of Electronics and Computer Science of Latvia, European patent Bulletin, January 7, 2009.
7. Bilinskis I., Sudars K., Min M., Annus P., *Advantages and limitations of an approach to bioimpedance data acquisition and processing relying on fast low bit rate ADCs,* Baltic Electronic Conference BEC 2010, Tallinn, Estonia, 4.-6. October 2010.
8. Artyukh Y., Bilinskis I., Roga S., Sudars K., *Digital Representation of Analog Signals leading to their Energy-efficient Processing*, Green Information Technology (GREEN IT 2010), Singapore, 25.-26. October 2010.
9. Sudars K., *Data Acquisition Based on Nonuniform Sampling: Achievable Advantages and Involved Problems,* “Automatic Control and Computer Science” Magazine, Allerton Press, 2010, Vol. 44, No. 4, pp. 199-207.
10. Bilinskis I., Skageris A., Sudars K. *Method for fast and complexity-reduced asymmetric image compression*, “Electronics and Electrical Engineering”, No. 4(110), May, 2011, Presented in International Conference “Electronics 2011”, Kauna, Lithuania, 17-19 May 2011.

11. Artyukh Y., Bilinskis I., Rybakov A., Sudars K., Vedin V., Modular Multi-channel Data Acquisition Systems, “Automatic Control and Computer Sciences” Magazine, Allerton Press, 2008, Vol. 42, No. 3, pp. 113–119.

The results are presented in following scientific conferences:

1. Workshop on Digital Alias-free Signal Processing (WDASP’07), London, UK, 17 April 2007
2. International Conference “Electronics 2008”, Kauna, Lithuania, 20-22 May 2008
3. 10th International Conference “Digital Signal Processing and its Applications” (DSPA'2008), Moscow, Russia, 2008
4. Baltic Electronic Conference BEC 2010, Tallinn, Estonia, 4-6 October 2010
5. Green Information Technology (GREEN IT 2010), Singapore, 25-26 October 2010
6. International Conference “Electronics 2011”, Kauna, Lithuania, 17-19 May 2011

2. DAQ Systems for Information Gathering and Supplying to Computers

"Data acquisition is defined as process of sampling of real world physical conditions and conversion of the resulting samples into digital numeric values that can be manipulated by a computer" [31]. This popular definition of data acquisition (DAQ), while basically true, covers only the general part of this process. Actually the essence of the DAQ task is supplying computers with information gathered from some quantity of sources. Carriers of that information are signals and various types of sensors are used for obtaining information from these sources usually placed on and connected to objects of natural or technical origin. Most types of the sensors convert the primary information into continuous-time or analog signals given as variable in time voltage or electrical current. Data acquisition from only this type of sensors is considered in this work. As the sensor signals are analog, a particular but most important task of DAQ systems (DAS) is converting these signals into their digital counterparts or digitizing. That is done by using analog-to-digital converters (ADC). The data gathered from some quantity of signal sources, after digitizing, are transferred to a computer. Obviously, that requires multiplexing of them. This operation has to be performed at some stage of DAQ, either by multiplexing analog sensor signals or by multiplexing digital signals after their digitizing.

Data acquisition is an essential part for many applications and this function will play an increasingly important role in the future. It is hard to imagine world without cameras for imaging, radars for plane monitoring, cardiographs for medical diagnosis and sensor devices for security etc. All of them are specific data acquisition systems. Many signal sources are around us and life quality of people could be significantly improved, if these signals would be acquired, analyzed by computers and some feedback generated for suppressing negative and amplifying positive factors. For example, environment monitoring, based on DAQ, provides vital information about varying pollution or flooding conditions, DAQ systems supply ambient intelligence systems or systems for medical diagnostics, remote patient monitoring in healthcare etc. DAQ application field rapidly grows and DAQ applications are diversified. That leads to increased demands for DAQ systems capable of data acquisition from larger and larger quantity of signal sources, operating at increased speed, at higher and higher input signal frequencies, in a wider resolution range while it is required that DAQ system designs have to be less complicated and consuming significantly reduced power.

The first Chapter of the thesis is an introduction into the current situation in the field of data acquisition. Basically there are a few DAQ systems and technologies that are usually used. They are briefly described and compared. Their advantages and limitations are specified and the problems that have to be resolved to develop more effective DAQ methods and algorithms are defined.

2.1 Conventional DAQ methods and systems

Data acquisition consists of several stages. It starts with measuring of physical phenomenon (temperature, light intensity, pressure, force etc). Then necessary physical property first has to be transformed into electrical signal. It can be done using transducers or sensors. At the next stage acquired electrical signal has to be prepared for the further processing and digitized (the signal may need to be amplified, filtered or demodulated etc.; some of these procedures can be done after signal digitization). After digitization all information about primary signal are carrying discrete signal sample values. The final is acquired data pre-processing and transmitting part.

As the acquired data are to be given as discrete quantities so that they could be transferred to computers, the analog sensor signals have to be digitized to obtain their representations in the digital domain. Sensor signal digitizing and processing usually is performed on the basis of the classic Digital Signal Processing (DSP) theory and techniques. It might be said that DAQ is one of the widely used application of DSP. Relatively many various DAQ systems are currently produced and offered by many companies. On the other hand most of them actually are operating on the basis of a few basic DAQ principles that might be considered as classic as they have remained unchanged for a long time. Therefore performance of the existing DAQ systems mainly depends on the currently achieved perfection of the involved microelectronic elements.

2.1.1 Basic theoretical background of the conventional DAQ systems

Theoretical background of virtually all currently available DAQ systems depends on theoretical relationships and principles discovered and described about 60 years ago. Shannon`s sampling theorem represents the basic one of those principles. According to this theorem, under certain conditions every analog signal can be fully represented by periodically taken discrete signal samples. Then the original analog signal can be recovered from discrete signal samples according to the following relationship:

$$x(t) = \sum_{n=-\infty}^{\infty} x[n] \cdot \mathrm{sinc}\left(\frac{t-nT}{T}\right) \tag{2.1}$$

Where $x(t)$ – is original analog signal recovered from discrete signal sample values; $x[n]$ – discrete signal sample values; t – time; T – is sampling period or time interval between two near standing signal samples; n – integer, which points discrete signal sample number. Interesting is the fact that this theorem is also known also as Whittaker and Kotelnikov sampling theorem. It seems that all these authors discovered this theorem independently in parallel.

The Shannon sampling theorem works well, if discrete signal samples are taken equidistantly according to periodic sampling. Another significant condition required by sampling theorem is so-called Nyquist limit. The Nyquist limit or the Nyquist frequency f_s defines the minimal signal sampling frequency that has to be used for periodic sampling of analog signals with the bandwidth B to ensure recovery of analog signals from their discrete signal samples according to relationship (2.1). This Nyquist frequency is at least two times larger than the upper frequency of the signal bandwidth:

$$f_s \geq 2B \tag{2.2}$$

Where f_s – is analog signal sampling frequency; B – is analog signal bandwidth upper frequency.

Ignorance of this condition leads to corruptions of recovered signal due to the aliasing effect, what means that the original analog signal then cannot be correctly recovered.

These are two basic theoretical principles are related to analog signal representation with its discrete signal samples. Description of the typical hardware implementations of multi-channel data acquisition systems follows.

2.1.2 Typical implementations of DAQ systems

According to the definition, the data acquisition systems have to contain the following functional blocks:

- Sensors (transducer) to convert some physical parameters into electrical signals;
- Signal conditioning block to convert sensor signals into a form that can be converted to digital values;
- Analog-to-digital converters that convert conditioned sensor signals into sequences of digital signal sample values;
- Other functional blocks to transmit and process acquired digital data etc.

Two of the most popular DAS architectures are given in Figure 2.1.

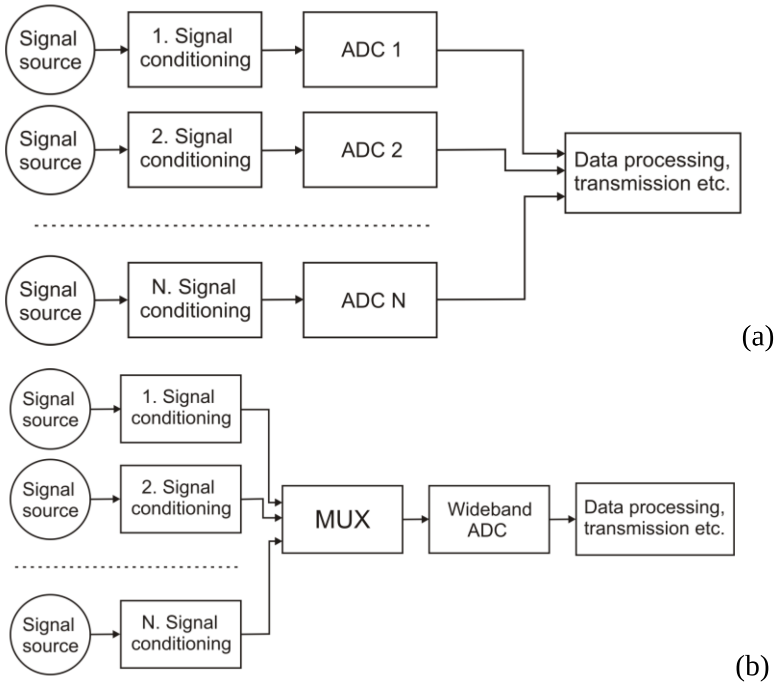

Figure 2.1 Two traditional DAS architectures: (a) based on many ADCs and (b) based on a single multiplexer and a wideband ADC.

As it can be seen from Figure 2.1, one of the possible DAS architectures is based on usage of many analog-to-digital converters – one ADC per channel. In the centre of the other DAQ system hardware architecture is a multiplexer, which sequentially switch all inputs to wideband ADC. The essential difference between both DAS architectures is where the signal digitizing is accomplished. In the case of many ADCs usage the analog signal digitizing can be organized close to signal sources.

Each of these DAQ system architectures has its own advantages and drawbacks. For example, architecture shown in Figure 2.1 (a) has multiple analog-to-digital converters, what makes system hardware more complex. On the other hand, the system analog hardware part in this case is simpler (it does not contain a multiplexer at the front-end of the system) and ADCs can be placed closer to the input signal sources, what protects acquired input signals from noise and leads to increased resolution (dynamic range).

In the case of multiplexer based DAQ architecture, the sampling frequency of each channel can be calculated by dividing the ADC sampling frequency with the channel count. Therefore it is very hard to achieve with this architecture at the same time big channel count and large sampling rate per channel. More detailed comparison of these structures is given in the Section 2.3. These two DAS architectures basically are used for supplying computers with data taken from signal sources located more or less closely. That often is not the case. There are many DAQ applications that have to acquire data from signal sources scattered over some area. To cover the needs of these DAQ applications, sensor networks are used. Currently they are intensively explored in the world.

2.1.3 Sensor networks

Sensor networks can be divided into two large groups – wireless sensor networks and wired sensor networks. Today wireless sensor networks has drawn much larger attention from researchers due to its promising and potential applications. Wireless sensor network concept defines that all sensor nodes are autonomous and communications between them are without usage of wires. It makes design of them much difficult in comparison with wired sensor networks.

In wireless sensor networks all sensor nodes – also called motes – are merged into one system with common goal – acquire data from environment around sensors and transmit acquired data to data center, where those can be analyzed. Data center – also sometimes called wireless sensor network sink – stores collected data and provides sensor network gateway functions if it is necessary. Only in particular cases data analyzing procedures can be delegated to sensor nodes due to its insufficient computation power, what is closely related to energy saving and cost of sensor nodes. Therefore only simplest data processing algorithms can be processed in sensor nodes. Nevertheless wireless sensor networks enable new dimensions in ambient intelligence, environment monitoring, process control and in many other applications [55].

Data acquisition is only common issue with sensor networks, what covers the scope of this dissertation. There sensor networks are surveyed as one particular data acquisition system with its own data acquisition philosophy. Important difference between sensor networks and simple data acquisition system is that sensor networks cover much larger functions range and data acquisition is not only function, what they are capable to provide. In general data acquisition is integrated part or subsystem of sensor networks. It will be clearly visible later, when the structure of sensor node will be given.

In some applications data acquisition can be very simple as it shown in Figure 2.2, where some target detection is shown. To detect target is enough with ON-OFF signal acquisition (for example, is particular area poisoned or not). In these cases where signals with narrow bandwidth are acquired and full signal waveform is not necessary to know the data acquisition is one of the simplest parts of all sensor system. Then more complicated part of sensor network is communications between sensor nodes and data transmitting to data center [55].

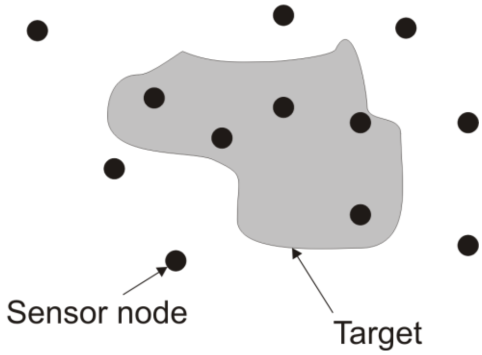

Figure 2.2 Illustration of target detection by a sensor network.

In many applications sensor networks are used together with data distribution networks as it is shown in Figure 2.3. It provides additional functionality and enlarged applicability to sensor networks.

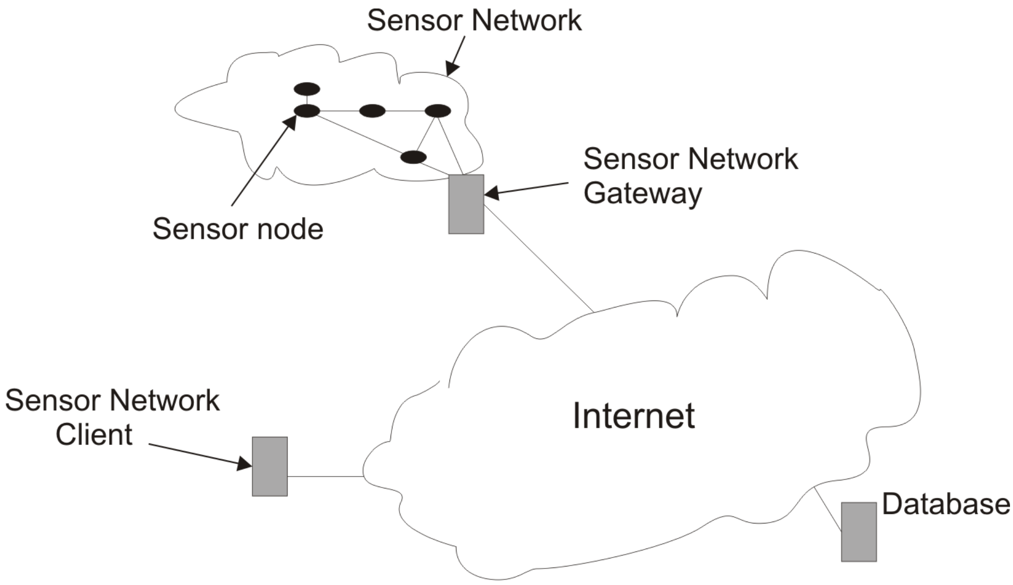

Figure 2.3 Typical architecture of sensor network and data distribution network.

In Figure 2.3 sensor network, used for data acquisition purpose, is connected with data distribution network – *Internet*. It provides additional functionality. User can remotely access sensor network, get acquired data from it through sensor network gateway and do all other necessary manipulations with acquired data. Achieving more automation level of system it can be done by computer programs of OSI model higher levels [55].

Wireless sensor networks usually have time variant topology, because some of sensor nodes can went out of order due to battery discharge or change its location due to some environment impact. It is illustrated in Figure 2.4.

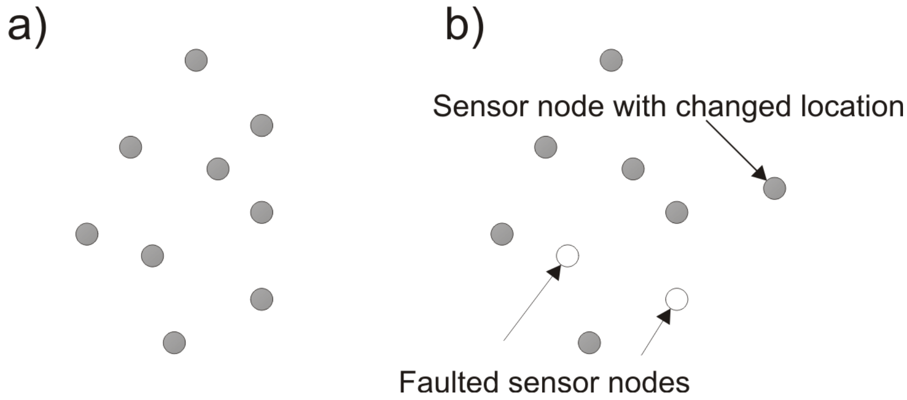

Figure 2.4 Deployment of the wireless sensor network nodes (a) in *ad hoc* manner and (b) deployment changes after long enough time period.

Networking in wireless sensor networks is a complicated issue, because communications media between nodes is an air and sensor nodes can be scattered over a geographic region in *ad hoc* manner (or in the better case according to mesh network topology, if it is specially planned). It means that each sensor node will receive signals from neighbours all the time with signal propagation delay if these signals are strong enough. All these conditions require additional intelligence from sensor nodes and it makes their organization more complicated. Therefore many network protocols are designed for wireless sensor networks [55].

Sensor node is quite complicated structure. It is shown in Figure 2.5 where typical organization of wireless sensor node is given [55].

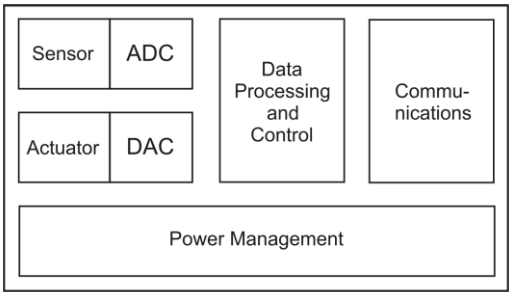

Figure 2.5 Sensor node building blocks: power, sensing, analog/digital conversion, data processing, (wireless) communication and their system integration.

As it can be seen in Figure 2.5 in general wireless sensor network mote (sensor node) consists of some essential functional blocks:

- Sensor block with ADC – provides primary signal digitizing function with all necessary preparations included (signal sensing with sensor, signal conversion into electrical form, signal condition and signal conversion into sequence of digital sample values);

- In some applications actuators with digital-to-analog converters (DACs) can be included not only for monitoring environment, but also for affecting it and reacting on sensed impacts;
- Autonomous power supply block (power management) – supplying sensor node with necessary energy and provides possible all functions related to energy storage, power conditioning, energy scavenging from the environment etc.;
- (Wireless) communication block – provides communication links with neighbor nodes, network gateway or central base station (depending on network architecture and communication protocols) etc.;
- Data processing and sensor node control block – this block provides necessary computation power for sensor node. It is needed for signal pre-processing, appropriate coding for data transmitting, controlling other functional blocks of sensor node etc.

In many applications each sensor nodes have to be as small as possible, their operational life should exceed several years and many other requirements. Therefore implementation of all these functional blocks into one robust sensor node is challenging from design point of view.

More detailed studies of sensor networks including acquired data transmitting and communications between sensor nodes are out of scope of this work.

2.2 Simultaneous DAQ: two different interpretations

The term „simultaneous DAQ", in general, means parallel acquisition of data from some multitude of signal sources simultaneously at the same time instants. Obviously often it is important to ensure fulfillment of that condition, to perform DAQ simultaneously. That is often crucial for correct evaluation of reaction of an object to some test excitation or for monitoring functioning of objects performed on the basis of DAQ and analysis of the acquired data. However this term not always is used in an acceptable way. The problem is that this might lead to wrong conclusions.

Description of the requirements for „simultaneous DAQ" given in [32] represents a typical case of this. The essence of the given there misleading statements concerns DAQ systems made according to the basic structures shown in Figures 2.1 (a) and 2.1 (b). It is explained that only using a separate ADC in each of the DAQ channels provides for „simultaneous DAQ". This term here is actually used in the sense that only such a structure allows to take signal sample values in all of the input channels exactly at the same time instants. That of course is true. However the conclusion, defined on the basis of this, the conclusion that only the basic scheme of Figure 2.1 (a) and not the scheme given in Figure 2.1 (b) (based on MUX and a single ADC) can be used for „simultaneous DAQ", this conclusion is misleading.

Let us explain what seems to be wrong with this approach to the term of „simultaneous DAQ" and this conclusion. The basic task for a DAQ system is obtaining information from a multitude of sensors, pre-processing this information and transferring it to a computer. Signals carry this information and it is picked up by the mentioned sensors. What is the best approach to acquire data so that they represent the essential information is another question. Broadly speaking, this information can be considered on the level of signal instantaneous sample values (case 1) or on the level of some sensor signal parameters in time, frequency or modulation domains (case 2). Definitions and requirements of „simultaneous DAQ" in both these cases would differ. Actually just saying „simultaneous DAQ" is not enough. It should be clear what sort of data are to be acquired simultaneously.

In this work, DAQ is considered as a process ensuring obtaining of data sufficient for reconstruction the waveforms of the respective signals provided by sensors. When data are acquired from a number of sensors in parallel, it is not necessary to sample all of the involved signals at the same time instants. It is required instead that the acquired data should contain sample values of these signals taken under conditions providing for reconstruction of the original signals. That ensures that the acquired data contain all information about the processes going on, being observed and reflected by the multitude of the sensor signals. Multi-channel DAQ should be simultaneous in this sense and it does not then matter if that is done on the basis of the basic scheme of Figure 2.1 (a) or the scheme given in Figure 2.1 (b).

2.3 State-of-the-art in the area of DAQ

To give an impression of the state-of-the-art in the area of DAQ, let us briefly consider achievements of a typical company developing and manufacturing of DAQ hardware and software.

2.3.1 Multiplexer or multiple ADC based DAQ systems

As all companies have to work on the best possible level of quality to ensure their competitiveness, performance of these products more or less characterize the currently achievable precision, operational speed, covered frequency range, number of channels and other related metrological parameters. Typical parameters of modern DAQ systems, currently available on the market, are given in Appendix 1. Although only the most important parameters of data acquisition systems are given, they reflect the performance of these systems built according to the structures shown in Figure 2.1 (a) and 2.1 (b).

Other significant factors besides the mentioned performance characteristics are the system cost and functionality. Signal pre-processing function currently can be and often is a part of a DAQ system. For example, company "*National Instruments*" provides DAQ boards, which can be plugged into PC. There is a FPGA chip on the board providing for additional functionality, specifically, for performing necessary pre-processing of the acquired signals.

Typical representatives of DAQ systems are also given in Appendix 1.

Not only the primary parameters like channel count, sampling frequency per channel etc. are important characterizers of DAQ systems. The system functionality also plays significant role. DAQ systems often are made with some extra features included. As all DAQ system hardware is built on the basis of specific electronic components, the characteristics of these components usually determine the achievable DAQ performance. The most responsible microelectronic elements for any DAQ system is the used analog-to-digital converter, converting continuous signals into their discrete counterparts by performing the sampling and quantizing operations, and a multiplexer (MUX) used for multiplexing either analog or digital signals.

The achieved ADC perfection is very high and the parameter range covered by various types of ADC is very wide. Specifically, one of the fastest and ultra-wideband ADC is currently produced by company *MAXIM*. It is *MAX 109* chip, which supports high sampling rate, up to 2.2 Gsps. However it is an expensive device with high power consumption and its dynamic range is quite narrow 8 bits (low resolution). "*Nationals Instruments*" has announced development of currently the world's fastest and very precise ADC. It is capable of sampling at 3.6 Gsps and provides for 12 bit resolution. Nevertheless its power consumption also is quite large 2.06 W [33].

Much wider dynamic range has ADCs operating at considerably lower sampling frequencies. For example, *MAX11040* chip from *MAXIM* has 24 bit resolution, but its sampling frequency is only 64 Ksps. Available parameters of currently existing ADCs are given in Appendix 1. Note that all the best parameters cannot be available at the same time for one converter. That means, if ADC has high sampling frequency then its resolution will be low etc.

Similar situation is with available multiplexers – each MUX is designed for its own applications. Therefore one multiplexer cannot be the best in all categories. Available parameters of current multiplexers are summarized in Appendix 1.

Many applications exist, where data acquisition is integrated part. In these cases the characterizing parameters are hardly extractable from other system descriptive parameters. Anyway it impacts all system performance. For example, data acquisition is definitely a part of some automated test equipment, offered from many companies. If the specific data acquisition task with particular signal pre-processing procedures should be solved, in many cases the system hardware architecture can be customized to the given specific application.

2.3.2 Sensor nodes

Today sensor networks are developed all around the world starting with small researcher groups and ending with prominent companies and organizations. Few prominent companies and organizations in the field of developing and manufacturing wireless sensor networks for data acquisition are *Crossbow*, *Ember*, *Microstrain*, *IMEC* etc. Detailed descriptions of them are given in Appendix 2.

To get insight about typical parameters of wireless sensor network nodes, an example of one sensor node – *TelosB* mote from *Crossbow* – is considered. This sensor node *TelosB* is shown in Figure 2.6.

Figure 2.6 Sensor mote TelosB from Crossbow illustrating state-of-the-art in the field wireless sensor networks.

TelosB mote has following specification: IEEE 802.15.4 compliant;

- 250 Kbps, high data rate radio;
- TI MSP430 microcontroller with 10kB RAM;
- Integrated onboard antenna;
- Data collection and programming via USB interface;
- Open-source operating system;
- Optional integrated temperature, light and humidity sensor.

As it can be found from *Crossbow* web page, *TelosB* mote platform is an open source, low-power wireless sensor module designed to enable cutting-edge experimentation for the research community. The *TelosB* bundles all the essentials for lab studies into a single platform including: USB programming capability, an IEEE 802.15.4 compliant, high data rate radio with integrated antenna, a low-power MCU with extended memory and an optional sensor suite.

2.4 Comparison of two common DAS hardware architectures

In the case of multiplexer based DAQ architecture each channel sampling frequency can be calculated dividing ADC sampling frequency with channel count. Therefore with this architecture big channel count and large sampling rate per channel is very hard to achieve at the same time [32]. This fact is illustrated in the next Table.

Table 2.1 Signal bandwidth per channel in both common DAQ architectural cases.

DAQ system architecture based on single MUX and wideband ADC			**DAQ system architecture based on many ADCs**		
Number of channels acquired	Sampling rate per channel [KHz]	Signal bandwidth [KHz]	Number of channels acquired	Sampling rate per channel [KHz]	Signal bandwidth [KHz]
1	120	60	1	120	60
2	60	30	2	120	60
3	30	15	3	120	60
4	15	7.5	4	120	60
5	7.5	3.75	5	120	60

Usage of DAQ system architecture based on many ADCs increases overall system sampling frequency and signals with higher bandwidth can be acquired, but it can be costly and can’t be recommended for all cases. Wider bandwidth of acquired signal is achievable, because each channel uses the full throughput of an individual ADC converter [32].

DAS hardware architecture based on usage of many ADCs provides better operational speed and accuracy than multiplexer based DAS architecture, because several sources of error like settling time and channel-to-channel crosstalk can be avoided. Both these errors sources are because of analog multiplexer imperfections and can’t be met in the case many ADCs DAS architecture type.

Settling time is parameter, which shows how fast multiplexer inputs can be switched with output. This parameter also is called transition time and it impact DAS system operation rate especially at high rates. For reason that DAS hardware architectures based on usage of many ADCs have a separate ADCs for each input, transition time between channels is not an issue. That means you can acquire data at very high speeds [32].

According to [32] channel-to-channel crosstalk occurs when the signals on one or more multiplexed channels interfere with the signal on the channel that is being switched. Crosstalk is inherent to the multiplexing process and distortions become larger as someone increase the number of channels or the signal frequency. Crosstalk phenomenon occurs because of parasitic capacitance across each open switch couples. Due to it a portion of each channel signal goes to the output and distorts the multiplexed signal.

All common DAQ hardware architecture drawbacks and advantages are summarized in Table 2.2.

Table 2.2 Summarized comparison of two the most common DAQ system hardware architectures.

DAQ system architecture based on single MUX and wideband ADC	DAQ system architecture based on many ADCs
Digitization only after signal multiplexing (large system analog part)	Digitization can be close to signal source
Simpler system hardware and less power consumption	More complex system hardware and large power consumption
Sampling rate per channel is inversely proportional to the channel number	Sampling rate per channel is independent on channel number
Acquired signals are less protected from environmental noise and impact of other signals	Acquired signals are more protected from noise and can be measured more precise with increased resolution
Signal sample values from all channels only can be taken sequentially	Signal sample values from all channels can be taken at the same time instant

It will be shown later that designing multi-channel DAQ system these two common hardware architectures could be changed, if the uniform sampling is not just only sampling approach, what is considered. The uniform sampling is just a special case from the general NU signal sampling group, where all signal sample values are taken equidistantly. When DAQ system hardware organization is designed from many signal sources, the most appropriate signal sampling should be chosen and trading-off among their properties has to be done.

2.5 Specific approaches to signal conversions involved in DAQ operations

As it is shown in the previous sections, acquisition of data from real-world information sources usually requires conversion of analog signals into respective digital signals. Achieved quality of DAQ strongly depends on these analog-to-digital conversions. The existing DAQ systems mostly are based on the classical theory and procedures for these conversions. However the drawbacks of this approach have been noticed a long time ago and there have been attempts to use also non-traditional methods and techniques for that. Application of NU sampling for analog-to-digital conversions used at DAQ is described and discussed in the following Chapter 3.

Signals can be represented by particular information in both the time (or space) and frequency domain. How it is known, for full signal representing in frequency domain it is enough with signal amplitudes and phases. The same can be done in time domain employing various sampling schemes. Here representing signals digitally by using only timing information and novel trend in data acquisition called compressive sensing is briefly considered. The results achieved in this area also are reviewed.

2.5.1 How signals can be represented using only timing information

Interesting fact is that many examples can be found in the nature, where timing instants are carrying all information about signal. For biologist it is known that human inner ear conveys information from ear to the brain in the form of almost identically shaped nerve impulses or spikes. Then the information about the acoustic signal is represented by the timing information in the form of spike trains [56]. It was just one example and many others can be found.

Only under particular conditions explored by Logan in 1977 bandpass signals can be represented by sequences of timing instants alone $\{t_k\}$ [42]. This specific signal class of bandpass signals is called real-zero signals. In this case signals are uniquely represented by their zero crossings (these are time instants at which the signals change their sign) without additional knowledge about sampling specifics [35]. Examples of signals represented by timing information are given in Figure 2.7.

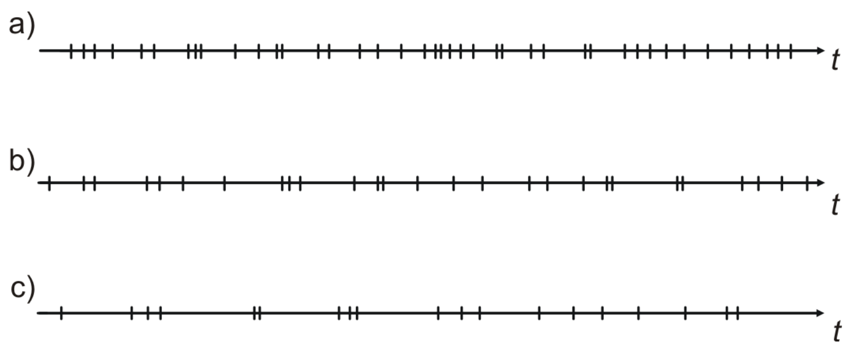

Figure 2.7 Several sequences of timing instants.

Satisfying requirement to know some knowledge about signal sampling scheme in advance the many representation signal methods by timing information can be found. This additional knowledge can be information about sampling scheme organization, targeting DAS signal class etc. Note, that the discrete signal processing can be involved in any signal representation phase, if only the appropriate processing algorithm exists.

After representing signals by timing information, the signal reconstruction or specific processing of time instants is required, in order to recover original signal waveform. This might be understandable as inverse procedure to signal sampling.

One specific signal sampling scheme, where signals are represented by timing information, is based on detection of signal and reference function crossings. Representing signals in such a way, the sequence of crossing time instants is carrying all information about the original signal. Of course, if the sampling is organized properly – providing sufficient sampling point count N at some time period θ. Time period θ is also known as signal observation window. A priori knowing reference function waveform, the original discrete signal sample values can be recovered from the crossing instants very easy. Going further the obtained discrete signal samples can be converted into original continuous signal, if it is necessary. Doing this the specific reconstruction algorithm is needed, because all discrete signal samples of the original signal are localized nonuniformly.

In many cases sine-wave as reference is preferred. Nevertheless many other possible functions have to be taken into account. It is known that signal sampling based on signal and sine-wave crossings was explored long time ago. As it can be found in papers [25, 58] the image representation by zero and sin-wave crossings was explored in 1987. Since it many related papers appeared, continuing research and finding nontraditional signal representations applicability in the field of DAQ.

Usage of sinusoid-crossing sampling leads to attractive simplification of sampling scheme hardware. It is because threshold detection can be implemented only with one comparator. While in the case of uniform sampling designing of analog-to-digital converters are either expensive (as it is with flash architectures ADCs, which requires a number of comparators) or slow (ADCs by successive approximation architecture) [53]. The sampling based on detection of signal and sine-wave crossing instants will be illustrated and quite overwhelm discussed later.

2.5.2 Threshold level sampling and direct signal recovery from threshold crossings

Another specific signal sampling scheme is threshold level sampling, where reference function is one or many constant levels. According to this sampling in general signal can be represented by two vectors – threshold level crossing timing instants and numbers of crossed level (or with related information, exploiting ideas from sigma-delta modulation), if only one level threshold level sampling or real-time system design without acquired data storage in memory is not considered. In that case it is sufficient with timing information only [41].

This sampling approach together with asynchronous data processing circuits is well suited to particular DAQ cases where acquired signals from information sources are rare impulses. Then this approach can provide very low energy consumption.

Level crossing sampling more detailed is illustrated in Figure 2.8. As it can be seen from Figure 2.8 (a) the each time instant is detected when signal intersects some constant reference level. The sequence of detected crossing time instants (can be seen in Figure 2.8 (b)) together with level number are carrying all information about continuous signal, of course, if sampling conditions are proper.

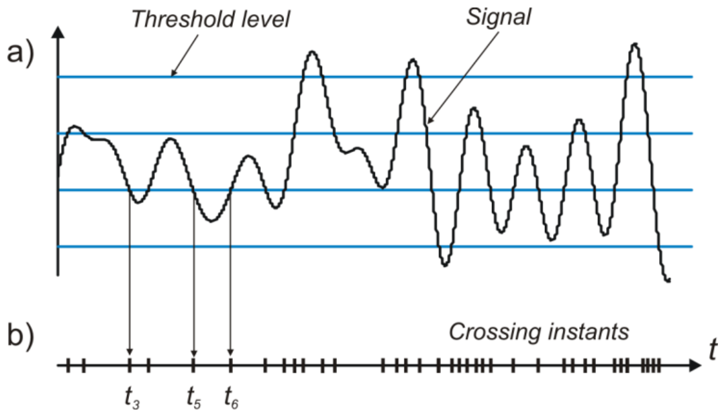

Figure 2.8 Fixed threshold level sampling is illustrated.

Manipulation with threshold levels is the main tool, how the signal sampling conditions can be managed. In the simplest case threshold levels are fixed in the time. However, exploration of much complex level crossing sampling schemes is became popular lately, where threshold levels change their value in time and the process could be signal dependent. This is called adaptive level crossing sampling.

Recovery algorithms are important part of any NU sampling scheme. It provides inverse transformation from timing information back to signal original waveform. In general all recovery algorithms can be divided in two large groups – direct and indirect reconstruction algorithms. Indirect recovery algorithms provide signal reconstruction via Fourier Transform. Other algorithms direct recovery class provides signal reconstruction in time domain. To this algorithm class belong all interpolation and approximation algorithms – polynomial curve-fitting, cubic-spline interpolation etc.

According to this sampling scheme the signal waveform can be recovered quite precise directly from level crossing instants and information related to crossed level number. Additional precision is achievable with some digital filtering procedures etc.

In some application cases even with one bit ADC (one threshold level sampling) is sufficient to achieve high accuracy. For example, in paper [29] the high accuracy Fourier Transform interferometry, without oversampling, with a 1-bit analog-to-digital converter is considered.

2.5.3 Compressive sampling/sensing

Compressive sampling also known as compressive sensing (CS) is relatively new paradigm that goes against the common wisdom in data acquisition. According to it signal can be represented and reconstructed by fewer signal samples or measurements in comparison with traditional Shannon sampling method. For certain signals it can be done beyond Nyquist frequency requirement. A good introduction about compressive sensing can be found in article [27].

According to compressive sampling concept, the information about a signal *s(t)* is obtained by following expression:

$$y_k = \langle s(t), \varphi_k(t) \rangle,\ k = 1,2,\ \dots,\ m. \tag{2.3}$$

Information about original signal are carrying a set of correlation coefficients y_k. In formula (2.3) *s(t)* – is an original signal waveform; $\varphi_k(t)$ – is set of particular waveforms or basis functions.

Choose of basis function set $\{\varphi_k(t)\}$ is the main tool to control signal sampling conditions. This particular approach like other NU signal sampling techniques requires reconstruction process to obtain back original signal waveform. Therefore each particular compressive sampling method has to be considered together with reconstruction algorithm.

In compressive sensing expression (2.3) is standard procedure to digitize original signal waveforms and get *footprints* from them. Actually, the original signal is not represented by pure signal sampling values as it is in case of traditional uniform sampling, but with signal and particular function correlation coefficients.

There exists a large number of varieties what waveforms $\{\varphi_k(t)\}$ can be. If these are Dirac delta functions (or spikes) then it leads to traditional uniform sampling. In another case if these are sine-waves then y_k are coefficients of Fourier transformation.

There are two main principles: *sparsity* and *incoherence*. Sparsity principle underlying CS says that during the compressive sampling process the obtained small coefficients y_k can be discarded without significant loss of information about original signal waveform *s(t)*. Second principle – *incoherence* – shows the connection between two function basis. One is signal sensing basis and the other is signal representation basis. Coherence measures the largest correlation between any two elements of sensing basis $\Phi=\{\varphi_k(t)\}$ and signal representation basis $\Psi=\{\psi_k(t)\}$ (there is assumption that signal can be fully represented with finite number elements of this function basis, as it is shown in formula 2.4). Compressive sensing is mainly concerned with low coherence pairs of function basis, and then the described technique provides the most remarkable results.

Signal model in the case of compressive sensing:

$$s(t) = \sum_{i=1}^{n} x_i \psi_i(t)\,, \tag{2.4}$$

Where *s(t)* – is original signal; x_i – are coefficients of *s(t)* and $x_k = \langle s(t), \psi_k(t) \rangle$; $\psi_i(t)$ – is signals representation basis.

Compressed signal is obtained after sparsity procedure. It is subset, what remains from all coefficients $\{y_k\}$. Therefore it can be written that now $k \in M$, where $M \subset \{1,\ldots,m\}$. After compression the coefficients count *n* is significantly smaller than waveform count *m*. It can be written $n << m$.

Reconstruction of compressed signal can be done according to ℓ_1-norm minimization algorithm. Note, that ℓ_1-norm is defined following:

$$\|x\|_{\ell_1} = \sum_i |x_i| \tag{2.5}$$

Reconstructed signal vector can be obtained following $s' = \Psi x'$, where x' is solution of the convex optimization program:

$$\min_{x' \in R^n} \|x'\|_{\ell_1} \ \ subject\ to\ \ y_k = \langle \varphi_k, \Psi x' \rangle,\ \forall k \in M\ . \tag{2.6}$$

Expression (2.6) means that among all objects $s' = \Psi x'$ we pick that coefficient sequence with minimal ℓ_1-norm. Anyway, there exist also other reconstruction methods and many variations of this reconstruction method involving linear programming.

2.6 Conclusions

Performance of a wide variety of computer systems to a large extent depends on the perfection of their DAQ subsystems supplying these computer systems with the information obtained from real-world sources. Much has been already done to develop DAQ systems capable of fulfilling these functions under conditions dictated by various applications. The overall situation in this field is considered and discussed in Chapter 2. Analysis of the currently used data acquisition system specifics reveals some essential facts and leads to the following generalized conclusions:

1. While many DAQ systems are manufactured and used, they mostly belong to one of two basic types of DAQ systems: (1) multi-channel systems for DAQ based on multiplexing inputs to a central ADC connected via interface to a computer; (2) multi-channel systems for so-called simultaneous DAQ using a separate ADC in every input channel.
2. DAQ functions usually are considered as input signal conditioning, analogy-to-digital conversions and transmitting the digital signals, obtained from all inputs, to the computer. Processing of data more often than not is the responsibility of the host computer.
3. The essential function of signal digitizing usually is performed on the basis of the classical concepts of uniform periodic sampling and fixed-threshold quantizing.
4. The sampling rate of for DAQ systems based on multiplexing inputs to a central ADC directly depends on the clock frequency at which the multiplexer is switched and the rate

of sampling signals in each input channel is inversely proportional to the number of inputs. Consequently the quantity of DAQ system inputs usually is restricted to relatively small numbers, usually up to 16. More complicated systems contain a hierarchy of multiplexers. In this case there might be more inputs however this type of DAQ systems then can be used only for data acquisition from low-frequency sources.

5. Using a separate ADC in every input channel allows avoiding these restrictions. Therefore this type of DAQ systems can be used for obtaining data from high frequency signal sources. The factors limiting their applications are relatively high complexity (ADC in every channel) and multiplexing of ADC output signals needed for transmitting them sequentially to the host computer. Additional drawback of this type of DAQ systems is relatively high power consumption narrowing the area of their applicability for autonomous DAQ.
6. The quality of developed and produced DAQ systems improve all the time, however this progress is mostly based on the achievements in the area of semiconductor device development and production technologies. The theoretical basis for signal digitizing exploited for DAQ, in general, has remained the same classical one for many years.

The last conclusion is true for most of the currently produced DAQ equipment. On the other hand, there have been various R&D efforts addressing the problem of data acquisition under conditions more demanding than usual. Some of significant publications in this field are discussed above. They are dedicated to consideration of essential problems in the area of signal digitizing, data pre-processing and compressing. In general, they reveal a very important fact:

The classical theory covering signal digitizing (sampling and quantizing) and digital representation of analogy signals is not exclusive. These signal conversion operations can be performed in various ways, not only according to the rules of periodic sampling and traditional quantizing.

In particular, the applicability of NU sampling and low-bit rate quantizing has been investigated over a long period of time and this approach is directly related to DAQ functions [22, 23, 43, 44]. These methods and algorithms are applicable for achieving a number of essential advantages, such as performing of DAQ in a wide frequency range, elimination the dependency of the sampling rate in a channel on the quantity of channels in a system, data compression/reconstruction, reducing the complexity of DAQ systems and others. That leads to the following conclusions:

1. The currently used classical theory covering signal digitizing (sampling and quantizing) and digital representation of analog signals is not exclusive. These signal conversion operations can be performed in various ways, based on the signal digitizing theory

developed in a few past decades, including theory of randomized signal processing, NU sampling and quantizing and DASP.

2. To achieve progress in the area of DAQ, efforts have to be put in this work basically in the directions of developing methods and algorithms for application-specific DAQ. That is considered to be the key factor for achieving the capability of more precise data acquisition in a wider dynamic range from a larger quantity of signal sources at increased operational speed, widened signal bandwidth and increased energy-efficiency.
3. Selecting and using the most effective type of digital representation of analog input signals is really important for that.
4. Data pre-processing in many cases should be included in the list of functions to be fulfilled by a DAQ system as algorithms for parallel processing of raw digital signals can be developed and used at that stage for effective data representation and compression.

Reduction of power consumption, simplification of system hardware, simplification of algorithms for acquired data pre-processing and enlargement of system channel quantity, accurate signal acquisition are still very desirable for DAQ systems.

3. Data Acquisition Based on NU Sampling: Achievable Advantages and Involved Problems

To convert an analog sensor signal into its digital counterpart, it has to be digitized on the basis of the sampling and quantizing operations. No doubt that periodic sampling is currently the most used and widespread sampling method. This type of sampling is also called uniform or equidistant sampling as the intervals between the taken sample values in that case are constant. However there are other methods for sampling. Attention is drawn to a non-traditional approach to sampling performed in the process of data acquisition, specifically, to NU sampling. The achievable advantages and application potential of this approach are based on exploitation of the capabilities offered by the NU sampling procedure carried out in the process of the sensor signal digitizing [22, 23, 30, 43, 44, 54].

Usage of NU sampling makes it possible, first of all, to enlarge the frequency range where information carried by the analog signals can be represented in the digital domain. To achieve that, these signals, in the process of their digitizing, must be sampled non-uniformly in a right way to avoid overlapping or aliasing of signal components whenever their frequencies exceed half of the mean sampling rate. Skilful using of NU sampling then opens up the possibility of getting valuable positive advantages but that leads also to specific difficulties related to processing of this type of digital signals, including reconstruction of the original signal waveforms from them. However, if these signals could be reconstructed, then a number of typical problems arising at development of data acquisition systems can be resolved in a simple and effective way.

Application potential of this non-traditional approach to data acquisition from sources of continuous in time sensor signals is discussed in this Chapter. It is shown that using NU sampling at digitizing such signals opens up a possibility of obtaining a number of practically valuable benefits under the condition that appropriate algorithms are used for processing them. However this approach requires also more complicated processing of the acquired data, especially at reconstruction of the original waveforms. Problems of this kind and ways how to resolve them are discussed.

The knowledge accumulated over a long period of time in the area of non-traditional Digital Signal Processing (DSP) has been used to develop the theory of Digital Alias-free Signal Processing (DASP). It is also very useful for gaining benefits at data acquisition and for finding the right solutions to the involved problems [22, 23]. The later largely are related to the task of the original waveform reconstruction from the acquired data and to the problems arising from the specific properties of the irregular signal sample value sequences obtained in result of NU sampling. As soon as the sampling process is nonuniform there might be bias errors if the sampling procedure is not performed in a right way and cross-interference between components of a signal occurs. This fact has to be taken into account. How that could be done and at what costs is explained in Section 3.1 – 3.3.

Sometimes NU sampling is deliberately used with clear purpose to gain some specific advantages. In such a case the sampling nonuniformities are just a side effect defining the costs due to usage of NU sampling methods. However in some application areas data can be acquired only at unpredictable random time instants as it is, for example, in the case of fault tolerant data acquisition. DASP theory helps also in this case. A number of typical data acquisition cases, where the considered approach to data acquisition can be successfully used, are discussed in Section 3.4. The specific problem of image data compression and image reconstruction is considered in Section 3.5. In Section 3.6 problems concerned with wideband signal digitization in enlarged dynamic range problems are considered with the following conclusions at the end of Chapter.

3.1 Aliasing effect in DSP, is it possible to avoid it?

Frequency overlapping or aliasing is a well known effect significantly limiting the frequency range where signals can be digitally processed on the basis of the classical DSP theory and existing microelectronic elements. Whenever continuous time signals are digitized and then processed on the basis of DSP, the sampling rate f_s of the used periodic sampling limits the bandwidth of the original analog signals. Then the restrictions, defined by the Sampling theorem, have to be satisfied to avoid the uncertainty due to the fact that all frequencies belonging to the sequence: f_o; $f_s \pm f_o$; $2f_s \pm f_o$; $3f_s \pm f_o$;... $nf_s \pm f_o$ are indistinguishable.

Let us briefly consider the essence of aliasing to see what can be done to avoid the limitations imposed on DSP in result of this effect. Suppose there are two sinusoidal signals $x_0(t_k) = 2\pi f_0 t$ and $x_n(t_k) = 2\pi(f_0 + nf_s)t$. Both of them belong to the indicated above row of aliasing frequencies. Suppose that they are sampled at the frequency f_s. Then we obtain

$$\begin{aligned} x_0(t_k) &= \sin 2\pi f_0 t_k = \sin 2\pi k \frac{f_0}{f_s} \\ x_n(t_k) &= \sin 2\pi(f_0 + nf_s)t_k = \sin(2\pi k \frac{f_0 + nf_s}{f_s}) = \sin(2\pi k \frac{f_0}{f_s} + 2\pi kn) \end{aligned} \tag{3.1}$$

as $t_k = kT, k = 1,2,3,...$ and $T = \frac{1}{f_s}$, where T is the sampling interval or period of the sampling frequency.

Now compare these two original analog signals and their digital counterparts. Note that while the original signals are clearly different sine functions, the respective digital signals are equal. They provide the same sequences of sample values. In other words, the compared digital signals completely overlap and they evidently are aliases.

The obvious way to avoid this uncertainty is to require that the frequency $f_o<f_s/2$ and that all frequencies in the spectrum of the input signal above $f_s/2$ are taken out by analog low-pass pre-filtering. Whenever that does not represent a problem, periodic sampling of signals is preferable as it leads to significant advantages. However the widely spread belief that the limitations defined by the Sampling theorem are unavoidable is not right.

Indeed, the equality of both digital signals in (3.1) is due to the fact that the sampling interval T has a constant value. In other words, both these digital signals are overlapping because sampling is performed periodically and this signal overlapping or aliasing can be avoided if the signal sample values are taken non-uniformly, if the sampling operation is nonuniform.

This fact has not escaped attention and published descriptions of attempts to use NU sampling to avoid aliasing started to appear in 1960-ties [15] and they were quite popular in 1970-ties [16-21, 36-40, 45-49]. Balakrishnan, for example, considered the well known fact that periodic sampling is always in fact a random process as the signal sample value taking actually happens at random time instants t_k as there is random jitter of them. At this type of sampling the signal sample values are taken at time instants

$$t_k=kT+\tau_k\,, \quad k=0,\,1,\,2,\,... \tag{3.2}$$

where $\tau_k\,, \quad k=0,\,1,\,2,\,...$, is a random variable.

While consideration of this jittering usually was focused on the problem how to suppress it, Balakrishnan draw attention to the potential usefulness of the involved jittering. Relatively many other publications proposing and discussing deliberate randomization of signal sampling followed. Gradually it became clear that there is a possibility to avoid the described uncertainty due to frequency overlapping or aliasing and that this possibility is based on application of NU signal sampling [16, 45].

Indeed, imagine that the signal frequencies are sampled non-equidistantly, obviously then all the digital replicas of signal frequencies will differ. That opens up the principal possibility of distinguishing between them without mentioned cutting-off of the analog signal spectra by low-pass pre-filtering of them.

On the other hand, it is not so easy to gain from NU sampling, to develop practically applicable designs of analog/digital systems successfully exploiting advantages of this technique. Whenever signals are sampled nonuniformly, processing of the obtained digital signals has to be done specifically and correctly, to avoid errors due to the cross-interference between signal components and to other negative effects related to the specifics of randomized sampling.

Suppose a signal $x(t)$, continuous in time, is sampled at time instants t_k, $k=1, 2, 3, \dots$ and a sequence of sample values $x(t_k)=x_k$ taken at these time instants is obtained. It becomes possible to use this sequence of the sample values $\{x_k\}$ for representing the original analog signal in the digital domain if certain requirements, depending on the specific sampling mode used, has been satisfied. While in the cases of periodic sampling the signal sample values have to be taken at a rate at least twice exceeding the upper frequency in the spectrum of the signal, it is less clear what requirements have to be satisfied in the cases where signals are sampled nonuniformly. They depend, in general, on the used specific method for NU sampling, on various parameters characterizing the sample value taking process and also on the used approach to extraction of the information carried by the signal. The sampling model (3.2) actually has limited application. It was shown [22, 23] that so-called additive random sampling has proved to be a much better NU sampling option. The basic difference between the NU sampling procedure based on (3.2) and the additive random sampling is that the introduced randomness in the second case accumulate and this do not happen in the first case. This difference is significant as the accumulative effect of the introduced randomness at the additive random sampling leads to a number of important advantages.

3.2 Using of NU sampling for data acquisition

Various methods and techniques are used for implementation of NU sampling [22, 23]. The most popular are the following methods for NU sampling: (1) additive sampling and (2) random skipping of some quantity from the periodically given sampling points. Actually, both methods can be implemented in pseudo-random way. Each of the methods has its own advantages and drawbacks, of course. Let us consider the basic specifics of NU sampling relevant to data acquisition.

3.2.1 Basics of additive sampling

In the case of the mentioned additive sampling, the sample values are taken from signals at time instants t_k defined as follows [23]:

$$t_k=t_{k-1}+\tau_k\,, \quad k=0, 1, 2, \dots \tag{3.3}$$

where τ_k are random or pseudo-random variables.

As it has been proved, the successive sampling intervals $\tau_{k,}$ τ_{k+1} should be statistically independent and identically distributed. Remarkable properties of the sampled signals are achieved under this condition. First of all application of this type of sampling makes it possible to avoid aliasing even when the mean sampling rate does not exceed the upper frequency in the spectrum of a signal. On the other hand, randomizing of the signal sampling instants leads to further considered negative effects complicating processing of the digital signals obtained in result of such sampling. To reduce these negative effects to some extent, a simple method can be used. The idea is really very simple: the randomness introduced at sampling should be minimized for that. This means, in terms of equation (3.3), that the distribution of the random or pseudo-random variables τ_k should be characterized by relatively small ratios σ/μ, where μ is the mean sampling rate and σ is standard deviation of τ_k. Usually the desirable properties of sampling are obtained at even small values of the ratio σ/μ. Excessive randomization of the sampling process actually is just harmful.

3.2.2 Ensuring unbiased estimation of signal parameters.

Additive sampling has a very valuable property. Specifically, the sampling point density function *p(t)* characterizing this type of sampling, with *t* increasing, tends to the constant level $1/\mu$. It is shown that usually there are no problems in achieving that. The point is that signal waveform instantaneous values are sampled under this condition with equal probability. And that is very important as only then the nonuniformly sampled signals can be processed without systematic or so-called bias errors. It is shown in [23] that the estimates $\hat{A}$ of many various signal parameters A, defined on the basis of functional conversions F_A according to

$$\hat{A} = \frac{1}{N}\sum_{k=1}^{M} F_A[x(t_k)], \tag{3.4}$$

where N is the number of signal sample values taken within the time interval Θ during which the signal is observed.

If the sampling operation is performed in accordance to (3.3), then the expectation $E[\hat{A}]$, as it is shown in [23], is given as

$$E[\hat{A}] = \frac{1}{N}\int_0^{\Theta} F_A[x(t_k)]p(t)dt, \tag{3.5}$$

If the sampling point density function $p(t)=1/\mu=const.$ and $N\mu=\Theta$, then

$$E[\hat{A}] = \frac{1}{\Theta}\int_0^{\Theta} F_A[x(t_k)]dt = A, \tag{3.6}$$

Therefore estimation of signal parameters A under these conditions is reduced to estimation of the mean value of the functionally converted signals and the expected value $E[\hat{A}]$ of these parameters is equal to them. And the additive sampling procedure, performed according to (3.3), leads to such sampling characteristics. Therefore this approach is preferable. Whenever it is used in a right way there are no systematic or bias errors in parameter A estimation.

This fact is significant for a number of reasons.

First, there are other methods for NU sampling and they have to be evaluated before using for data acquisition because not all of them satisfy the above conditions for unbiased signal parameter estimation. For example, periodic sampling with fluctuations of the sampling instants, even if these fluctuations are significant, does not satisfy the requirement $p(t)=1/\mu=const.$

Second, the criteria for unbiased parameter estimation cover a wide range of signal parameters, including Fourier coefficients estimated for signal conversion from the time to the frequency domain. Therefore the defined conditions for avoiding bias errors are essential also for achieving unbiased signal waveform or image recovery from the acquired data.

3.2.3 Implementation of DAQ on the basis of additive NU sampling concept.

The concept of NU sampling can be used for multi-channel DAQ in various ways. Let us consider two typical cases of simultaneous DAQ performed at time instants t_k. Data then are taken from M sensor signal sources in one or another way as shown in Figure 3.1.

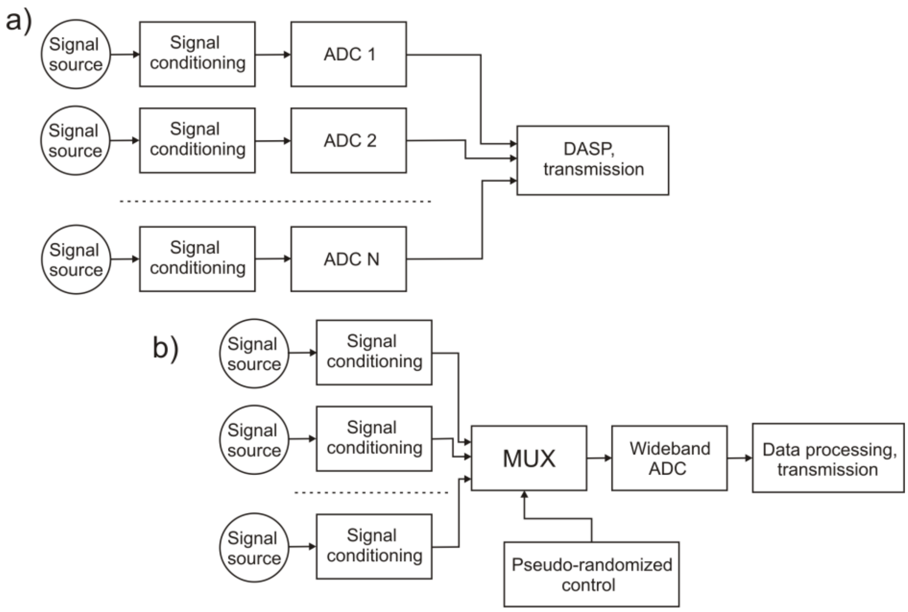

Figure 3.1 Two multi-channel DAQ system structures modified according to requirements of NU sampling: (a) structure based on usage of NU sampling performed by many ADCs and (b) structure for data acquisition based on NU multiplexing of input signals.

In general, these DAQ system structures seemingly do not differ from the already discussed typical multi-channel DAQ system structures given in Figure 2.1. Actually they differ significantly as they perform the functions of DAQ using two different approaches to this task. While systems shown in Figure 2.1 perform DAQ functions according to the rules of periodic sampling, the systems given in Figure 3.1 perform these functions on the basis of NU sampling. Consequently, the capabilities and characteristics of them differ strongly. Whenever DAQ is based on periodic input signal sampling, the achievable higher frequency of input signals, as well as the achievable number of DAQ channels, is limited by the sampling frequency. Introduction of the NU sampling concept into the procedures of DAQ takes out this limitation. That leads to the possibility of obtaining various benefits valuable for practical applications. How that can be done on the basis of DAQ systems given in Figure 3.1 is shown and discussed in Sections 3.4 and 3.5.

However introduction of the NU sampling concept into the procedures of DAQ preconditions also some more or less damaging negative effects. Consideration of the basic drawback, typical for NU sampling based DAQ, follows. This is the effect of cross-interference between signal components that appears whenever signals are sampled nonuniformly.

3.3 Relevant specifics of NU sampled signals

An example of a typical signal sampled nonuniformly is shown in Figure 3.2.

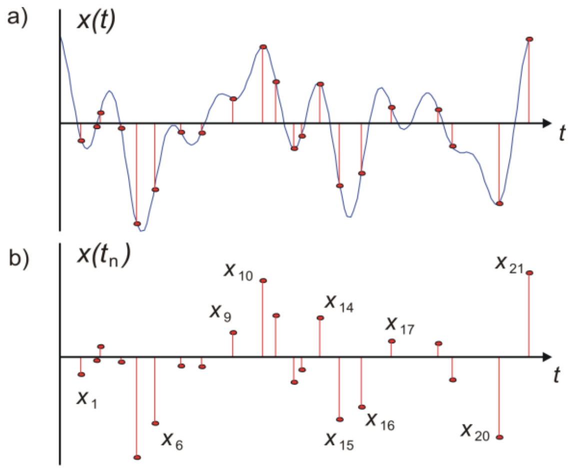

Figure 3.2 Digitizing based on NU sampling: (a) analog signal; (b) digital signal obtained in result of additive NU sampling.

Whenever a signal is digitized, it should be possible to reconstruct the original signal from the obtained discrete signal sample value sequence. In the case of periodic sampling, it can be done whenever the signal sampling frequency f_S is high enough. Shannon sampling theorem defines this frequency limit saying that a continuous signal can be sampled and converted back into its original form if the sampling frequency f_S is at least twice higher than the upper frequency f_u present in the spectrum of the signal. This frequency limit is called Nyquist frequency (see Chapter 2.1.1 about DAQ theoretical basis). If a signal has frequencies exceeding this limit then overlapping or aliasing of signal components at frequencies f_S+f, f_S-f, $2f_S+f$, $2f_S-f$ ... takes place. Obviously, then it is impossible to reconstruct the original signal from the sequence of its sample values.

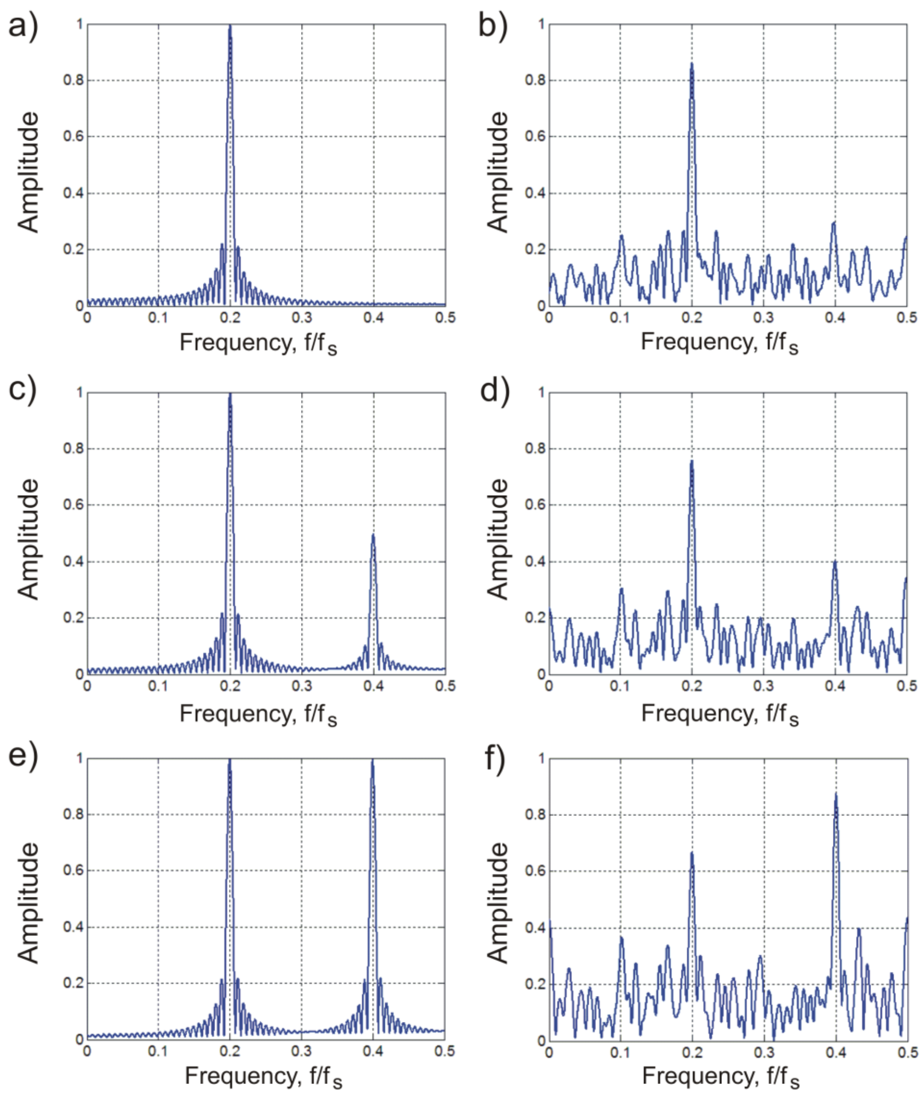

Figure 3.3 Impact of the cross-interference between signal components on spectral estimations.

Aliasing can be avoided if signals are sampled according to proper methods for NU sampling and the obtained sample value sequences are processed by taking into account the specifics of the used sampling approach. It means that using of NU sampling sometimes makes it possible to enlarge the frequency range where information carried by the analog signals can be represented by digital data. For example, if the DAQ for measurements is considered.

And that is exactly why it is suggested in this Chapter to use NU sampling for data acquisition. The point is that skilful using of NU sampling leads to significant advantages. On the other hand, using of this type of sampling leads also to specific difficulties and problems. Most of them are due to the fact that whenever signals are sampled nonuniformly, cross-interference (CI) between signal components occurs. If nothing is done to take care of the consequences of this phenomenon, substantial errors distort the results of processing the digital signal obtained in this way. Figure 3.3 illustrates how this CI affects digital signal processing in the cases of NU sampling.

Suppose that classical Discrete Fourier Transform (DFT) is performed over data obtained in result of periodic and NU sampling of a signal given as a single sinusoid at a specific frequency. Then obtained spectra will look similar to the spectrograms given in Figure 3.3 (a) and (b), respectively. At the first glance it seems that the spectrogram obtained in the case of NU sampling has additional noise related to the randomness present at sampling. Actually that is not exactly right. Studies of the involved processes have revealed [22] that the NU sequence of sampling points, defining the signal sampling process, and the particular signal frequency fully determines the pattern of the spectrogram. The spectrum is deterministic and each peak in it can be traced back to the signal sinusoid. Amplitudes of these peaks are proportional to the amplitude of this sinusoid. Therefore the signal frequency interferes with other frequencies in the spectra and actually symmetric CI takes place, as can be seen by comparing Figure 3.3 (c) with Figure 3.3 (d) illustrating the CI between two signal components in the case where the amplitude of the second component is smaller. These two diagrams might be compared with the spectrograms given in Figure 3.3 (e) and 3.3 (f) obtained in the case where the amplitude of the second component is enlarged.

As it is shown in [22, 51], the CI coefficients for a given NU sampling point process are given as:

$$(A_iC_m)=\frac{2}{N}\sum_{k=0}^{N-1}\cos(2\pi f_m t_k)\cos(2\pi f_i t_k)$$
$$(A_iS_m)=\frac{2}{N}\sum_{k=0}^{N-1}\sin(2\pi f_m t_k)\cos(2\pi f_i t_k)$$
$$(B_iC_m)=\frac{2}{N}\sum_{k=0}^{N-1}\cos(2\pi f_m t_k)\sin(2\pi f_i t_k)$$
$$(B_iS_m)=\frac{2}{N}\sum_{k=0}^{N-1}\sin(2\pi f_m t_k)\sin(2\pi f_i t_k) \tag{3.7}$$

and

$$A_iC_m = A_mC_i \qquad A_iS_m = B_mC_i \qquad B_iC_m = A_mS_i \qquad B_iS_m = B_mS_i \tag{3.8}$$

Where N – count of signal discrete values; f_S – sampling frequency; f_m – frequency on which DFT is carried out; f_i – frequency on which signal component is expected; t_k – time instants, when signal sample values are taken; k – signal sample number $k = 0, 1, 2... N\text{-}1$; m – frequency number $m = 1, 2, 3... M$.

CI coefficients allow estimating how each signal component impacts all other components at all frequencies f_m. That could be done by using the CI coefficient matrix.

$$C = \begin{bmatrix} (A_1C_1) & (A_1S_1) & (A_1C_2) & (A_1S_2) & \ldots & (A_1S_M) & (A_1S_M) \\ (B_1C_1) & (B_1S_1) & (B_1C_2) & (B_1S_2) & \ldots & (B_1C_M) & (B_1S_M) \\ (A_2C_1) & (A_2S_1) & (A_2C_2) & (A_2S_2) & \ldots & (A_2S_M) & (A_2S_M) \\ (B_2C_1) & (B_2S_1) & (B_2C_2) & (B_2S_2) & \ldots & (B_2C_M) & (B_2S_M) \\ \ldots & \ldots & \ldots & \ldots & \ldots & \ldots & \ldots \\ (A_iC_1) & (A_iS_1) & (A_iC_2) & (A_iS_2) & \ldots & (A_iC_M) & (A_iS_M) \\ (B_iC_1) & (B_iS_1) & (B_iC_2) & (B_iS_2) & \ldots & (B_iC_M) & (B_iS_M) \end{bmatrix} \tag{3.9}$$

To eliminate the impact of the CI, this matrix has to be inverted and then the reconstructed values of the Fourier coefficients are calculated by using the following matrix:

$$\begin{aligned} a_1 &= \hat{a}_1(\alpha_{11}) + \hat{b}_1(\alpha_{12}) + \hat{a}_2(\alpha_{13}) + \hat{b}_2(\alpha_{14}) + \ldots + \hat{a}_M(\alpha_{1M-1}) + \hat{b}_M(\alpha_{1M}) \\ b_1 &= \hat{a}_1(\alpha_{21}) + \hat{b}_1(\alpha_{22}) + \hat{a}_2(\alpha_{23}) + \hat{b}_2(\alpha_{24}) + \ldots + \hat{a}_M(\alpha_{2M-1}) + \hat{b}_M(\alpha_{2M}) \\ a_2 &= \hat{a}_1(\alpha_{31}) + \hat{b}_1(\alpha_{32}) + \hat{a}_2(\alpha_{33}) + \hat{b}_2(\alpha_{34}) + \ldots + \hat{a}_M(\alpha_{3M-1}) + \hat{b}_M(\alpha_{3M}) \\ b_2 &= \hat{a}_1(\alpha_{41}) + \hat{b}_1(\alpha_{42}) + \hat{a}_2(\alpha_{43}) + \hat{b}_2(\alpha_{44}) + \ldots + \hat{a}_M(\alpha_{4M-1}) + \hat{b}_M(\alpha_{4M}) \\ &\ldots\ldots\ldots\ldots\ldots\ldots\ldots\ldots\ldots\ldots\ldots\ldots \\ a_M &= \hat{a}_1(\alpha_{(M-1)1}) + \hat{b}_1(\alpha_{(M-1)2}) + \hat{a}_2(\alpha_{(M-1)3}) + \hat{b}_2(\alpha_{(M-1)4}) + \ldots + \hat{b}_M(\alpha_{(M-1)M}) \\ b_M &= \hat{a}_1(\alpha_{M1}) + \hat{b}_1(\alpha_{M2}) + \hat{a}_2(\alpha_{M3}) + \hat{b}_2(\alpha_{M4}) + \ldots + \hat{a}_M(\alpha_{M(M-1)}) + \hat{b}_M(\alpha_{MM}) \end{aligned} \tag{3.10}$$

Where α_{ij} are the elements of the inverted matrix inv(C).

To perform reconstruction of the original waveforms from the data obtained in result of signal digitizing based on NU sampling, the briefly described CI effect has to be taken into account. Otherwise significant errors will distort the signal processing results. And that under certain conditions might represent a problem. Indeed, these calculations take time and that in turn makes it difficult to reconstruct data in real time.

However, there are also other methods how to cope with NU sampling irregularities and the CI effect. And recovery of nonuniformly sampled signals is a rather wide subject out of scope for this work.

3.4 Using NU sampling to obtain specific benefits for DAQ

Various specific and valuable for practical applications advantages can be obtained by exploiting NU sampling techniques. Several methods of this kind are considered in this Section.

3.4.1 Data acquisition from high frequency signal sources

As proper application of NU sampling leads to elimination of aliasing, this specific approach to signal sampling can be used to enlarge the frequency range where information carried by high frequency analog sensor signals can be represented by digital data (for example, in cases of signal demodulations). A structure shown in Figure 3.1 (a) can be used for data acquisition directly from high frequency signal sources if operation of the used ADCs is based on quantizing signal sample values taken from the input signal at time instants dictated by a NU sampling point process. In such a case the usage of the additive sampling point process is usually preferable. The upper frequency of the signal spectrum sometimes can exceed the mean sampling rate several times. However the data obtained under these conditions then must be treated with the specifics of NU sampling taken into account [12, 13, 23].

3.4.2 Increasing the quantity of input channels

The structure of the DAQ system used for data acquisition from a multitude of sensors is based on multiplexing of analog signals and it is illustrated in Figure 3.1 (b). The difference between the traditional structures of this type (given in Figure 2.1) and this one is in operation of the multiplexer. Whenever it connects inputs to the ADC periodically, the number of inputs is limited by the achievable multiplexer switching rate as the sampling rate of each input then is *n* times lower, where *n* is the number of inputs (see Chapter 2.4). Replacing the periodic multiplexer switching by randomized allows using of the total bandwidth of channels more efficiently. Therefore that makes it possible to increase the number of inputs several times for specific class of signals [14]. Of course, the obtainable increasing of this input number depends on specific conditions.

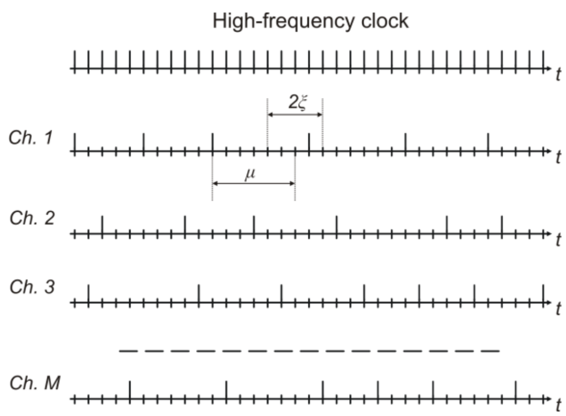

Figure 3.4 Particular implementation of simultaneous multi-channel data acquisition from M sources.

Note that the variables τ_k in the equation defining the additive NU sampling procedure in this case are digital and pseudo-random. The smallest digit of these pseudo-random time intervals τ_k is equal to the period Δt of the high frequency clock used for controlling the data acquisition process. This parameter also defines the upper frequency limit for the data acquisition bandwidth B_u. Obviously, according to the Nyquist criterion, $B_u = 1/2\Delta t$. The mean value of the time intervals τ_k between acquiring data from a particular source is equal to μ and they are distributed in the interval $\mu \pm \xi_k \Delta t$, where ξ_k are pseudo-random numbers uniformly distributed in a specified interval (in the case of the considered example, this interval is equal to [0, 2]).

3.4.3 Data acquisition at object testing

Exploiting NU sampling techniques and gaining advantages on that basis is a considerably less complicated task under conditions typical for the cases where data are acquired from some biomedical or industrial objects being tested. Then the information that has to be obtained is related to the characteristics and properties of the object and the signals taken off the respective object during the tests carry it. These signals reflect reaction of the object on the used some specific excitation signals. Diagram, shown in Figure 3.5, illustrates this situation. The fact that data acquisition then is performed under conditions where the test signal characteristics, including its spectrum, are given is very useful. Taking this information into account makes it possible to reduce significantly the complexity of the following data processing process. Indeed, to take out the errors due to the CI discussed in Section 3.3, usually data processing has to be based on calculations of CI coefficients, composing of the matrix (3.9), inverting it, obtaining the elements α_{ij} of the inverted matrix inv(C) and then estimating the Fourier coefficients. In the cases of data acquisition at object testing the situation is specific. As the spectra of the test signals then are given, the frequencies of the output signals are known whenever the objects are linear. The specific NU sampling point streams used at data acquisition are also given. Using of this significant a priori information leads to substantial simplification of the algorithms to be used at reconstruction of the waveforms or their parameters. All cross-interference coefficients then can be pre-calculated, matrix C also can be composed and inverted so that all elements α_{ij} of the inverted matrix inv(C) also could be pre-calculated. Therefore the Fourier coefficients in this case can be calculated by directly using the equation system (3.10). That dramatically simplifies and speeds-up the involved calculations.

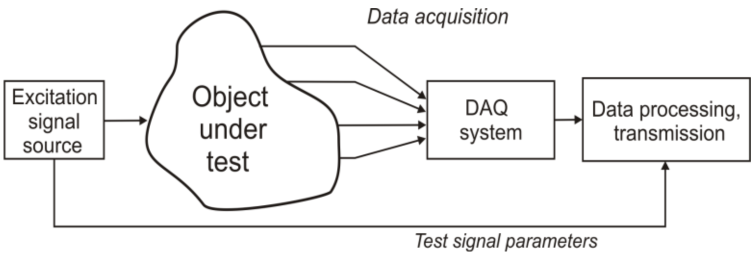

Figure 3.5 Diagram illustrating the conditions for data acquisition at linear object testing.

That leads to the conclusion that gaining practically valuable benefits from using the NU sampling approach is much easier for applications related to data acquisition at linear object testing. Using of this approach for data acquisition in the specific case of bioimpedance signal analysis in a wide frequency range of the test signals (up to a few GHz) is described in [51].

3.4.4 Fault tolerant data acquisition

Suppose data are acquired under conditions where the spectra of the involved processes are restricted at relatively low frequencies. Then application of NU sampling is not needed and data might and should be acquired at periodically repeating time instants. Attention is drawn to the possibility of improving the performance of the data acquisition system on the basis of NU sampling even under these conditions if it is needed to protect this system against unpredictable explosive noise bursts. Then the concept of NU sampling and specific data processing typical for NU sampling still proves to be quite useful.

Time diagrams shown in Figure 3.6 illustrate the data acquisition process under normal conditions in Figure 3.6 (a) and under the impact of noise bursts in Figure 3.6(b).

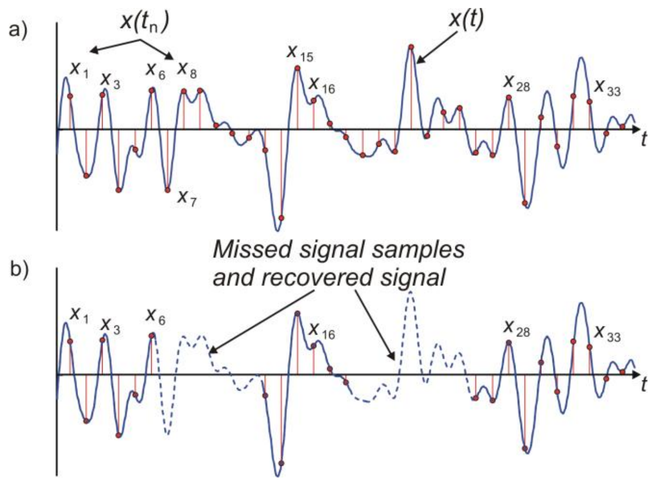

Figure 3.6 Impact of noise bursts on signals: (a) periodically sampled continuous signal, (b) the same signal with bursts of lost data and the recovered parts of faulted signal (recovery performed using CI method discussed above).

Data acquisition system protection against unpredictable explosive noise bursts also is a subject falling within the interest area of DASP, because the signals under impact of noise bursts become NU in a specific way. It means that sometimes DAQ systems should be ready and prepared to such accidents that might happen. In other words, their fault tolerance sometimes has to be improved. And the concept of NU data representation proves to be useful for that. The idea of improving fault tolerance on this basis is simple. The essence of it is as follows: to improve fault tolerance on the basis of the NU sampling concept, the data should be acquired periodically as usual and facilities usually used for processing of nonuniformly acquired data should be added to the system and used for data reconstruction [12, 13, 24, 50]. This means that under normal data acquisition conditions redundant equipment would be used. The role of this equipment would be to recover the data lost under impact of the noise bursts.

3.4.5 Asymmetric data compression/reconstruction

Essential are the advantages related to data compression that are obtainable if proper NU sampling procedures are used for DAQ. To compare the conditions for data compression in the cases of classical DAQ and non-traditional approach to fulfilling this function, consider the diagrams given in Figure 3.7.

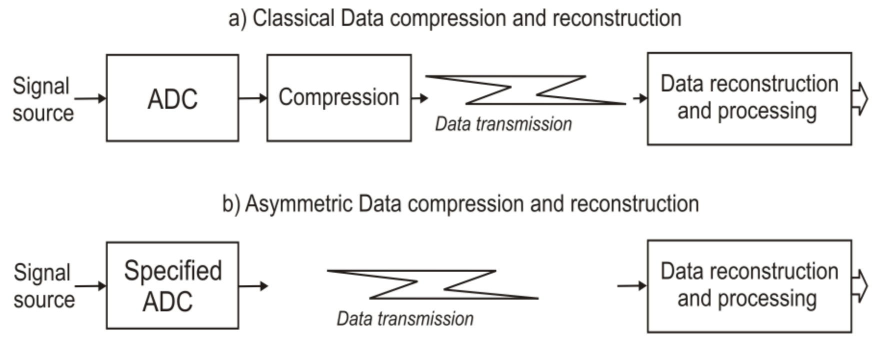

Figure 3.7 Standard data compression/reconstruction scheme (a) and the structure (b) used for data compression/reconstruction in the case where the compression is based on properties of NU sampling.

Standard data compression/reconstruction schemes look like the structure given in Figure 3.7 (a). This diagram reflects the fact that in this case, to compress and decompress the data, they are processed twice. Naturally that requires using of computing resources twice and that takes time. Using of the NU sampling procedures makes it possible to reduce the volume of data representing the respective input sensor signals simply by taking out some quantity of the signal sample values or perform other simple operation. It means that in this case no calculations are made at data compression. Then the structure used for data compression/reconstruction looks like the one shown in Figure 3.7 (b). The computational burden related to reconstruction of the compressed data then is totally placed on the data recovery side of the system. This data acquisition paradigm seems to be with high application potential as it is well suited for significant reducing of the acquired data massive as well as the data compressing costs in terms of equipment volume, weight and power consumption. The basic advantage is that this type of complexity-reduced data acquisition and compression is fast [22]. Note that compressive sensing described in subsection 2.6.3 also belongs to this asymmetric data compression/reconstruction paradigm.

Specifics of asymmetric data compression/reconstruction are considered in some detail on the example of 2D data acquisition given in the following Section 3.5. Image data acquisition, compression and reconstruction are discussed there.

3.5 Asymmetric 2D image data acquisition/reconstruction

3.5.1 Asymmetric 2D image data compression

The considered method for asymmetric data acquisition/reconstruction can be used in a wide application area, including 2D data compression and reconstruction [10]. Therefore this method can be exploited for image encoding, transmission (or storage) and reconstruction. Actually this task is quite complicated. It is considered in this Section and a standard test image, shown in Figure 3.10 (a), is used for that. This standard test image I can be defined by its $M \times N$ matrix of pixels or elements as follows:

$$I = \begin{bmatrix} e_{11} & e_{12} & e_{13} & e_{14} & e_{15} & e_{16} & \dots & e_{1N} \\ e_{21} & e_{22} & e_{23} & e_{24} & e_{25} & e_{26} & \dots & e_{2N} \\ e_{31} & e_{32} & e_{33} & e_{34} & e_{35} & e_{36} & \dots & e_{3N} \\ e_{41} & e_{42} & e_{43} & e_{44} & e_{45} & e_{46} & \dots & e_{4N} \\ \dots & \dots & \dots & \dots & \dots & \dots & \dots & \dots \\ e_{M1} & e_{M2} & e_{M3} & e_{M4} & e_{M5} & e_{M6} & \dots & e_{MN} \end{bmatrix} \tag{3.11}$$

According to the considered method, to compress the original 2D data, many of pixels have to be replaced by zeroes in accordance to the basics of NU sampling. The question is how to do that in a way that would make the task of the compressed image reconstruction easier. Various approaches have been considered and tested. The best of so far found approaches is based on design and usage of a mask containing logic 1 and 0. An example of it is given as matrix (3.12) and it is shown also in Figure 3.9.

Full cycle of original image compression and reconstruction is organized in accordance to the flowchart shown in Figure 3.8. Note that this particular signal/image compression procedure differs from the popular Compressive Sensing approach.

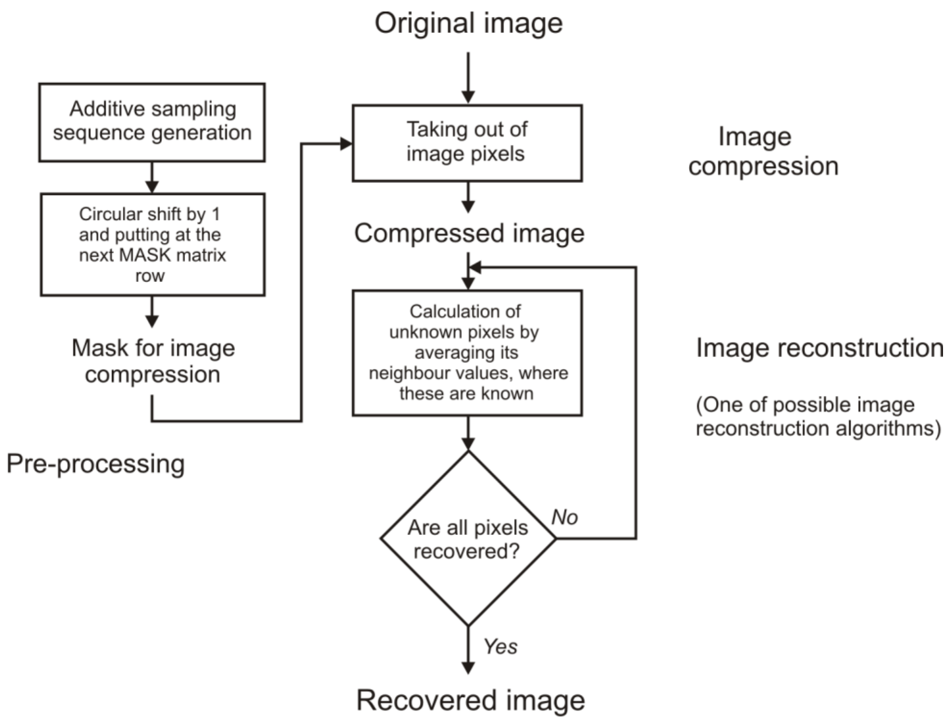

Figure 3.8 Flowchart of asymmetric image acquisition/reconstruction.

An example of the compression matrix H or mask, used for the considered asymmetric data acquisition, is given as:

$$H = \begin{bmatrix} 0\,1\,0\,0\,0\,1\,0\,0\,1\,0\,0\,1\,0\,0 \ldots 0 \\ 0\,0\,1\,0\,0\,0\,1\,0\,0\,1\,0\,0\,1\,0 \ldots 0 \\ 0\,0\,0\,1\,0\,0\,0\,1\,0\,0\,1\,0\,0\,1 \ldots 1 \\ 1\,0\,0\,0\,1\,0\,0\,0\,1\,0\,0\,1\,0\,0 \ldots 0 \\ 0\,1\,0\,0\,0\,1\,0\,0\,0\,1\,0\,0\,1\,0 \ldots 0 \\ \ldots\ \ldots\ \ldots\ \ldots\ \ldots\ \ldots\ \ldots\ \ldots \\ 0\,1\,0\,0\,1\,0\,0\,0\,1\,0\,0\,0\,1\,0 \ldots 0 \end{bmatrix} \tag{3.12}$$

To generate this mask, taking out of pixels is done in a specific way by using additive sampling sequence given in Figure 3.9 (b) and generated according to formula (3.3). The mean distance μ of two neighbouring pixels left in the image is equal to 5 and width of the uniform distribution of pseudo-random numbers ξ is equal to 3. The same sampling sequence is used also at the next image rows. They are only circularly shifted by one pixel each time to the right. The mask matrix needed for implementation of image compression in such a way has been generated by using the following MATLAB M-language code:

```
rand('state',1232);
h=1;
tmp=zeros(1,512);
while h<=512; % additive sampling flow
    tmp(h)=1;
    % xi random variable
    xi=round(2.495*(rand-.5));
    tau=5+xi;
```

```
    h=h+tau;
end;
maska=zeros(512,512); % MASK generation
for r=1:512;
    maska(r,:)=circshift(tmp,[0 r]);
end;
```

The mask and the used additive sampling point process can be seen in Figure 3.9.

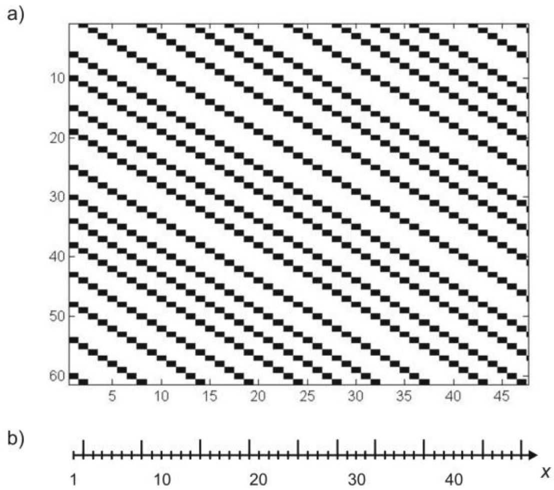

Figure 3.9 Image mask (a) showing the part of image pixels that will be taken out (in white colour) and the pixels that will remain after image compression (black colour); (b) the respective additive sampling point process used for generation of the mask.

The compressed image is obtained in a very simple way, just by using logic or scalar multiplication of generated mask matrix with the image matrix:

$$I_c = I \times H = \begin{bmatrix} 0\ e_{12}\ 0\ 0\ 0\ e_{16}\ 0\ 0\ e_{19} \ldots\ e_{1N} \\ 0\ 0\ e_{23}\ 0\ 0\ 0\ e_{27}\ 0\ 0 \ldots\ e_{2N} \\ 0\ 0\ 0\ e_{34}\ 0\ 0\ 0\ e_{38}\ 0 \ldots\ e_{3N} \\ e_{41}\ 0\ 0\ 0\ e_{45}\ 0\ 0\ 0\ e_{49} \ldots\ e_{4N} \\ \ldots\ \ldots\ \ldots\ \ldots\ \ldots\ \ldots\ \ldots \\ 0\ e_{M2}\ 0\ 0\ e_{M5}\ 0\ 0\ 0\ e_{M9} \ldots\ e_{MN} \end{bmatrix} \tag{3.13}$$

As can be seen, pixel taking out in a row is organized so that the remaining pixels are arranged in accordance to a realization of an additive sampling point process used for generation of the mask. Then the mask itself is formed by stacking this type of pixel rows that are shifted by one step horizontally per each vertical step, as it is shown in Figure 3.9 (a).

The compressed image is obtained in this way. Apparently image compression performed in such a way is a quite inexpensive and technically effective operation. The complexity of this type of image compression is much lower than the complexity of the usually exploited rather complicated standard image compression algorithms. That apparently represents a significant advantage of the proposed and described 2D data compression algorithm.

3.5.2 Reconstruction of the compressed image

Two approaches to sparse image reconstruction were considered and studied. Both of them have a common first recovery stage. The result obtained after this stage is shown in Figure 3.10 (c). According to the suggested reconstruction method, part of all unknown image pixels can be calculated at this stage by processing its neighbour pixel values if these are known. In this particular sampling case, the maximum count of the known pixels in close proximity (considering 2D 4-pixel connectivity case) can be 2. These pixels can be approximately calculated averaging its neighbour pixel values:

$$\begin{aligned} \hat{e}_{mn,l} &= 0.5(e_{m-1,n} + e_{m,n+1}), \ \textit{for the left side estimates} \\ \hat{e}_{mn,r} &= 0.5(e_{m+1,n} + e_{m,n-1}), \ \textit{for the right side estimates} \end{aligned} \tag{3.14}$$

Where $m = 1, 2, 3 \ldots M$, $n = 1, 2, 3 \ldots N$. The matrix of the recovered image pixel values after the first reconstruction cycle is the following:

$$\hat{I}_{r1} = \begin{bmatrix} \hat{e}_{11} & e_{12} & \hat{e}_{13} & 0 & \hat{e}_{15} & e_{16} & \hat{e}_{17} & 0 & e_{19} & \ldots & e_{1N} \\ 0 & \hat{e}_{22} & e_{23} & \hat{e}_{24} & 0 & \hat{e}_{26} & e_{27} & \hat{e}_{28} & 0 & \ldots & e_{2N} \\ 0 & 0 & \hat{e}_{33} & e_{34} & \hat{e}_{35} & 0 & \hat{e}_{37} & e_{38} & \hat{e}_{39} & \ldots & e_{3N} \\ e_{41} & \hat{e}_{42} & 0 & \hat{e}_{44} & e_{45} & \hat{e}_{46} & 0 & \hat{e}_{48} & e_{49} & \ldots & e_{4N} \\ \ldots & \ldots & \ldots & \ldots & \ldots & \ldots & \ldots & \ldots & \ldots & \ldots & \ldots \\ \hat{e}_{M1} & e_{M2} & 0 & \hat{e}_{M4} & e_{M5} & 0 & 0 & \hat{e}_{M8} & e_{M9} & \ldots & e_{MN} \end{bmatrix} \tag{3.15}$$

At the next stages this process can be continued iteratively (finding unknown pixels, which have known neighbouring pixels and then calculating them).

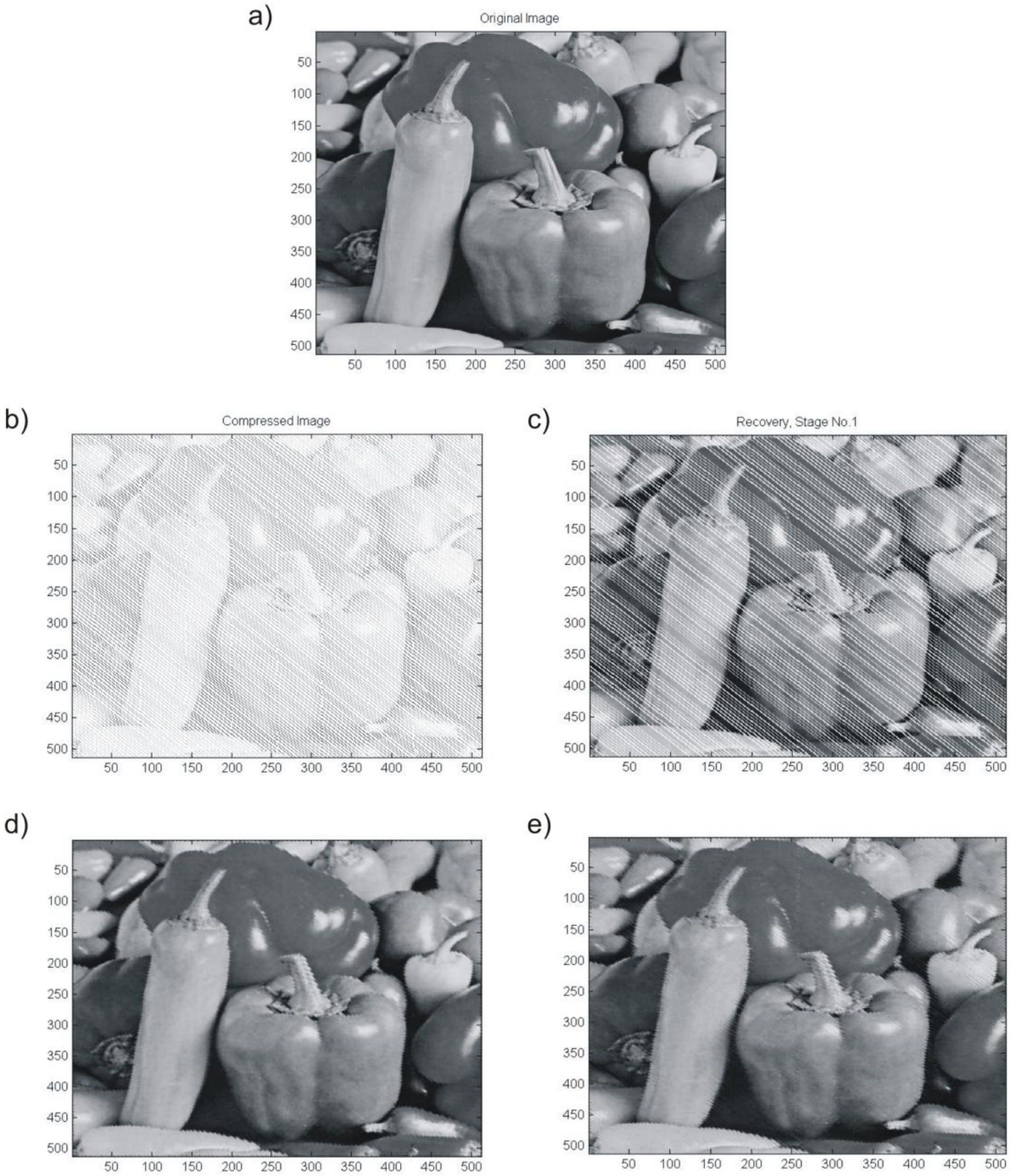

Figure 3.10 Example of asymmetric DAQ compression/reconstruction: (a) the original image by size 512×512 pixels; (b) sparse image after losing 80.27% of its pixels; (c) the image recovered at the first recovery stage; (d) image recovered by calculating unknown pixels from their neighbours and (e) recovered image obtained on the basis of SECOEX method.

Evidently there are exceptions for the estimates of the first and last rows:

$$\begin{aligned} \hat{e}_{1n,l} &= e_{1,n+1} \textit{ for the left side estimates} \\ \hat{e}_{Mn,r} &= e_{M,n-1} \textit{ for the right side estimates} \end{aligned} \qquad (3.16)$$

At the last recovery stages the unknown pixels are calculated from the four estimated pixels: $\tilde{e}_{36} = 0.25(\hat{e}_{26} + \hat{e}_{35} + \hat{e}_{37} + \hat{e}_{46})$.

The essence of the method is iteratively finding unknown pixels by averaging known values of the neighbouring pixels until all unknown pixels of the compressed image are replaced by the estimated pixel values. All the pixel values are estimated in this way after a few cycles and the full image is recovered. The following MATLAB code is used for fast performance of the first iteration at the first image recovery stage:

```
% X is compressed image before Recovery stage No.1
tmp=X; % temporary variable
for r=1:511;
    X(r,:)=tmp(r,:)+(circshift(tmp(r,:),[0 1])+tmp(r+1,:))/2;
end;
for r=2:512;
    X(r,:)=X(r,:)+(circshift(tmp(r,:),[0 -1])+tmp(r-1,:))/2;
end;
% Now X is result after Recovery stage No.1, iteration No.1
```

The average relative error, obtained in this particular case at image reconstruction performed in accordance to the described method, is equal to 0.1648 %. This parameter shows how close the recovered pixel values are to the respective true image values.

The second considered reconstruction method is based on application of SECOEX method. There exist also other options how to recover the compressed image and some other approximation algorithms are applicable. Application of this SECOEX method (it is well described in [22]) leads to the result shown in Figure 3.10 (e). In this particular case, the average relative error of image recovery is 0.3147 %, what actually is worse than the result obtained by the previous method. While this larger error can be explained by the particularities of the processed test image signals, image reconstruction based on the SECOEX method is much more complicated and more time consuming in comparison with the developed method.

This considered example of asymmetric data acquisition draws attention to the capabilities of this imaging method, it is not given for comparison of various image reconstruction algorithms. The asymmetric 2D data acquisition/reconstruction has significant advantages for application cases where computational power is limited and transmitting of the acquired data is expensive in terms of spent time, memory and equipment resources.

The discussed method for asymmetric 2D data acquisition/reconstruction so far has been considered as a tool for rational encoding and reconstruction of grey-scale images. The applicability of this method has been widened to cover also processing of colour images. Actually this widening of the functionality is straightforward and there are no serious problems in handling colour images on this basis. The illustration of the results obtained in this way are given in Appendix 7.

An experimental system has been developed and made for studies of the described image compression method. The photo of this system is given in Appendix 7 Figure A7.6. The device is developed on the basis of the modified digital video camera module *Omnivision OV7620* supplied with the hardware and software of the video module *CMUcam3*.

3.6 Wideband signal digitizing in enlarged dynamic range

As it is shown in the previous section, usage of NU sampling provides various advantages in the data acquisition. Obtaining of these advantages mostly is tied to the possibility of representing wideband sensor signals digitally if the data acquisition is based on NU sampling.

In many cases it is important to perform analog-digital conversions at high frequencies to support applications of digital electronics in various fields. However it is not so easy to achieve this capability, as it is shown in [34] in regard to the specific case of software-based radio. The frequency range, where the currently available 10 to 12 bit ADCs are applicable, often is not wide enough. On the other hand, the dynamic range of the ADCs, applicable for analog-digital conversions in GHz frequency range, is limited by the achievable quantization bit rate usually not exceeding 4 bits [26, 57]. These typical problems, arising at attempts to convert analog signals into their digital counterparts in a wide frequency range extending up to GHz frequencies, are studied and a specific approach to resolution of them is suggested in this Section.

This approach is based on application of special Digital Alias-free Signal Processing techniques [22]. They are well suited for processing of signals digitally at much higher frequencies than it can be done on the basis of the classical Digital Signal Processing. Although it is easier to use them for estimation of wideband signal parameters, including their spectra, it has been shown that it is also possible to digitize wideband signals and reconstruct their waveforms [24, 50]. However the so far developed methods for signal waveform reconstruction do not cover real-time applications, because the method for waveform reconstruction discussed in [12, 13, 24], specifically, is based on the direct and inverse Discrete Fourier transforms. The problem is that it takes time to execute these transforms. In other words, it is difficult to reconstruct data obtained in result of NU sampling in real time. A possible approach to resolution of this problem is studied further. Various options in resolution of the task of wideband signal digitizing and their waveform real time reconstruction in sufficiently wide dynamic range are considered in this Section.

3.6.1 Current trends in development of ADCs

Evidently both operations of sampling and quantizing are of vital importance for analog/digital conversions of signals so that improvements obtained at performance either one of these operations impact positively the whole digitizing process. Indeed, quality of data acquisition from sensors strongly depends on such characteristics of the analog-to-digital converters (ADCs) as the highest applicable sampling rate and the quantization bit rate. While the first of these parameters define the frequency range that can be covered by the respective DAC, the second parameter determines how large are the errors corrupting rounding-off of the sample values taken from the input signal at their sampling. These parameters are cross-related. At a given perfection level of ADC manufacturing technology, the achievable highest quantization bit rate depends on anis limited by the needed highest sampling rate.

Currently produced ADCs, capable of taking signal sample values at rates measured in Gsps, typically provides for 6 to 8 bit quantizing. For example, currently offered on the market ADCs MAX109 with 8-Bit resolution from MAXIM fall within this ADC category. In particular, input bandwidth and the highest sampling rate of 2.2 Gsps MAX109 provide for signal digitizing in a rather wide frequency range extending up to 1.1 GHz. There are also reported R&D results showing the feasibility of making low-power 4 bit 2.5 Gsps ADC [57] and covering even a wider signal frequency range by 4 bit ADCs [26].

Thus there are ADCs that can operate in a wide frequency range. The problem is that their relatively narrow dynamic range limits the application area of these devices. Resolution provided by 4 to 8 bit quantizing in many cases is not sufficiently high. In addition, there are other disadvantages related to such low bit-rate ADCs, specifically, significant unpredictable errors due to spurious frequencies appearing in the spectra of the digital signals obtained in result of using this type of ADCs that are characterized by high power consumption.

3.6.2 Waveform recovery by digital filtering

To achieve the possibility of using 10 to 12 bit ADCs for wideband signal digitizing at frequencies exceeding the mean sampling rate, the pseudo-randomized version of this type of sampling is used. A typical realization of the used pseudo-randomized additive sampling point sequences is shown in Figure 3.11.

Bandwidth of the signals $x(t)$ is limited, the upper frequency f_u of the signal spectrum does not exceed the frequency limit f_{lim}, inequality $f_u<f_{lim}$ is satisfied. NU sampling is carried out according to the model of pseudo-randomized additive sampling [22]. The basic parameters characterizing this additive pseudo-randomized sampling scheme is the period T_c of the high frequency clock used for generation of the sampling point stream defining the sampling instants; the mean sampling rate 1/μ, where μ is the mean value of the sampling intervals equal to nT_c, $n=1, 2, 3,\ldots$.Therefore $\mu = nT_c$ and $f_{\lim} = \frac{1}{2T_c}$. Problems met at reconstruction of the original signal waveforms, under the conditions that the upper frequency in the spectra of input signals might exceed the mean sampling rate but not the indicated frequency limit defined by the clock frequency, are studied and approaches to resolution of them are looked for.

Figure 3.11 illustrates filtering of signal sample value sequences obtained in result of pseudo-randomized sampling process under these conditions. A realization of an input signal sample value sequence x_k is given in the upper part of this diagram. All of the sample values are placed on the time grid dictated by the used clock frequency. As can be seen, the intervals between these sample values are not constant, they are pseudo-random. Each of these sample values are multiplied by the respective filter coefficient and at each filtering cycle, at calculation of an output signal value at a given time instant.

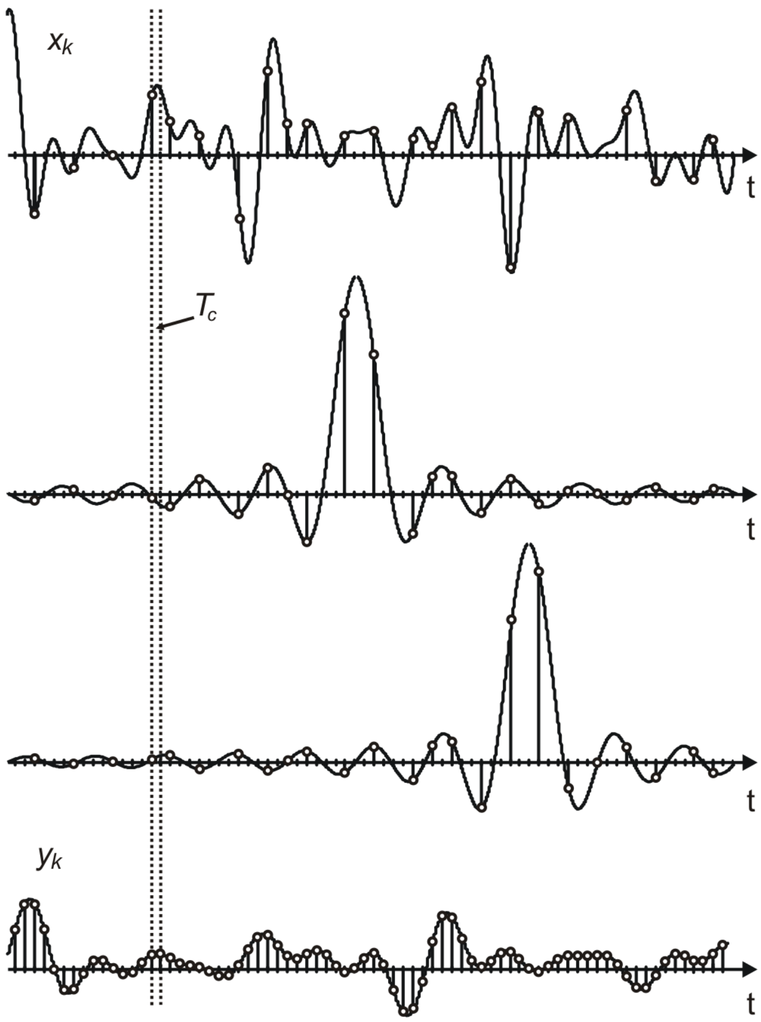

Figure 3.11 Conditions for filtering signal sample value sequences obtained in result of pseudo-randomized additive sampling process.

Note that the filter coefficients in fact are sample values of the filter impulse response. This function is step-by-step shifted at filtering and the step size is equal to the clock period. While the whole filter coefficient set is used for filtering, the number of them used at specific filtering cycles is reduced several times. It is shown that different coefficient sets are used for obtaining two output signal values.

The information carried by the NU signal sample value sequences, obtained in cases where the signals have been sampled according to this type of sampling point processes, provides not only for elimination of the aliases but it could be also successfully used, under certain conditions, for obtaining accurate spectral estimates and recovered waveforms of a wide class of signals. That has been confirmed experimentally [22, 24]. As it has been demonstrated by using the iterative approach to signal processing based on direct and inverse DFT, not applicable for analog-digital conversions in real-time, a different approach to this task has to be found. Using iterative special digital filtering for that was considered.

Consider using a low-pass digital filter for reconstruction of a signal from the sample values of it obtained in result of the described pseudo-randomized sampling. The calculation of the filter coefficients is based on a sampling model, according to which the signal is sampled periodically at the clock frequency. Relatively many signal samples are pseudo-randomly taken out as shown in Figure 3.11. The remaining sample values then are to be filtered. They are placed on the time axis nonuniformly according to the additive sampling point process discussed. Filtering is iterative. Structure of the electronic system, used for reconstruction of a signal waveform from the sample values, obtained in result of the described pseudo-randomized sampling, is shown in Figure 3.12.

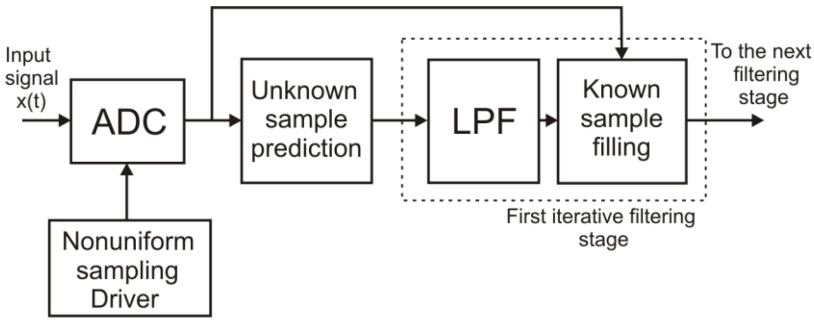

Figure 3.12 Structure of the electronic systems used for iterative reconstruction of signal waveforms, when signal is sampled according to NU sampling Driver.

Digitizing of the input signals is performed by using a 12 bit ADC. At the first stage of it the missing signal sample values are replaced by some values predicted in various ways. The results are given in Figure 3.13, where the empty places are filled either by zeroes (version1), by adding to each given sample values copies of it, placed on both sides of the known values (version 2) or by averaging each pair of the given sample values and using the result for filling the empty places, remaining after applying the procedure 2 (version 3). The outputs of this iterative filtering process are used, at all filtering stages, only for filling the empty places with sample values recovered with iteratively improved precision.

Examples of the obtained results are given in Figure 3.13. While signal waveforms are reconstructed in this way, the precision obtainable at sufficiently low mean sampling frequencies is not acceptable. The basic reason why waveform reconstruction with high enough precision was not achieved is related to behavior of the involved iterative filtering process. It does not tend to the zero error value. Some systematic error remains. It varies under variable sampling conditions but, in general, this error is too large.

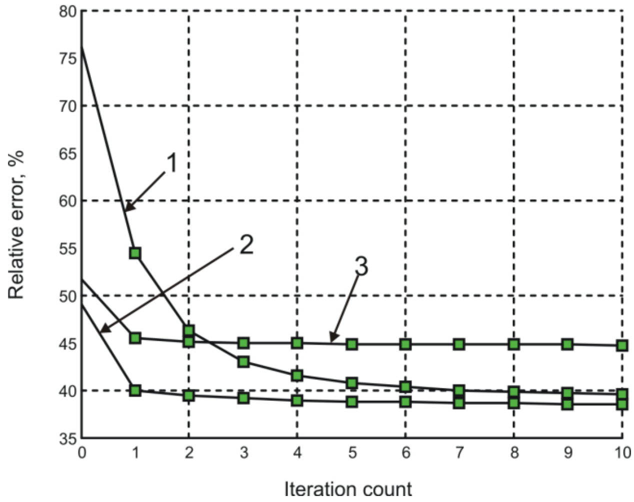

Figure 3.13 Reduction of signal waveform reconstruction errors by iterative filtering.

To achieve improved results, the option of using both high bit rate ADC and high sampling rate ADC in parallel was considered. The results obtained then indeed are much better. Discussion of this approach follows.

3.6.3 Combining precise sampling with low-bit very fast sampling in parallel

Improving previous signal sampling/reconstruction scheme shown in Figure 3.12 the sampling operation can be organized in a different way adding to the precise ADC another one, which has to be very fast (therefore with relatively low-bit resolution according to the current development trends of ADCs). This is illustrated in Figure 3.14. Now the empty places of discrete signal are not necessary to predict and it is suggested to these unknown signal samples measure with fast low-bit resolution ADC.

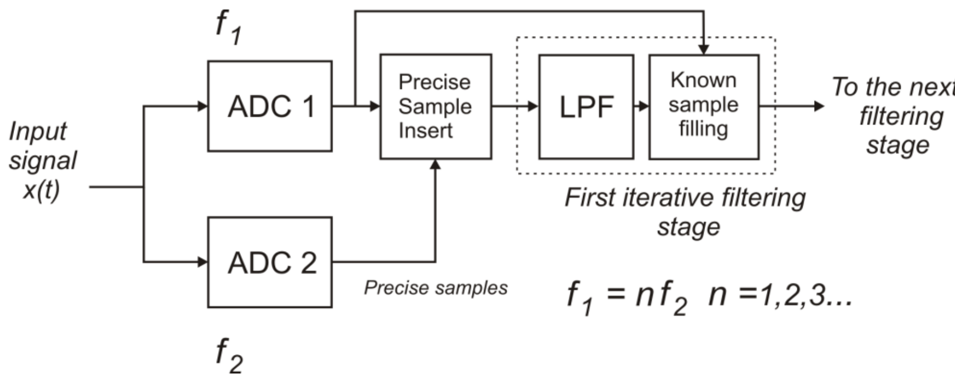

Figure 3.14 Structure of the electronic systems used for iterative reconstruction of signal waveforms, when signal is sampled using two ACDs in parallel.

Suppose the iterative filtering procedure is repeated when results of 4 bit fast periodic sampling are used for filling the spaces remaining empty after the precise signal sample values have been taken at time instants according to the described additive random sampling. Then the conditions for waveform reconstruction are more favourable and the obtained results also are significantly improved. They are displayed in Figure 3.15. As can be seen, only a few iterations have to be made to get the results, obtainable under the given conditions. While these results are relatively good, the waveform reconstruction error is not suppressed to a level that would be achievable if the same signal would be digitized by a hypothetical 12 bit ADC that would be capable of taking signal sample values at the clock frequency. To improve the waveform reconstruction, using of yet another one of the randomized procedures, namely, randomized quantizing is suggested.

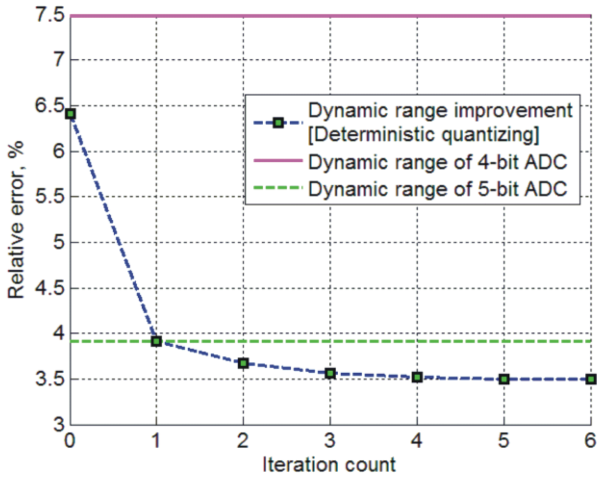

Figure 3.15 Results of waveform reconstruction when precise undersampling and low-bit fast periodic sampling procedures are used in parallel.

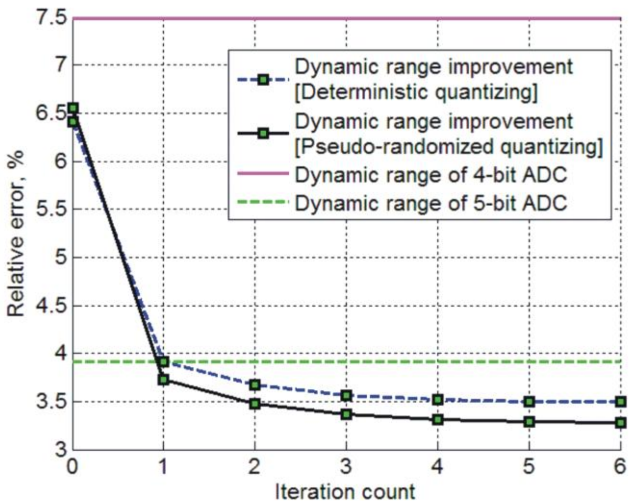

Figure 3.16 Waveform reconstruction precision improvement due to pseudo-random quantizing of the 4 bit signal sample value sequences.

Introduction of pseudo-randomized quantizing of the sample values (the pseudo-randomized signal quantizing is described in the next Chapter), obtained in result of considered fast 4 bit periodic sampling, is considered. That is aimed to increase the achievable waveform reconstruction quality even more.

The obtained results are shown in Figure 3.16.

The precision improvement, achieved in this way, is evident. While it seems to be relatively small, the actual quality improvement of the waveforms reconstructed in this way is more significant, as introduction of randomized filtering eliminates also the spurious frequencies in the spectra of the reconstructed signals usually distorting the spectra of 4 bit digital signals.

3.7 Conclusions

There are a number of advantages achievable at data acquisition using NU sampling. They are essential for various practical applications of data acquisition, especially at high frequencies. However there are also problems that have to be resolved. They are related to the specifics of digital data obtained in result of NU sampling. It is computationally burdensome to cope with the data nonuniformities and recalculate data as if they would have been obtained in result periodic sampling. Specifically, cross-interference between signal discrete components occurs whenever NU sampling is used. It is shown that this type of problems could be resolved and the knowledge accumulated in the area of DASP is useful for that.

Specific methods for wideband signal digitization in enlarged dynamic range is considered, where all signal samples are nonuniformly sampled and can be placed on periodic grid. Sampling is based on the combination of one precise ADC with another very fast ADC working in parallel. This is useful approach for precision improvement of wideband digital signals. The approach involves iterative Low-pass digital signal filtering, what provides computing efficiency in comparison with usage of methods based on direct and inverse DFTs. The obtained research results of data reconstruction carried out in the case of data acquisition using the procedure of NU sampling confirm the feasibility of real-time waveform reconstruction based on iterative filtering.

A number of benefits achievable for DAQ by using the concept of NU sampling are described to show the application potential of DASP methods for data acquisition. Considered approaches are beneficial especially for:

- DAQ based on pseudo-randomized multiplexing;
- Asymmetric data compression/reconstruction;
- Data acquisition from objects under tests;
- Improving fault tolerance of data acquisition.

NU sampling has high potential in the field of 2D data acquisition or image data acquisition. To show this, the example of asymmetric image data compression/reconstruction was considered. The standard test image has been taken and compressed taking out 80 % of its pixels according to the asymmetric DAQ concept. After that it was successfully reconstructed with 0.1648 % of average relative error. Thus it has been shown that application of NU sampling makes it possible to perform very simple image data compression. The achieved compression rate, in the case of the considered example, is equal to 5. It is shown that the developed method and algorithm can be used also for 2D data acquisition for colour image data compression and reconstruction with the same compression rate of 5.

4. Methods for Data Acquisition Exploiting Advantages of Pseudo-randomized Quantizing

Rational data acquisition to a large extent depends on signal digitizing and the method used for quantizing the sampled signal sample values directly impact performance of the used digitizers. Three basic quantizing models, specifically, deterministic, randomized and pseudo-randomized quantizing, are considered in this Chapter in the context of DAQ with the focus on the third method. DAQ based on pseudo-randomized quantizing has been investigated and it has been found that this method suits well the specific conditions for DAQ. On the other hand, while advantages of pseudo-randomized quantizing are significant, at first glance it seems that electronic implementation of this approach to quantizing is much more complicated than in the cases of deterministic and randomized quantizing. That probably is the reason why pseudo-randomized quantizing is seldom used. In search for effective data acquisition procedures, an approach to complexity-reduced DAQ based on this type of quantizing has been developed and investigated. The obtained results are described and discussed. It is shown that the design complications due to such quantizing, if it is implemented in a right way, actually are much less significant than might be expected. Impact of signal quantizing on DAQ resolution and DFT coefficient estimation precision is considered and the potential of pseudo-randomized quantizing for resolution improvement is shown.

Specifics of DAQ based on pseudo-randomized quantizing are considered in more detail in the particular case of bioimpedance measurement data acquisition and pre-processing.

4.1 Impact of signal quantizing on efficiency of data acquisition

4.1.1 Deterministic, randomized and pseudo-randomized quantizing

As it is described in [23], signal quantizing could be reduced to one of three quantizing methods. These methods are: deterministic quantizing DQ, randomized quantizing RQ (also known as dithering) and pseudo-randomized quantizing PRQ. No doubt that currently the method for deterministic signal quantizing is the most popular and the most used method in the world. Nevertheless there are also other quantizing methods and they have their particular advantages over the deterministic quantizing.

Suppose a continuous in time signal $x(t)$ is sampled at time instants t_k, $k=1, 2, 3, \dots$ and the obtained sequence of sample values $x(t_k) = x_k$ are quantized according to one of the considered above models. Let us denote the quantized signal values by $\hat{x}_k$. Then in the case of deterministic quantizing, we can write:

$$\hat{x}_k = n_k q\,, \tag{4.1}$$

where n_k is the number of threshold levels below the respective signal value x_k and q is quantization step.

The quantized signal value, obtained at randomized quantizing, is defined by the same expression:

$$\hat{x}_k = n_k q\,, \tag{4.2}$$

However there is significant difference between both cases of quantizing. While only the respective analog signal $x(t)$ is quantized in the case of traditional deterministic quantizing, in the case of the pseudo-randomized quantizing an auxiliary random noise $\xi(t)$ is generated in the range [$-0.5q,+0.5q$] and is added to the signal $x(t)$ before the quantization procedure. Therefore at randomized quantizing actually a mixture $x(t)+\xi(t)$ then is being quantized and the properties of the quantization noise to a large extent depend on $\xi(t)$.

The quantized signal value, obtained at pseudo-randomized quantizing, is defined as:

$$\hat{x}_k = (\xi_k - \frac{1}{2})q + n_k q\,, \tag{4.3}$$

where ξ_k is the value of the pseudo-random noise in interval [0 1] used at $t = t_k$ for pseudo-randomizing of the quantizing operation.

For better understanding signal waveforms of the deterministic quantizing and the pseudo-randomized quantizing are shown in Figure 4.1.

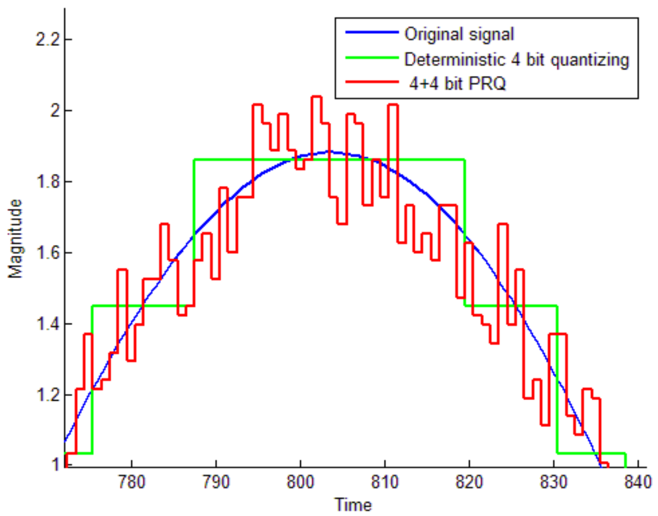

Figure 4.1 Waveforms of a signal (blue curve) quantized according to rough 4-bit deterministic quantizing (green line) and rough pseudo-randomly quantizing (red line).

It is shown in [23] that RQ and PRQ quantizing methods could be implemented on the bases of deterministic quantizing using ordinary analog-to-digital converters. In the case of randomized sampling the random values in the interval [*-0.5q,+0.5q*] should be added to continuous signal *x(t)* at the start of the conversion. Little more complicated it is in case of pseudo randomized quantizing. Implementing PRQ the added random values should be a priori known and later used for correction estimation simply concatenating additional bits to the output of analog-to-digital converter. This quantizing method makes sense only in cases of relatively rough ADCs usage.

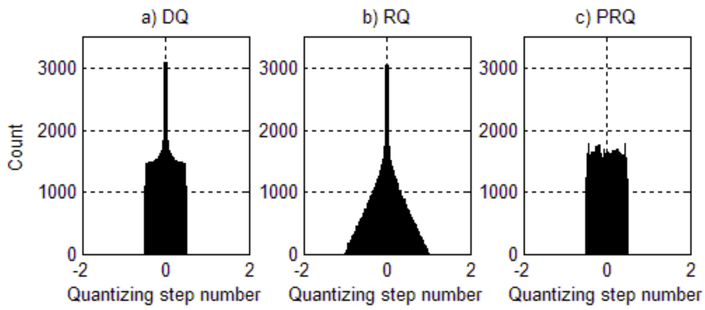

Figure 4.2 Empirical distributions of quantizing errors are shown in the cases of (a) deterministic quantizing, (b) randomized quantizing and (c) pseudo-randomized quantizing.

Typical empirical distributions of quantizing errors are shown in Figure 4.2. These distributions are obtained at quantizing a single component of a signal according to the considered DQ, RQ and PRQ methods. As it can be seen, errors in the case of randomized quantizing fall into diapason [*-q, +q*]. As it is twice larger than the error distribution intervals for DQ and PRQ, it could seem that randomized quantizing is the worst method of all. However that is not true. First, the probability of larger errors is small. Second, it is very easy to implement this quantizing method it has its applicability in enhancement of signal resolution, in particular, it effectively eliminates spurious frequencies.

As can be seen from these spectrograms, spurious frequencies, present in the noise of deterministic quantizing, are taken out by randomization of quantizing and the less powerful noise is obtained in the case of pseudo-randomized quantizing. While the specific properties of all these quantization models have been studied and are known for a long time (for example see [23]), the application value of randomized quantizing is still underestimated. That can be explained by the fact that application of multi-bit ADC strongly prevails and randomized quantizing is significantly better than deterministic in the cases of rough quantizing.

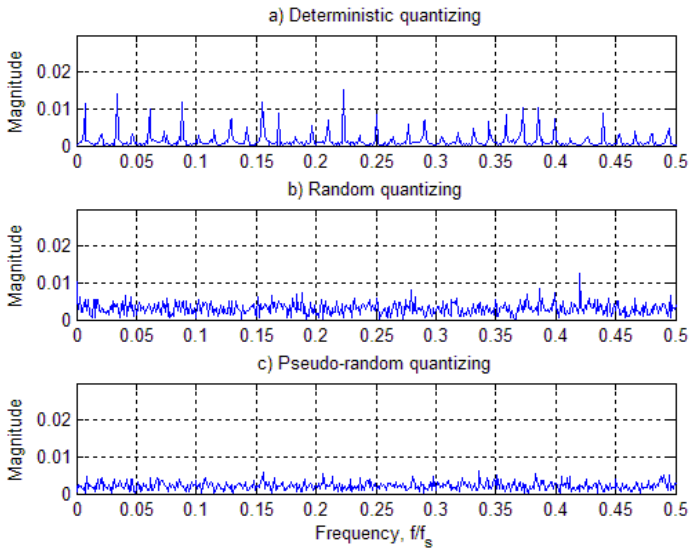

Figure 4.3 Typical spectrograms of the quantization noise obtained by quantizing the same signal in the cases of: (a) deterministic, (b) randomized and (c) pseudo-randomized quantizing.

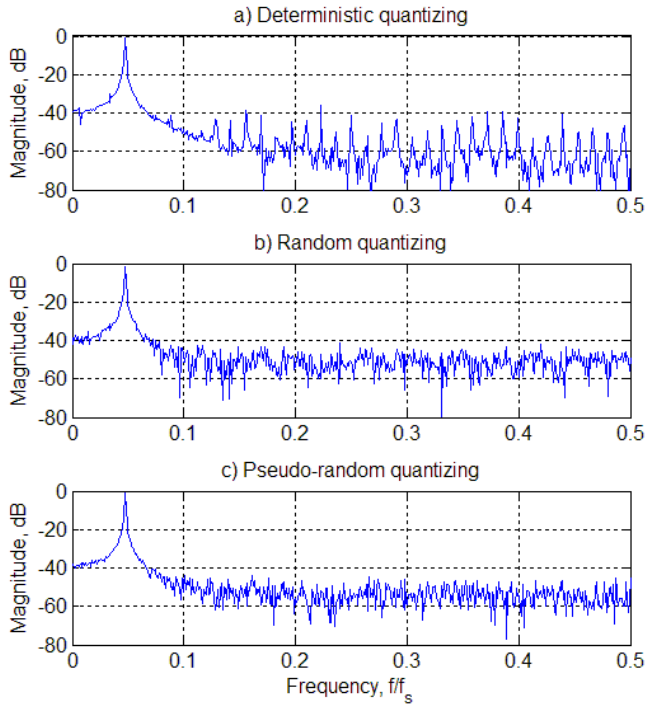

Figure 4.4 Typical spectrograms of quantized sine-wave function according to (a) deterministic quantizing DQ, (b) random quantizing RQ and (c) pseudo-randomized quantizing PRQ.

Typical spectrograms of rough 4 bit quantizing are illustrated in Figure 4.4. The single sine wave function is quantized according to DQ, RQ and PRQ methods to show the difference between them. As it can be seen the RQ and PRQ spectrograms does not contain spurious frequencies in comparison with deterministic quantizing. The difference between randomized and pseudo-randomized quantizing has smaller dynamic range which appears as higher background noise at spectrograms.

4.1.2 Method for elimination of spurious frequencies

It is well known that spurious frequencies distort spectra of digital signals obtained by using the traditional simple method for fixed-threshold deterministic quantizing. Then, to suppress the errors due to these spurious frequencies, either quantizing bit rate has to be increased or the quantization operation has to be randomized by using so-called dithering. The first option obviously leads to increased computational burden and additional power consumption. Therefore the second option seems to be and actually is better. Quantizing with dither, or randomized quantizing, indeed helps to remove the spurious frequencies. To implement this method, a random noise (dither) is generated and added to the analog signal at the input of ADC. That is usually done to eliminate spurious frequencies in the spectra of the signals quantized according to this method. And, indeed, the desired positive effect is achieved in this simple way. Although the quantization error is increased in this case from ±1/2 LSB (Least Significant Bit) ±1 LSB, the dynamic properties of the quantization noise are improved substantially. As dithering eliminates the spurious frequencies, the bit-rate of such quantizing could be to some extent reduced. In other words, quantizing with dither helps to reduce the number of bits in the numeric sample values. That slightly reduces the bit flow that has to be further processed and the power consumption is reduced accordingly.

More effective in this sense is so-called subtractive dithering. It is a more complicated method for pseudo-randomized quantizing that outperforms quantizing with dither as it provides for significant improvement of statistical characteristics of the quantization noise. In particular, it provides for unbiased estimation of signal parameters and for effective decorrelation of the quantization noise from the input signal. This noise is always white even at rough small bit-rate quantizing [22, 23]. However the price for this advantage is the increased number of bits $(\xi_k\text{-}1/2)q$ that has to be processed.

This type of quantizing usually is performed as shown in Figure 4.5 (a). A pseudo-random noise is generated, added to the input of ADC and then subtracted from its output. The quantized signal sample values in this case are given in expression (4.3). Errors of signal sample value quantizing in this case do not exceed $\pm\, q$ or, in other words, ± 1/2 LSB.

Consider definition (4.3) of the quantized sample values. The first part of it reflects the pseudo-random noise used and the second part gives results of quantizing. Both parts contribute to the number of bits that has to be processed.

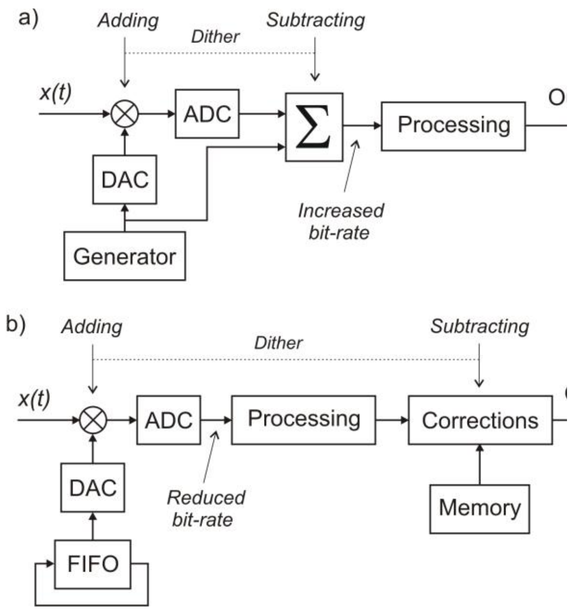

Figure 4.5 Illustration of two approaches to composition of system architectures in the case of systems performing functions of data acquisition and pre-processing. (a) structure of the system in the case where subtractive dithering is used in the traditional way; (b) structure of the system built as suggested.

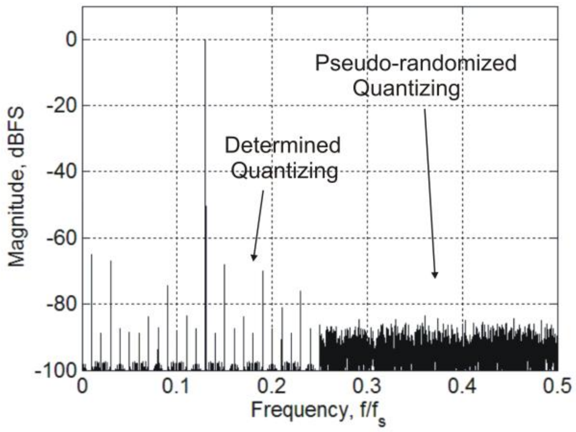

Figure 4.6 Spectrogram of a signal calculated partly for the signal quantized classically (lower frequencies) and partly for the signal quantized according to the pseudo-randomized quantization method.

It is suggested how to avoid processing of the increased number of bits $(\xi_k\text{-}1/2)q$ and how to improve the energy efficiency of designs based on this method of quantizing. Suppose that such a quantizer is included into a subsystem performing some linear transformations of the input signal, for example, this system fulfils the task of spectrum analysis. It is suggested to generate and add the generated pseudo-random noise $\{\xi_k\}$ to the input of ADC, as it is usually done at quantizing with dither, but not to subtract it from the output of the respective ADC. Then there are no additional bits that have to be processed. The signal with the dither added is quantized and only the bits n_kq of the second part of (4.3) are processed as shown in Figure

4.5(b). The first part of (4.3), obviously, does not depend on the input signal and can be pre-processed and the obtained results then can be used as corrections of the spectral estimates obtained without taking values $(\xi_k\text{-}1/2)q$ into account.

The spectrogram given in Figure 4.6 has been calculated under conditions typical for the classical deterministic quantizing (part of the spectrogram in the lower frequency region) and for quantizing performed according to the method for pseudo-randomized quantizing (second part of the spectrogram). As can be seen, the used subtractive dithering leads to significant reduction of the spurious frequencies. The point is that in this case this positive effect has been achieved as suggested by processing a 9 bit digital signal without increasing the bit rate for additional 5 bits as it would be if the subtracting dithering would be applied in the usual way. To achieve the same spurious frequency reduction level on the basis of the classical quantizing, 12 bit digital signal would have to be processed.

This method can be used in many cases for improving energy efficiency of systems in addition to other undertakings targeting achievement of the same goal. Implementation of it is simple enough and costs little.

4.2 Improving resolution of data acquisition

4.2.1 Improving ADC resolution

To increase ADC resolution, oversampling with filtering off the quantization noise in a large part of the covered frequency range can be used. This is a well-known technique that still draws attention and is suggested for applications [28]. As it is shown in this article, the quantization noise energy is distributed over the frequency range spreading from DC to half of the sampling frequency f_s. Increasing of the sampling rate (oversampling) makes it possible to reduce proportionally the quantization noise level within a fixed length frequency interval. Such oversampling and filtering increases the Signal-to-Noise Ratio (SNR) and an additional bit of resolution is obtained if the input signal is oversampled by a factor of four.

While this approach to improving resolution of ADC certainly works, in many cases application of it simply does not make sense. Indeed, why to use 8 bit ADC (for example, MAX109) for sampling a signal at 2.2 Gsps and then narrow the signal bandwidth 16 times from 1.1 GHz down to 68.75 MHz to reach 10 bit resolution if there are less expensive ADCs capable of covering this frequency range at even better resolution and much lower power consumption? Nevertheless the basic reasoning behind this approach to resolution improvement is sound and it, if modified, could be used under certain conditions for achieving DAC performance improvement without oversampling.

An essential problem complicating signal processing in the mentioned frequency range is aliasing. Signals with components at frequencies measured in hundreds of MHz have to be sampled at a very high sampling frequency f_s. Suppose that frequency downconverting for some reasons is not applicable. Then using of oversampling and narrowing the frequency range of the sampled signal by low-pass filtering to increase the resolution, under the given conditions, is not possible. The input signal under the stated conditions must be sampled at the frequency f_s. However the frequency interval occupied by separate input signal frequencies can be subdivided into a number of smaller intervals. Various approaches to resolution of this task might be used. For example, a bank of narrow-band filters could be used for that. Then a large part of the quantization noise energy is filtered off by each of the used filters and the filter output signals are obtained and processed with increased resolution. The effect of improving SNR, usually targeted by using oversampling and low-pass filtering, then is achieved in this way.

The disadvantage of this approach evidently is in the necessity of using some quantity of filters for processing the ADC output signal in real-time. However, in the case of bioimpedance data acquisition and demodulation, using of these filters is not necessary. The same resolution improvement effect then can be achieved simply by performing Discrete Fourier Transform at a relatively small number of excitation frequencies. The bandwidth Δf covered by each of these filters, at a given sampling frequency f_s, is inversely proportional to the number N of the signal sample values processed. Indeed, we can write that $\Delta f = \frac{1}{T} = \frac{1}{N\Delta t} = \frac{f_s}{N}$, where Δt is sampling interval. Therefore the quantization noise energy, remaining in the frequency range of a signal component in this DFT case, is reduced N times as $\frac{f_s}{\Delta f} = N$. In other words, the same number of additional bits of resolution, that can be gained by oversampling M times, can be obtained by processing $N=M$ sample values at DFT. And the desirable effect of increasing the resolution or decreasing the Fourier coefficient estimation errors in this case is achieved in a much simpler way.

However that is true only in the case where the quantization noise is white, does not depend on the input signal and is distributed uniformly in the range [$-0.5q,+0.5q$], where q is quantization step. Only multi-bit quantizing, carried out according to various quantizing models, more or less satisfy these requirements. Quantization noise of rough 4 or 6 bit deterministic and randomized quantizing, in general, does not meet them [23]. Consequently, gaining of additional bit resolution at DFT can be expected only in the case where quantizing is performed according to the pseudo-randomized quantizing model. The quantization noise characteristics then do not depend on the input signal even in the cases of extremely rough fast ADCs.

To widen the application area of these fast ADC, resolution of them has to be improved. In other words, the errors of signal sample value rounding-off or quantizing have to be somehow reduced. However the conventional deterministic quantizing, used in the cases of all of the referred to types of ADC, has significant drawbacks so that this method, in comparison with randomized and pseudo-randomised quantizing, is the less efficient one [23].

4.2.2 Precision of DFT estimates in DQ, RQ and PRQ cases

Discrete Fourier Transform or DFT also has significant role in bioimpedance signal demodulation. For multi-channel data acquisition the transform should be performed on several frequencies. Therefore in this section the impact of signal quantizing on DFT coefficient estimation precision is considered. The errors of DFT estimations are compared in the cases where signals are quantized deterministically, randomly and pseudo randomly. Obtained results are shown in Figure 4.7 where signal consists of single component.

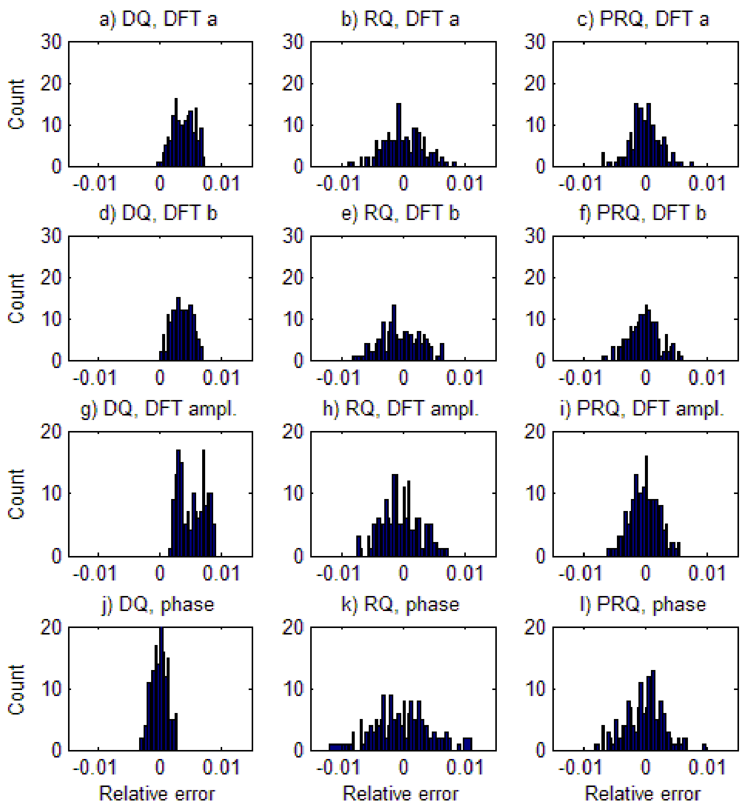

Figure 4.7 Empirical distributions of (a, b, c) DFT coefficient a estimates, (d, e, f) DFT coefficient b estimates, (g, h, i) DFT amplitude estimates and (j, k, l) DFT phase estimates are shown in cases where signal is quantized (a, d, g, j) deterministic quantizing DQ, (b, e, h, k) random quantizing RQ and (c, f, i, l) pseudo-randomized quantizing PRQ.

Histograms in Figure 4.7 are obtained under conditions where 512 points of signal are processed; the signal is quantized in full magnitude range with 4 bit rough ADC (but different quantizing method); the signal consists of one component with amplitude 1 and phase 1.0695 radians (which was arbitrary taken) on frequency 0.17 of sampling frequency.

Comparing all quantizing cases in Figure 4.7 is clearly shown that deterministic quantizing is the most accurate, but it has bias error which does not appear in cases of random and pseudo-random quantizing. The important fact what should be taken into account is that in cases of random and pseudo random quantizing the quantizing noise is very close to white. It means the signal dynamic range could be easily enlarged with low-pass filtering.

4.2.3 PRQ using reduced frequency additive pseudo-random values

Pseudo randomized quantizing usually is carried out so that a specific additive pseudo-random value is added to the input signal at quantizing each sample value. When the sample values to be quantized are obtained at a very high rate, there might be serious problems to generation the needed pseudo-random values as they have to be converted by a Digital/Analog Converter into analog form so that they could be added to the signal. The possibility of keeping these pseudo-random values constant for a number of quantization cycles is considered. Of course, it can cause some distortions and might reduce the quality of pseudo randomized quantizing. Nevertheless it could be allowed under specific conditions, which are evaluated in this section.

Empirical distributions of quantizing errors are shown in Figure 4.8. As it can be seen, the quantizing error distribution does not noticeably change from keeping the random increments fixed for 16 clock periods before taking the next random value. Illustrated is the case where 4 bits pseudo randomized quantizing is considered with 4 bit random values sequence added to the continuous signal *x(t)* (it could be written 4+4 bits PRQ quantizing). It means that values of the pseudo-random noise are changing at 16 times slower rate than the sampling rate used by the respective analog-to-digital converter. The distribution of the quantizing errors remains the same.

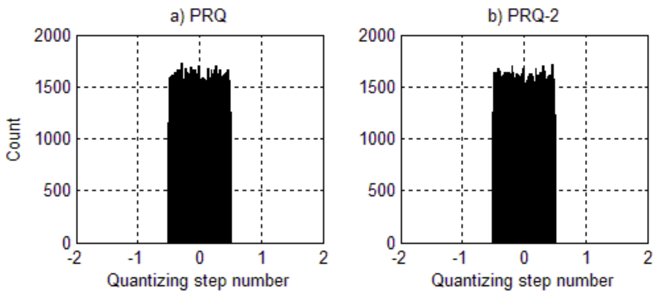

Figure 4.8 Empirical distributions of pseudo-randomized quantizing errors in cases where (a) ordinary PRQ is used and (b) modified PRQ is used.

Of course, the modified pseudo randomized quantizing with changed random increment affects the quality of further processing, because quantizing errors instead of pure white noise, which should be uniformly distributed over signal spectrum, becomes band limited. Also the necessary statistical properties of added random noise might be difficult to ensure.

Nevertheless in some cases incrementing of randomness is feasible and the processing quality of PRQ quantized signals does not suffer very much. The considered example of PRQ quantizing impact on processing quality is DFT coefficients estimation. Their error empirical distributions are shown in the next Figure.

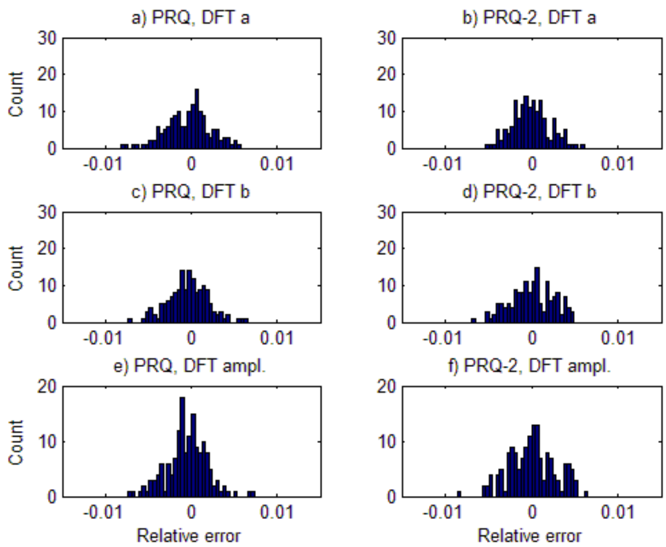

Figure 4.9 Comparison of DFT estimation error empirical distributions in the cases where (a, c, e) the random values is changed at every sampling event and (b, d, f) it is kept constant for 16 sampling intervals.

As it can be seen from Figure 4.9 diminishing of random values variability affects the DFT coefficients estimation precision. The histograms, which represent empirical distributions of DFT coefficient estimation errors, in the case of larger random increment are more inaccurate and their shapes become more blurred.

At first sight it is suggested to do not take random increment larger than 16, but it is case dependant and the detailed studies of the issue are necessary, including spectral analysis of DFT coefficients estimation errors etc. The spectral analysis would help to control appearance and expected energy of spurious frequencies etc. Also the number of processed signal samples is significant factor, which affects the choice of random increment value.

4.3 Particular case of bioimpedance data acquisition and processing

Using the DASP technology [22] for acquisition of data in a wide frequency range under the conditions typical for bioimpedance measurements has been already suggested and considered in [51]. As it is explained there, bioimpedance measurements are carried out to observe reaction of a biological object to some excitation current in a more or less wide frequency range [52]. Data for these measurements are acquired by digitizing signals picked up from electrodes placed on the object at various locations. The bioimpedance measurements are based on processing the data acquired from a number of such signal sources.

a)

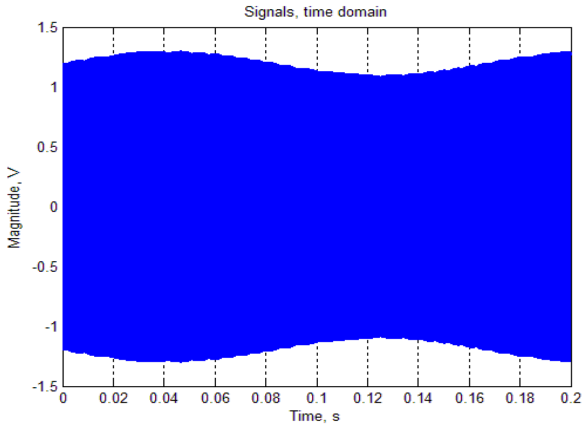

b) **Zoom**

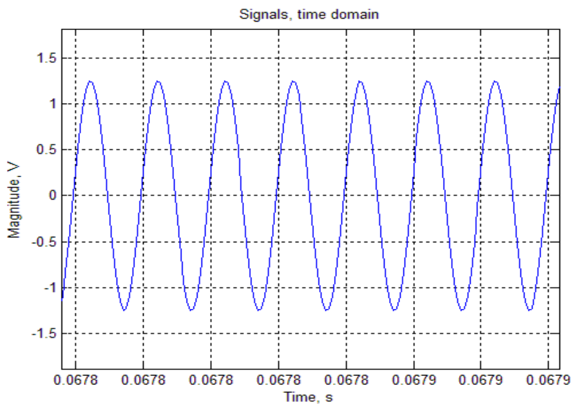

Figure 4.10 Typical signal in the data acquisition case of bioimpedance signal demodulation: (a) signal in the full scale and (b) zoomed signal.

The multitude of the picked up signals reflect the response of the object to the excitation process applied to the object being examined. The measurements have to be made in a way providing information characterizing this response in time and frequency domains. While parameters of the excitation current might vary from a case to case, typically it contains components at a number of frequencies. Consequently the bioimpedance measurements in many cases could be reduced to estimation of the signal spectra on specific pre-determined frequencies. The task of this spectrum analysis is made more difficult by the fact that the biological objects are dynamic. It means that the characteristics of these objects do change in time, the signals are modulated by these changes and that actually biomodulation of tissue impedance has to be analyzed in real time. In addition, the frequency range of interest is wide. While effective methods and techniques for bioimpedance measurements at frequencies up to several MHz have been developed and are used, there are problems when the spectrum analysis of the modulated bioimpedance signals has to be performed in the frequency range up to several hundreds of MHz or even up to several GHz. The involved data acquisition and processing tasks then become rather challenging. In particular, data have to be processed in real-time and with sufficiently high resolution.

Exploiting of DASP methods and techniques were considered in [51] for performing bioimpedance data acquisition and their real-time spectrum analysis with the emphasis on NU sampling. It is shown there how to reduce the required sampling rate and how to avoid cross-interference induced errors at bioimpedance signal demodulation and spectrum analysis in a wide frequency range. While the required performance improvement could be achieved in this way, the electronic systems implementing this approach are not so simple.

4.3.1 Processing of bioimpedance signals on the basis of complexity reduced DFT

As can be seen from (4.3), the pseudo-randomly quantized signal values contain significantly increased number of bits in comparison with deterministically or randomly quantized signals as the value of the pseudo-random noise ξ_k , used at quantizing, is added [22, 23]. Directly processing of the quantized signal (4.3) clearly leads to a complicated processing procedure. Fortunately, it is possible to avoid these complications. Suppose bioimpedance signal demodulation is based on DFT, on estimation of the Fourier coefficients. It is suggested to do that on the basis of the following equations:

$$\begin{aligned} \hat{a}_i &= \frac{2}{N}\sum_{k=1}^{N}\hat{x}_k \cos 2\pi f_i t_k = \frac{2q}{N}\sum_{k=1}^{N} n_k \cos 2\pi f_i t_k + \gamma_i^a \\ \hat{b}_i &= \frac{2}{N}\sum_{k=1}^{N}\hat{x}_k \sin 2\pi f_i t_k = \frac{2q}{N}\sum_{k=1}^{N} n_k \sin 2\pi f_i t_k + \gamma_i^b \end{aligned} \tag{4.4}$$

where γ_i^a and γ_i^b are corrections

$$\begin{aligned} \gamma_i^a &= \frac{2q}{N}\sum_{k=1}^{N}(\xi_k - \frac{1}{2})\cos 2\pi f_i t_k \\ \gamma_i^b &= \frac{2q}{N}\sum_{k=1}^{N}(\xi_k - \frac{1}{2})\sin 2\pi f_i t_k \end{aligned} \tag{4.5}$$

The point is that these corrections, taking into account impact of the specific sequence of the pseudo-random numbers used at quantizing, do not depend on the input signal. Therefore if a specific sequence of pseudo-random numbers is used at such quantizing repeatedly, these corrections remain constant, can be pre-calculated for all excitation frequencies and then they could be used according to equations (4.4). It means that the DFT complexity in the case of pseudo-randomized quantizing will be practically the same as in the cases of deterministic and randomized quantizing. Equal quantity of bits will have to be processed in all these cases.

Using the pseudo-randomized quantizing scheme would simply require taking into account these pre-calculated corrections at the Fourier coefficient estimation.

Comparison of the considered various approaches to quantizing from various points of view leads to the conclusion that pseudo-randomized quantizing often is preferable if the involved ADC is a low-bit device and quantizing is rough. In the case of the considered bioimpedance measurement application, using of fast low-bit ADCs exploiting pseudo-randomized quantizing could be especially attractive. Then there is marginal freedom in selection of the excitation frequencies and that makes it easier to gain from replacement of the *sin, cos* functions at DFT by rectangular functions assuming only the values ±1. Then the complexity of Fourier coefficient estimation can be significantly reduced. These estimates then can be obtained on the basis of the following equations which are modifications of (4.4) and (4.5):

$$\begin{aligned} \hat{a}_i &= \frac{Aq}{N}\sum_{k=1}^{N} n_k sign(\cos 2\pi f_i t_k) + \gamma_i^a \\ \hat{b}_i &= \frac{Aq}{N}\sum_{k=1}^{N} n_k sign(\sin 2\pi f_i t_k) + \gamma_i^b \end{aligned} \tag{4.6}$$

Where A is a coefficient taking into account the specifics of the approach. The needed corrections in this the case are calculated as

$$\begin{aligned} \gamma_i^a &= \frac{Aq}{N}\sum_{k=1}^{N} (\xi_k - \frac{1}{2}) sign(\cos 2\pi f_i t_k) \\ \gamma_i^b &= \frac{Aq}{N}\sum_{k=1}^{N} (\xi_k - \frac{1}{2}) sign(\sin 2\pi f_i t_k) \end{aligned} \tag{4.7}$$

The advantage of this approach to estimation of the Fourier coefficients is evident. Data can be processed in this case in a very simple and fast way. However the applicability of this approach is conditional. It can be used for estimations of the Fourier coefficients at frequency f_i only if the signal $\hat{x}_k$ does not contain components at frequencies (3, 5, 7,…) f_i. The required conditions usually can be provided for in the specific cases of acquiring and processing of data characterizing an object being tested by applying a specially generated test signal. If the object is linear and the indicated frequencies can be excluded from the test signal then the design complexity of the involved electronic system can be significantly reduced by using this approach.

4.3.2 Obtained results of the suggested method

Diagrams given in Figure 4.11 illustrate the precision obtainable at using the suggested methods for bioimpedance data acquisition and demodulation of the bioimpedance signals.

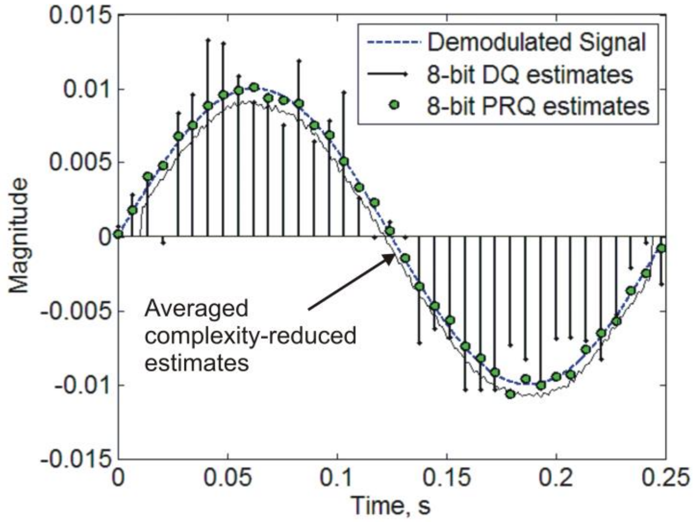

Figure 4.11 Estimates of the demodulated signal obtained by using deterministic quantizing (1) and pseudo-randomized quantizing (2). Averaged estimates based on the complexity-reduced approach using sign(sin) and sign(cos) functions are given as curve (3).

Note that the amplitude of the demodulated signal shown in Figure 4.11 is only 1% of a single carrier amplitude which is 1. There are 3 excitation frequencies with total magnitude 3. As can be seen, the estimates based on pseudo-randomised quantizing are significantly more precise than in the case of deterministic quantizing. Both types of the estimates have been obtained under equal other conditions.

Results obtained according to the suggested method (DFT in rectangular function basis) are achieved under easier conditions where demodulated signal values are taken with 10 times larger frequency in comparison with both other approaches. Also the additional filtering with 33 tap moving average filter is performed at the end of demodulation.

Results of comparing traditional DFT and DFT based on rectangular functions are shown in Figure 4.12. The quantizing is organized according to deterministic or pseudo random quantizing. These diagrams are obtained where test signal consists of one component on frequency 0.17 from the sampling frequency. At MATLAB simulations, 2000 signal samples were processed for calculation of each DFT estimate.

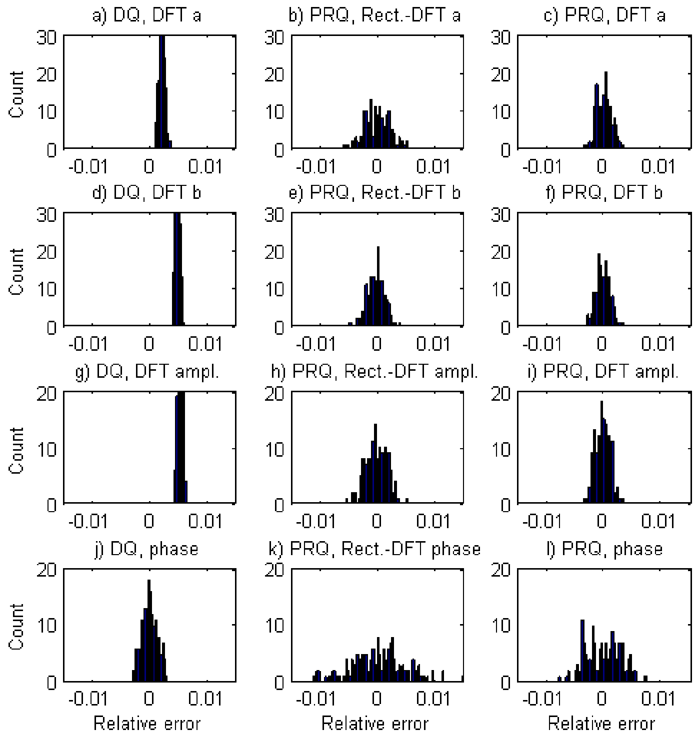

Figure 4.12 Comparison of traditional DFT and DFT based on rectangular functions in the case where a single harmonic is used at simulations as a signal. Histograms of estimation errors are shown in the cases where (a, d, g, j) deterministic quantizing is used, (b, c, e, f, h, i, k, l) the equivalent pseudo-randomized quantizing is used and (b, e, h, k) DFT based on rectangular functions is used, (a, c, d, f, g, i, j, l) traditional DFT is used.

As can be seen from Figure 4.12, in case of deterministic quantizing the DFT coefficients are estimated the most accurate, but due to its bias error, DQ does not provide sufficient precision. The best results provide traditional DFT together with pseudo randomized quantizing if phase histograms are not taken into account.

Histograms shown in Figure 4.13 are obtained under the same conditions as in the Figure 14 only in this case the test signal consists of two components on frequencies 0.17 and 0.225 from sampling frequency. Now the bias error, typical for deterministic quantizing, could not be clearly seen.

The accuracy of DFT estimates based on rectangular functions certainly is lower. The simple calculations reveal that in the case of bioimpedance signal demodulation where the signal carrier has amplitude 1 and the demodulated signal amplitude is 1% of it, particular relative errors of the demodulated signal amplitude could be 200% (see Figure 4.13 (h)). That of course is not acceptable. Therefore this approach to DFT based on using rectangular functions is not applicable for bioimpedance signal demodulation without additional signal processing carried out for improving this accuracy.

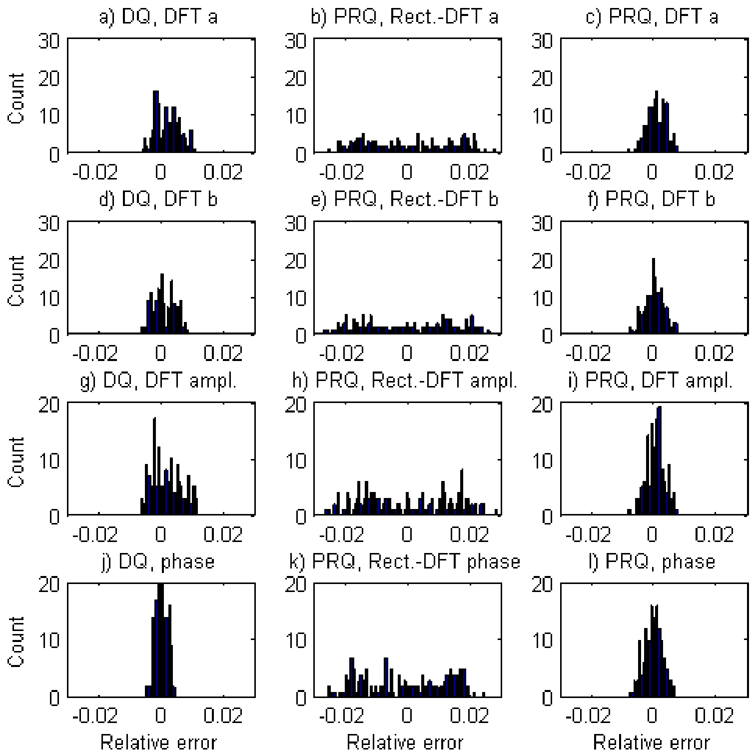

Figure 4.13 Comparison results of traditional DFT and DFT based on rectangular functions in the case where two harmonics are used at simulations as a signal. Histograms of estimation errors are shown in the cases where (a, d, g, j) deterministic quantizing is used, (b, c, e, f, h, i, k, l) the equivalent pseudo-randomized quantizing is used and (b, e, h, k) DFT based on rectangular functions is used, (a, c, d, f, g, i, j, l) traditional DFT is used.

4.3.3 Demodulated signal resolution improvement by filtering

After bioimpedance signal demodulation, the extra precision of processing could be obtained with ordinary digital filtering. For this purpose application of the moving average filter MAF is considered. If it is needed such filtering could be used iteratively. Also it is expected that using of other filter types, like low-pass filters LPF, would provide good results.

As with all signal resolution improvement methods, which are based on filtering, obtaining of enlarged number of signal sample values helps. The processed point count directly puts the limit on the achievable signal resolution improvements.

Figures in Table 4.1 illustrate comparison of signal quantization errors with and without filtering. As can be seen, the filtering in general reduces quantizing errors, no matter whether it is MAF or LPF filtering. Comparison of both filter applications, based on these results, is conditional. Moving average filtering efficiency depends on filter length, but not only. Results in Table 1 were obtained for LPF having cut-off frequency 0.15 of signal sampling frequency and the test signal bandwidth upper frequency does not exceed filter cut-off frequency. Finding optimal filter parameters was not attempted.

Table 4.1 Typical relative quantizing error readings.*

	Moving average filter MAF length	**3**	**5**	**7**	**9**
1	Deterministic 4 bit quantizing (without filtering)	0.1010	0.1010	0.1010	0.1010
2	Deterministic 12 bit quantizing (without filtering)	0.00037	0.00037	0.00037	0.00037
3	4+4 bit PRQ quantizing (without filtering)	0.0994	0.0993	0.1005	0.1004
4	4+4 bit PRQ quantizing, LPF	0.0431	0.0403	0.0426	0.0406
5	Deterministic 4 bit quantizing, LPF	0.0642	0.0642	0.0642	0.0642
6	4+4 bit PRQ quantizing, MAF	0.0399	0.0294	0.0274	0.0271

** The errors are statistical values and are not constants as it is given in table, because they are signal dependent.*

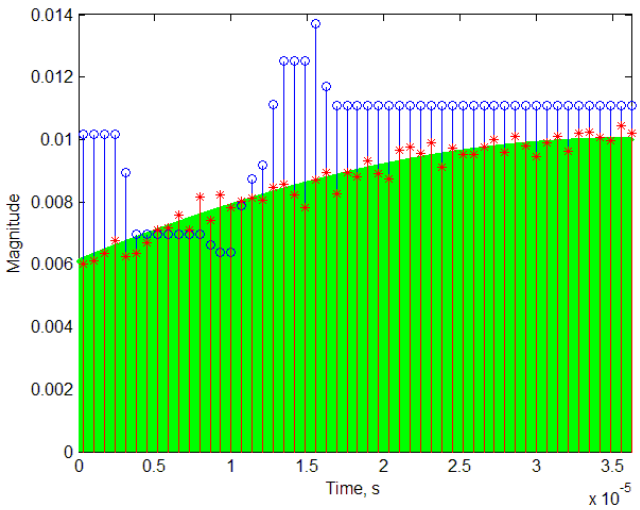

Figure 4.14 Demodulated signals are shown where the green background is the theoretical signal associated with the perfect demodulation, the blue discrete values are obtained in case of deterministic 8 bit quantizing and the red discrete values are obtained in case of 8+4 bit PRQ quantizing.

A fragment of DFT amplitude estimations is shown in Figure 4.14 as it is in bioimpedance signal demodulation. The modulated signal has 3 carriers on frequencies 0.13, 0.2, 0.33 of the sampling frequency 2.175 GHz with total amplitude 3. The demodulated signal does not exceed 1% of single carrier amplitude 1 and has upper frequency 4 KHz. The indicated results were obtained without additional demodulated signal filtering.

As it can be seen from Figure 4.14, PRQ quantizing provides better demodulated signal precision than the traditional deterministic quantizing.

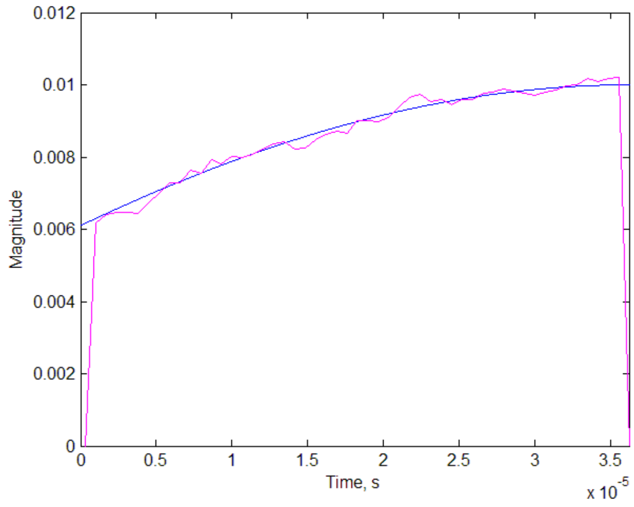

Figure 4.15 Demodulated signal is shown after filtering in comparison with theoretically perfect demodulation. The modulated signal is quantized according to PRQ method and moving average filter with length 3 is used.

Results in Figure 4.15 were obtained under the same condition as in Figure 4.14 with the difference that the demodulated signal is additionally filtered with 3 tap moving average filter. After this procedure the demodulation signal precision is achieved less than 2%. As it was shown, the demodulation signal quality could be improved with additional digital signal filtering.

4.3.4 Demodulation quality dependence on processed point count

The number of processed signal sample values plays an important role at bioimpedance signal demodulation based on DFT coefficient estimation. This issue is considered in this section.

Each point in Figure 4.16 was calculated by averaging 16 DFT estimates. Results are obtained after procedures: (a) carrier signal quantizing, (b) carrier demodulation and (c) demodulated signal filtering with moving averaging filters with core length 3.

Results illustrated in Figure 4.16 were obtained under the following MATLAB simulation parameters: sampling frequency Fs is 2.175 GHz; carrier signal frequencies are 290, 435, 725 MHz and 1.015GHz with amplitude 1 (for each carrier) and random phases; demodulated signal is quasi-stationary with amplitude 0.02; modulated signal is quantized according to 8 bit PRQ quantizing and after demodulation signal is filtered with 3 tap MAF.

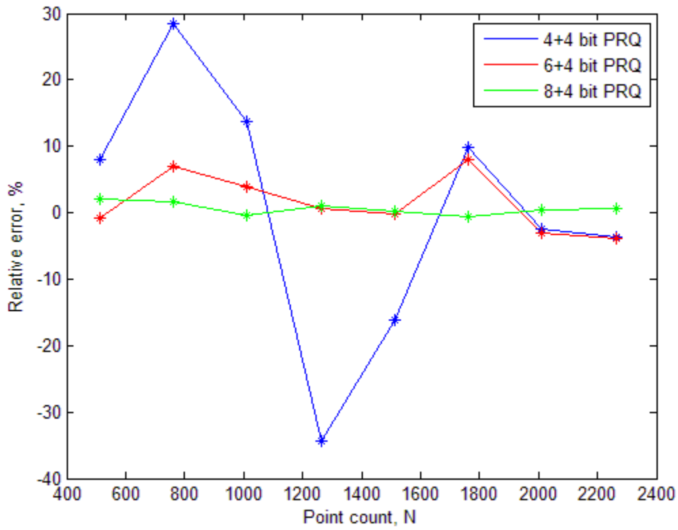

Figure 4.16 One realization of demodulation relative error dependence on processed point count N is shown in three cases: (a) 4-bit PRQ, (b) 6-bit PRQ and (c) 8-bit PRQ.

As it is shown in Figure 4.16, the important role plays point count, which falls into the signal processing time window. At first sight it would seem that better results provide larger point count, but it in general it is not quite true (if enormous points count is not considered). Much important is to ensure demodulation conditions where integer number of carrier periods falls into time window (including sampling frequency periods). Then windowed signal sample processing would provide optimal DFT coefficient estimation precision.

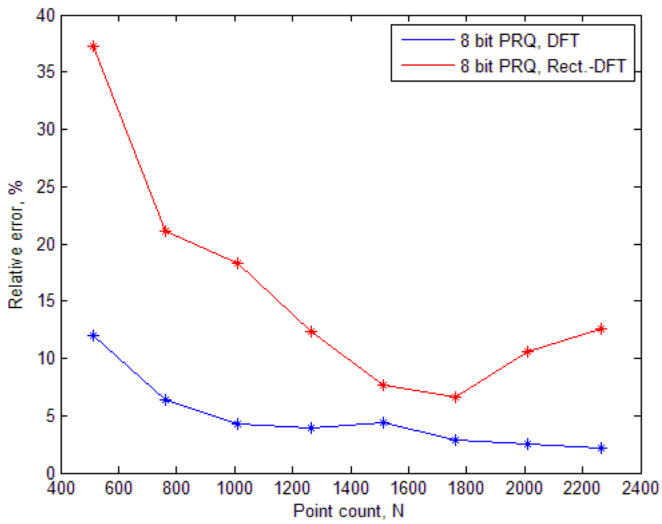

Figure 4.17 Averaged relative errors dependence on processed point count in cases where (blue curve) traditional DFT is used and (red curve) DFT based on rectangular functions is used.

In Figure 4.17 the traditional DFT is compared with DFT using rectangular basis functions. Placing carrier frequencies more irregularly, the averaged relative errors of bioimpedance signal demodulation were obtained, where each error was calculated by averaging 16 relative errors. Other simulation conditions remain unchanged. The general trend shows that enlarging of the point count provides for better demodulation signal quality, but it does not exclude the previous conclusion about the optimal time window size. This is true for both traditional DFT and DFT using rectangular basis functions involved in bioimpedance-signal demodulation.

4.4 Conclusions

Application specifics of the basic three signal quantizing methods (methods for deterministic, randomized and pseudo-randomized quantizing) for data acquisition are studied. All three of them are compared and their properties discussed in this Chapter. In many cases PRQ proves to be the best of them. That, of course, depends on the particular application. Actually the application potential PRQ for DAQ hardware designs is high as PRQ has significant advantages in comparison with DQ, PRQ specifically:

- Can be used in a wide dynamic range;
- There are no spurious frequencies in spectra of pseudo-randomly quantized data.
- Provides for decorrelation of data and quantizing noise;
- Eliminates systematic bias errors in estimates of basic signal parameters, including spectral;
- Provides for uniform quantizing noise distribution invariant to quantizing bit rate, essential for extension of the application range of rough quantizing;
- Ensures that distribution of the power spectrum of the quantizing noise is uniform independently of the original signal and the quantizing step size.

DFT is often needed for biomedical DAQ applications, where performance of bioimpedance signal demodulation is required. Methods for such signal processing are essential for design of medical equipment. This work considers bioimpedance signal demodulation based on calculations of DFT coefficients on several frequencies and the advantages of using PRQ are shown.

Due to these features, PRQ is an approach to quantizing that is rather valuable for achieving high performance of DAQ systems. That is confirmed by results obtained in the area of DAQ used for bioimpedance data acquisition. It is shown that in this application area:

- Improved resolution of very fast low bit rate ADCs (several GHz sampling frequency) at wideband low bit rate DAQ. In other words, PRQ reduces the quantizing bit rate, widening the application range of rough quantizing;
- Better digitized signal quality (in terms of signal sample values precision);
- Simplified, energy efficient DAQ hardware and bioimpedance signal processing.

In general, the obtained research results confirm that design and performance of DAQ systems often can be significantly improved by exploiting PRQ methods both for DAQ system hardware design and for data pre-processing software development.

5. Data Acquisition Based on Gathering Timing Information

As it is shown in the previous Chapters, taking sample values from continuous or so-called analog signals can be performed in a way differing from the classical approach to this operation, differing from the periodic sampling. Of course there should be a good reason for using sampling techniques significantly differing from this traditional sampling as the periodic sampling approach has a number of excellent properties and advantages. However it has also drawbacks, such as overlapping of frequencies (aliasing), excessive sample value taking from the signal parts slowly varying in time and others. Consequently it is often worth to spend time and efforts on finding some other special application-specific sampling methods better suited to conditions of a given specific application. Once the basic idea, the idea that the sampling operation actually can be performed in various ways, is accepted then it is not so difficult to find various unusual approaches to execution of this operation. On the other hand, application of different sampling methods leads to various digital representations of analog signals and that in turn leads to differing conditions for processing the digital signals obtained in result of using various specific sampling techniques. These conditions must be taken into account whenever it is attempted to change the approach to sampling from the classical to a specific one. Therefore, to avoid unexpected negative effects distorting results of digital signal processing, every new sampling technique has to be carefully studied before it is used.

5.1 Sampling based on detection of signal and reference function crossings

5.1.1 Sample value taking at the time instants of signal and reference function crossings

To get sample values from a signal, the signal can be compared with some reference functions at the time instants when the signal becomes equal to the reference, when the signal crosses the reference. This approach, as a technique closely related to zero-crossings, is discussed in [44] and in a number of other publications, specifically in [22]. Thus there are relatively many publications belonging to the subject area of non-traditional methods for analog signal digitizing. However sampling based on signal and reference sine-wave crossings has never been considered as a widely applicable alternative to the classical periodic sampling. This work is related to and further develops the sampling techniques suggested in [22].

The function of capturing the real world signals is important for many modern DAQ systems used in the areas of industry, medicine, defense etc. The importance of the role they play is growing. Sampling, based on detection of signal and reference function crossings (SRC sampling), provides many new features valuable for efficient data acquisition from the real life objects. Let us consider the concept, basic electronic schemes, advantages, drawbacks and other things of this sampling approach.

The features of this approach significantly differ from the characteristics of the classic solutions typically used for data acquisition systems. They, in fact, more often than not relay on uniform signal sampling. A number of typical essential features of the classic and SRC sampling approaches are given in Table 5.1.

Comparison of an analog input signal with a reference function is in the core of the SRC sampling approach. Detection of the time instants t_k when both inputs *x(t)* and *r(t)* become equal is how the SRC sampling operation is being done and this function could be performed in a simple way by using a single comparator. There are various possible approaches how to organize necessary multi-channel data acquisition for computers on that basis. Consideration of them follows.

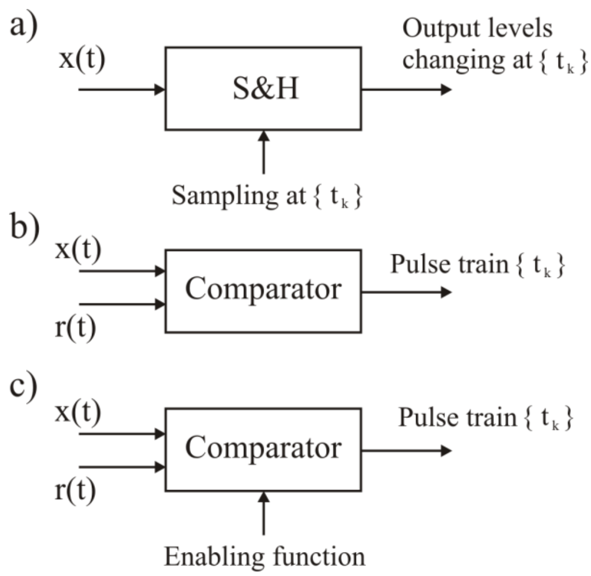

Figure 5.1 Various types of samplers used for performing the sampling operation. (a) sampler implementing the classical Shannon sampling; (b) sampler used for SRC based sampling; (c) sampler for SRC crossing based sampling controlled by an enabling function.

Figure 5.1 illustrates various approaches to implementation of the sampling operation. In the classical sampling case (see Figure 5.1 (a)) this operation usually is based on the 'Sample & Hold' circuit as shown in Figure 5.1 (a). In the case of SRC sampling scheme, the core element there is a comparator detecting the signal and the reference function *r(t)* crossing instants t_k (Figure 5.1 (b)). It compares the analog input from signal source with the reference function and forms trains of short pulses at the time instants $\{t_k\}$. They carry all the information taken from the original analog signal *x(t)*.

To add to the functionality of this signal/reference crossing detector, an enabling function is introduced as shown in Figure 5.1 (c). It is used for activating the comparator. The comparator fulfils its functions, compares the inputs and produces short pulses at the output when the crossing events occur only during the time intervals when it is activated by the enabling function. Figure 5.2 illustrates operation of such a sampler.

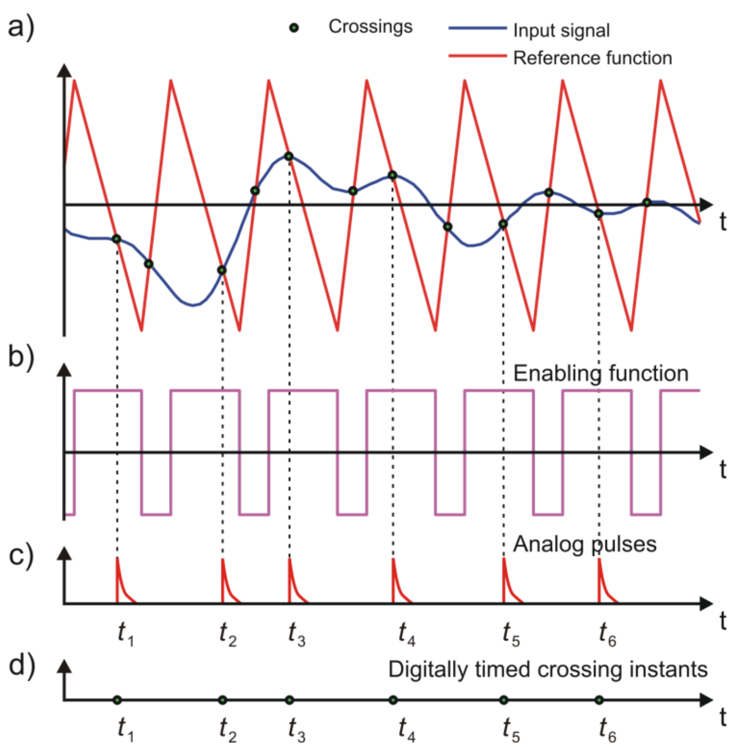

Figure 5.2 Functionality provided by SRC sampling scheme. (a) SRC sampling in the case of triangular reference function; (b) enabling function; (c) pulse train carrying information taken off the input signal; (d) another option of timing information presentation: a sequence of digitally timed crossing instants.

According to the discussed SRC sampling approach, the signal sample values are taken when the analog input signal intersects the reference function (Figure 5.2 (a)). In the illustrated SRC sampling case, the reference function is generated as an asymmetric sawtooth function with differing ascending and descending slopes. The sampling operation based on the signal and reference function crossing time instant detection is performed according to the equality:

$$x(t_k) = r(t_k),\ k=1,\,2,\,3\ldots \tag{5.1}$$

Where $x(t_k)$ - instantaneous input signal values, $r(t_k)$ - instantaneous reference function values, t_k - time instants at which the equality holds.

In result of the sampling operation, the time instants when the signal intersects the reference function are detected and given either as a train of analog pulses placed properly on the time axis, as shown in Figure 5.2 (c), or as a sequence of digitally timed crossing events (Figure 5.2 (d)). Note that only those crossing instants are used that fall within the time intervals when the comparator is activated by the enabling function (Figure 5.2 (b)).

The enabling function *z(t)* is a useful instrument that can be used for manipulation of signal sampling conditions. The comparator performing analog signal sampling is active only when the enabling function allows that. During the inactivated time intervals it sleeps and the power consumption of it then can be reduced.

Usage of the enabling tool is beneficial also from the functional point of view. By using this enabling function it is possible to ignore signal sample values and to control such conditions as the mean sampling frequency, minimal time duration between two sample values, sampling flow periodicity etc.

To avoid the situation when DAQ is halted because the comparator is deactivated by the enabling function, it is useful to put and use comparators in parallel, to perform DAQ form many channels according to Time Division Multiplexing Access principle. It gives the opportunity for utilizing the enabling function for multiplexing by sequential activating one comparator after another. Such manipulations could be done periodically what leads to the classical multiplexer functions or to non-periodical multiplexing what gives interesting opportunities to utilize enabling function for carrying out randomized multiplexing. These variations of the enabling function utilization are considered in the following Sections in more detail.

5.1.2 SRC sampling in the context of analog-to-digital conversions.

Traditionally conversions of analog signals into their digital counterparts are subdivided into two subsequent stages where:

- The first stage is the signal sampling operation;
- The second stage is quantizing of the signal.

Signals are sampled at the first stage and sequences of the taken signal sample values are then formed. In the case of the classic sampling (Figure 5.1 (a)), the signal sample values are given as voltage (current) levels, changing after each sampling event. In the case of SRC sampling, only the sequences of the crossing time instants are formed at the output of the sampler. Recovering of the original signal sample values happens in both cases at the second stage of the analog-to-digital conversions and the quantizing operation is performed in some way to fulfill this function. SRC sampling is specific and, consequently, signal analog-to-digital conversions that are based on this type of sampling are carried out also in an unusual way. Block diagram given in Figure 5.3 shows how the considered SRC sampling is exploited in the process of such conversions.

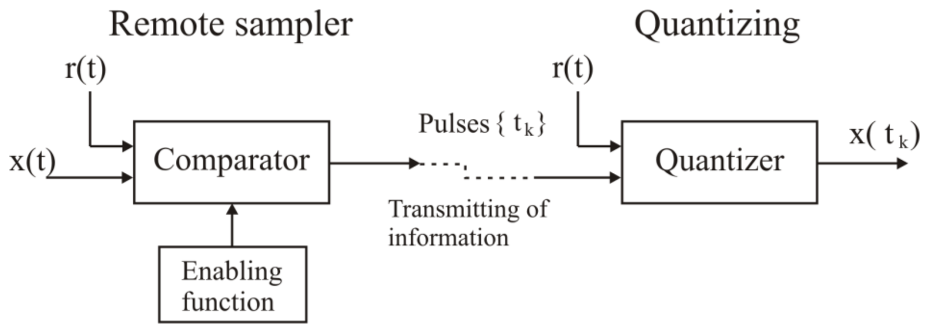

Figure 5.3 Basic scheme according to which the signal-to-digital conversions are performed on the basis of the considered SRC sampling.

The basic scheme shown in Figure 5.3 is, in fact, a specific analog-digital converter and that can be used for performing the sampling operation according to the considered here approach. The merit of it is the simplicity of the front-end design and the fact that it is well suited for remote signal sampling applications, specifically, for building distributed structure ADCs. The diagram given in Figure 5.3 draws attention to the fact that using of the considered SRC sampling makes it possible to distance the sampler at the front-end from that part of the whole ADC which performs quantizing of the sampled signal. That indeed is the case. As the output signal of the sampler then is a sequence of pulses with sharp leading edges, only the positions of the pulses on the time axis have to be preserved while the changes of their shape, due to the impact of the ambient noise, do not matter. Consequently the output signal of this type of samplers is much better protected against noise than the usually used samplers of Figure 5.1 (a). That leads to the possibility of performing this type of sampling operations in the close vicinity to the signal sources even if the output signals of the samplers have to be transmitted over relatively long transmission lines. The term Remote Sampler emphasizes that fact.

Thus, according to the considered sampling approach, the central element of the scheme in Figure 5.3 is the comparator used for detection of the time instants $\{t_k\}$ at which the signal $x(t)$ intersects the reference waveform. The physical output $y(t)$ of the comparator is formed as a pulse whenever the sampler is enabled by a function $z(t)$ and a crossing of the input signal $x(t)$ and the reference function $r(t)$ takes place. These pulses $y(t)$ at the sampler output are formed so that they carry the timing information indicating the exact crossing instants t_k of the signal and the reference function. In the framework of this work, it is assumed that the output pulses, having extremely short front edges of negligible duration, are formed with a constant delay after each crossing of the signal and the reference sine-wave function. Thus the sampler output signal is carrying the original information encoded as the sequence $\{t_k\}$ of the sine-wave crossing instants. It is transferred over some shorter or longer distance to the quantiser used for recovery of the input signal sample values. The signal sampling has to be executed in a way ensuring that the information carried by the input signal *x(t)* is fully transferred to the sampled signal given as the sequence $\{t_k\}$. Evidently fulfilling of this requirement is crucial for recovery of the input signal sample values encoded by this timing information. As it will be shown later, the timed event sequence $\{t_k\}$ has various properties that should be taken into account when designs of systems for data acquisition from the real world objects are considered.

The reference function *r(t)* is needed both for performing the signal sampling operation and for the recovery of sampled signal values. The reference waveform used for both these operations should be exactly the same. It concerns all parameters of the reference function, including the start time of the function. Any smallest deviation from this equality between both reference function replicas will cause distortions of the sampled digital signal and will degrade the quality of the following operations. Therefore it is crucial to achieve high precision at synchronization of the reference functions used for sampling and reconstruction (quantizing) of the signal.

Equally important is the question which type of the reference function is to be used. While there certainly are some options, sine-wave reference functions are used in the framework of this work as the best choice. The arguments in favour of that are given in Section 5.2.

As the above brief discussion of the SRC sampling approach in the context of signal analog-to-digital conversions shows, this approach differs from the classical sampling significantly. Comparison of both these methods for sampling follows.

5.1.3 SRC sampling in comparison with the classic approach to the sampling operation

Both the classical and the SRC sampling methods have various features essential for data acquisition applications. In Table 5.1 they are compared from the data acquisition viewpoint.

As can be seen, SRC based sampling has features that makes this approach well suited for applications related to simultaneous data acquisition from a large quantity of signal sources. Specifically, no switching of the analog signals are then performed and multiplexing of channels, provided for by proper application of the enabling function, is much simpler. Actually output signals of the samplers rather than their analog input signals are then multiplexed and that certainly is much better.

Table 5.1 Comparison of two alternative sampling approaches.

Classical sampling approach	**SRC sampling approach**
Signal sample value acquiring	
• Signal sample values are taken at predetermined time instants • Sample values are represented by respective voltage (current) levels • Uniformly spaced signal sample values • Remote sampling implementations usually not acceptable • Aliasing determined by Nyquist frequency	• Sample values are taken at the signal and reference function crossing instants • Sample values are represented by the time instants when the crossing events take place • Nonuniformly spaced signal sample values • Remote sampling applicable • Specific aliasing conditions • Reference function defines the envelope of the sampled signal instantaneous values
Signal sample value transmission	
• Requires transmission of constant levels • Sensitive to the ambient noise • Transmission acceptable only over short distances	• Based on transmission of time instants • Relatively insensitive to the ambient noise • Transmission might be performed over relatively large distances • Provides for data compression: transmission of a single pulse generated at the SRC instants is equivalent to transfer of a multi-bit code
Quantizing	
• Sample values are quantized directly	• Reference function values are quantized at the crossing time instants • High precision synchronization of the reference functions used for signal sampling and reconstruction is required
Multi-channel operation	
• Based on switching the analog input signals • Number of channels limited by hierarchic multiplexer structures	• No switching of analog signal performed • Multiplexing of channels, provided by enabling function, is much simpler • Well suited to data acquisition from a large quantity of signal sources • Data gathering is well suited to the specifics of implementations based on the Ultra Wideband communication techniques
Processing	
• Based on the classical DSP algorithms	• Typically specific algorithms are needed for processing • Applicability of standard algorithms achievable under certain condition • Complexity-reduced pre-processing is achievable in a relatively wide application range
Advantages for DAQ systems	
• Features and obtainable benefits are well known	• Reduced complexity and power consumption at the DAQ system front-end part • Significantly enlarged number of data channels

Remote sampling directly at the signal sources distributed over some 3D area becomes feasible. Thus SRC sampling is well suited for data acquisition from a large quantity of relatively low-frequency signal sources scattered over a relatively large area. Ultra Wideband communication techniques are well suited for high-speed sampled data transmission to the part of the data acquisition system where the sampled signals are reconstructed.

The content of Table 5.1 also shows that successful application of SRC sampling based for data acquisition largely depends on high-resolution detection of the signal and reference function crossing time instants and on the precision of the reference function generation and synchronization. Therefore attention has to be focused on achieving sufficiently good results in that direction. That is directly related to the problem of defining the most suitable reference function type. Let us consider this essential problem.

5.2 Sine waves as the preferred selection of the reference function

The reference function plays an important role at SRC based sampling. It affects the whole sampling process. Specifically, the crossing time instant streams and the characteristics of the digital signals, obtained in result of such sampling and the following sample value reconstruction, essentially depend on the features of the used reference function. The crossing time instant streams in turn determine the aliasing conditions, the applicability and efficiency of various algorithms for pre-processing the acquired data. Therefore serious attention has to be paid to the selection of the reference function type. It has to provide for:

- Relatively regular distribution of the crossing points along the time axis;
- Features of the digitized signals leading to rational algorithms for their digital pre-processing;
- Simple and effective high-precision generation of the reference functions with a few given parameters that can be stabilized in time and in regard to changing exploitation conditions of the respective electronic circuits.

Let us consider and compare two types of possible reference function candidates: variable parameter sawtooth functions (as shown in Figure 5.2) and sine-wave functions.

The first type of functions, the sawtooth functions, is relatively popular. They are currently used for similar applications almost exclusively. For example, they are usually exploited for Pulse-width modulation. The reason for such preference is the fact that their slopes are linear. Application of such reference functions in our case would ensure that bias in input signal level would lead to proportional shift of the crossing time instants along the time axis. Obtaining of this property, of course, is desirable if only the price for this is not too high.

The second possible type of the reference functions is sine-wave functions. While both types of the reference functions being compared would equally well provide for meeting of the first given above requirement (application of both of them would properly pre-condition relatively regular crossing event distribution in time), the sine-waves are non-linear and that at first glance makes them less suitable. However sine-waves have other features that make them more useful than the mentioned sawtooth functions. To show this, attention is drawn to the given equality (5.1). According to it, all instantaneous values of the signal sampled on the basis of the SRC method belong to the reference function. Consequently, the envelope of these sample values is constant independently from the input signal. And the reference function defines this envelope. Therefore in the case of the sine-wave reference, the envelope of the sample values is sinusoidal. This type of sampling is considered as Signal and Sine-Wave Crossing sampling or SWC sampling.

5.2.1 Constant envelope sampling

Diagrams in Figure 5.4 illustrate signal sampling performed according to the considered SWC sampling model in the case where sine-wave reference function is used. While sampling then is signal-dependent and essentially nonuniform, it is characterized by constant envelopes defined by the used sinusoidal reference function. As is evident from the given diagrams, the envelopes of the two obtained distinctly different digital signals are exactly the same. This is a significant positive fact leading to far reaching consequences for processing of this type of digital signals.

The various reference functions could be used while at the system implementation and design point of view the reference should be stable and easy to generate the same waveform. The sine-wave is one of those functions which match to above mentioned requirements very well. The reference function also has to be varying and has to cover all dynamic diapason of input analog signal. Therefore in the case of DAQ from real world objects the sine-wave function is recommended as reference function [1].

It was mentioned at previous discussion where the SRC signal sampling was considered that sine-wave function is well suited to be a reference function when the massive data acquisition is organized from many signal sources. The main reasons were the easy copy-ability of sine waveform and the applicability form many algorithms. The second reason will more clearly appear further when the processing of such a way sampled signals will be considered.

This specific sampling approach organized in mentioned way has following advantages:

- The switching of the original analog input signals is not planned;
- The sampling could be easily accomplished close to the signal source, while the remained part of DAQ system could be placed distantly. It is called the remote sampling;

- Under certain conditions it is possible to use classical DSP algorithms. These conditions are estimated at latter chapters;
- The front-end part of considered DAQ system is very simple and consist only from one comparator;
- It is possible to use new algorithms (for DFT, digital filtering etc.) that typically are complexity-reduced and not requiring multiplication of multi-digit numbers instead of classical ones;
- The power consumption of the basic electronic scheme might be ultra-low.

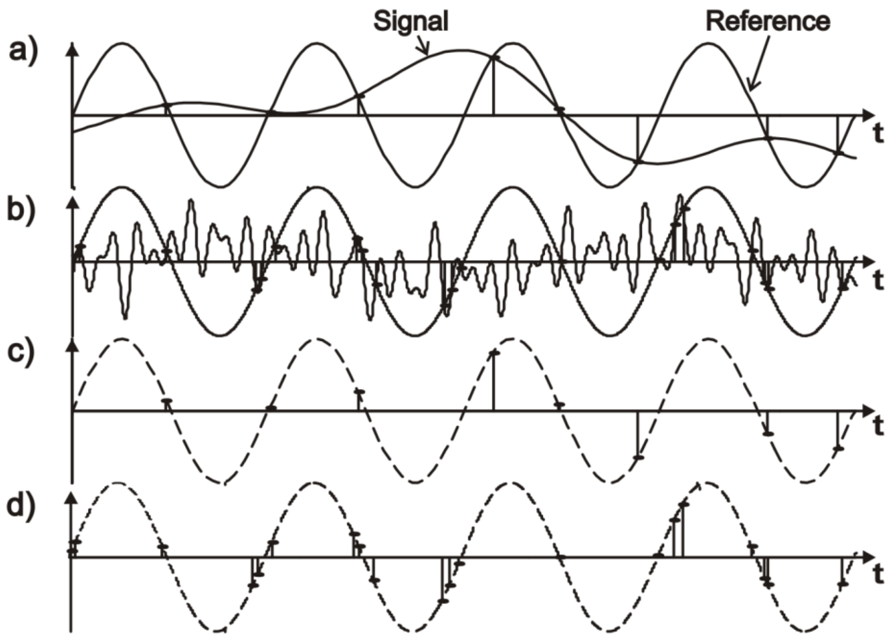

Figure 5.4 Illustration of a constant envelope sampling process based on a signal and a sinusoidal reference function crossings. (a), (b) diagrams illustrating sampling of two signals having components at differing frequencies; (c) signal digital sample value sequence of the signal shown in (a); (d) signal digital sample value sequence of the signal shown in (b).

Unfortunately there also exist some drawbacks of the considered sampling approach what needs attention:

- The sampled signals according with this sampling are nonuniform what means well known consequences with sampled signal further recovery, signal processing etc. However this topic is much deeper considered in latter chapters;
- In this case many classical signal processing algorithms doesn't work therefore there is need for developing the new applicable algorithms.

5.2.2 Potential of SWC sampling for simplifying some DSP algorithms

The fact that the envelope of the digital sample values, obtained in result of SWC sampling, is a sine function is unusual and meaningful. Indeed, it means that the digital signals reconstructed from the crossing point streams in that case always have one and the same sinusoidal envelope independently of the input signal. The signal only varies the crossing point positions on the time axis. In other words, all sample values then belong to a sine-wave function and they are nonuniformly distributed along the time axis.

This significant feature of SWC sampling might be exploited for reducing the complexity of the algorithms for pre-processing of signals. Such pre-processing usually is performed in the process of data acquisition and formatting in order to compress data and to simplify their handling. Algorithms for processing digital signals obtained in result of SWC sampling often can be significantly less complicated than the widely used conventional ones. In particular, it is possible in many cases to avoid multiplications of multi-bit numbers. The obtainable complexity reduction then is based on the well known relationships:

$$\begin{aligned} \sin(a)\sin(b) &= \frac{1}{2}[\cos(a-b)-\cos(a+b)] \\ \sin(a)\cos(b) &= \frac{1}{2}[\sin(a-b)+\sin(a+b)] \end{aligned} \tag{5.2}$$

The unique constant envelope feature of SWC sampling makes it possible to exploit these formulae and to develop rational algorithms, in particular, for Discrete Fourier Transform based spectrum analysis and waveform reconstruction. For example, the following equations can be used for calculation of Fourier coefficient estimates $\hat{a}_i$, $\hat{b}_i$ not requiring multiplication of multi-digit numbers as usual [1, 2, 6]:

$$\begin{aligned} \hat{a}_i &= \frac{A_r}{N}\sum_{k=0}^{N-1}(\sin 2\pi(f_r - f_i)t_k + \sin 2\pi(f_r + f_i)t_k) \\ \hat{b}_i &= \frac{A_r}{N}\sum_{k=0}^{N-1}(\cos 2\pi(f_r - f_i)t_k - \cos 2\pi(f_r + f_i)t_k) \end{aligned} \tag{5.3}$$

Where A_r, f_r are the amplitude and frequency of the sinusoidal reference function, t_k denotes the crossing time instants and N is the number of signal samples processed.

This approach to complexity reduction of algorithms for data pre-processing is usable only under the condition that the reference function is sinusoidal. This represents a strong argument in favour of using this type of reference functions. The problem related to the necessity of operating with sine and cosine functions in this case can be easily resolved by using look-up tables.

5.2.3 Generation of reference functions

Reference functions evidently play an important metrological role at signal digitizing. Their waveforms must exactly fit the respective definitions so that their parameters are very close to the defined values. The precision obtainable at data acquisition based on the considered type of signal sampling to a large extent depend on this. Therefore the issue of the reference function generation is important. It has to be taken into account that analog as well as digital generators of reference functions are needed and that in multi-channel data acquisition systems relatively many of such generators have to be used.

It might seem that generation of sawtooth type of reference functions is easy. Indeed, digital structures such as counters and DAC might be used for that. However then the structures of such generators would not be so simple and, in addition, generation of reference functions with relatively short periods would represent a serious problem.

Actually generation of precise sinusoidal reference functions in many cases prove to be considerably simpler. The fact that a sine-wave is a mono-harmonic function with all power concentrated at a single frequency helps a lot at their generation. That can be done on the basis of simple structures as narrow-band selective filters might be used for obtaining truly sinusoidal signals.

The arguments discussed in this Section leads to the conclusion that it makes sense to prefer and use the sine-waves as reference functions at sampling based on the detection of the signal and reference function crossing instants.

5.3 SWC sampled signal properties in the time domain

Periodic sequences of analog signal sample values are usually considered as the natural digital representatives of the respective original analog signals. As it is shown in Chapter 3, the signal sample sequences might be also non-periodic or, in other words, nonuniform. Thus the periodic sampling based digital signals are not unique, there are other types of digital signals that can be used for representing their analog signal counterparts. Let us show that the sequences of timed events might be added to the list of various types of digital signals that can be used for representation of analog signals.

If the crossings of a signal with a reference function are considered as events, then the sequences of these events, under certain conditions, might be considered as carriers of the information initially carried by the respective analog signals. Therefore it should be possible to reconstruct the mentioned analog signals from the respective sequences of timed crossing (sampling) events. If that is the case, then this type of timed event sequences could be considered as a specific digital representation of analog signals. As it is further shown, under certain conditions, that indeed can be done. The first condition is the requirement to add the parameters of the reference function to each of the used sequence of the timed crossing events. These timed event sequences become meaningful only if this information is *a priory* given.

5.3.1 Signal representation by timed sequences of events

To convert an analog signal into digital, sample values of the original analog signal usually are taken at some specifically defined sampling time instants and the digital signal is formed as a sequence of these sample values. As the definition of the sampling time instants of the signal sample value taking might differ, analog signals actually might be converted into their digital counterparts in various ways. The most popular approach is based on sampling signals periodically but it certainly is not exclusive. The sampling process might as well be also nonuniform. A specific signal digitizing technique suggested in [22] is considered in some detail in work. It is rarely used so far. According to it, signal sample values are taken at time instants when the signal crosses a sinusoidal reference function. Such digitizing of signals, based on their crossings of a given constant parameter reference sinusoid, has features unparalleled by other digital signals. For a wide class of input signals, the envelope of their digital counterparts is invariable. And that leads to a remarkable method for representing the analog signals. They might be fully digitally represented just by sampling time instant sequences rather than by the sequences of their sample values as usual. Consequently, the conditions for processing this type of digital signals are essentially specific as well. Therefore adding the described digital signal to the collection of other more conventional digital signal types widens the variety of the signal processing and the signal processing system design options. When development of a specific application is planned, this approach to signal digitizing is well worth considering. Basics of this signal digitizing approach are further discussed.

An essential informative parameter characterizing this kind of sampling is the ratio σ/μ, where σ is the standard deviation of the sampling intervals and μ is the mean value of them. This parameter, for the sampled signals in Figure 5.5 (a) and (b), is $\sigma/\mu=0.4863$ and $\sigma/\mu=0.9055$, respectively.

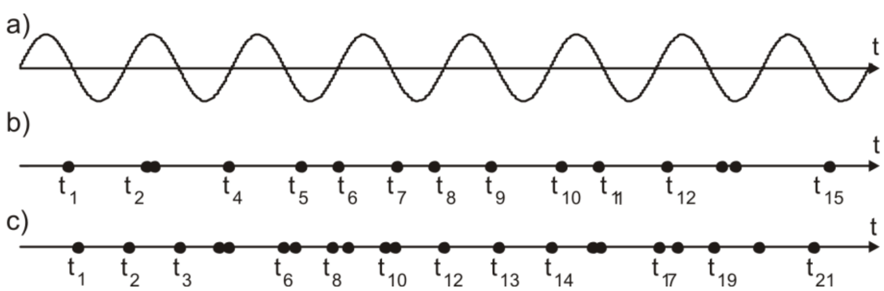

Figure 5.5 Sampling point processes fully representing the respective analog signals in the digital domain. (a) reference function; (b) point process representing the sampled signal shown in Figure 5.4(a); (c) point process representing the sampled signal given in Figure 5.4(b).

Empirical distributions of the sampling intervals in both of these cases are given in Figure 5.6. Evidently they strongly differ. The first one illustrates a sampling case that is much better than the second one. First of all it is better in the sense that it is more regular. The deviations of the sampling interval values from their mean value are less pronounced. Second, only a small number of the sampling intervals in that case are very short. That is not the case with the empirical distribution given in the Figure 5.6 (b). In that case, a considerable number of crossings occur very closely in time and that represents a problem for processing the respective signal sample values. It might be said that the nonuniformity of sampling in the second illustrated case is much stronger. And that is clearly shown in the given empirical distributions and follows from the numerical value of the ratio σ/μ.

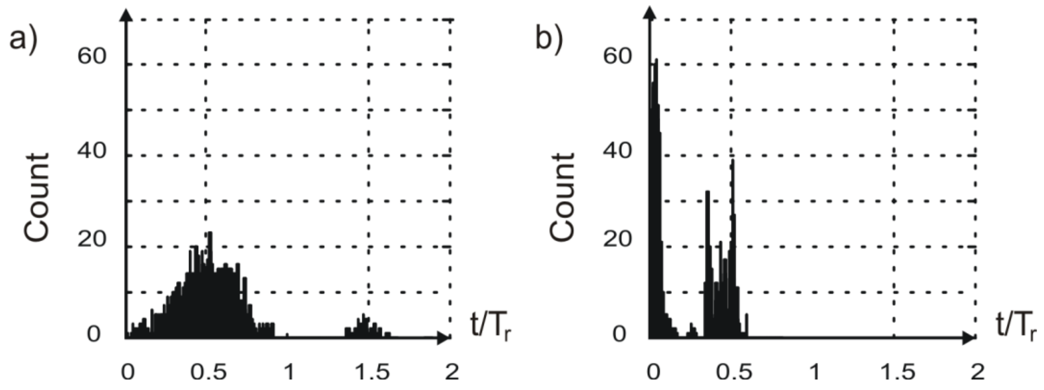

Figure 5.6 Empirical distributions of the sampling interval duration normalized to the reference period: (a) for the sampled signal shown in Figure 5.4 (a); (b) empirical distribution for the sampled signal shown in Figure 5.4 (b).

The displayed two cases of two differing signal sampling reveal the fact that this approach to sampling and to analog signal digitizing leads to digital signals that could be given either as sequences of signal sample values with envelopes defined by the used reference function or just as sequences of sampling (crossing) time instants $\{t_k\}$. Both types of the digital signals represent the respective analog signals equally well. The quality of this kind of digital signals, obtained by detecting the original signal crossings with a reference sinusoid, remains to be found out. This issue is discussed in [1] and to some extent in the following sections.

5.3.2 Trading-off the mean sampling rate against the time-resolution

Features of the digital signal formed in result of the analog input signal and the reference sinusoid crossings obviously depend on both of the involved processes. As the crossing point process might be considered as the digital signal representing the original analog signal, the basic features of concern are the regularity of the intervals between the sampling (crossing) points and the accuracy of the indicated crossing time instants. Both of these features to some extent depend on the frequency of the used reference sinusoid. Therefore the question arises how to select the appropriate value of this parameter of the reference function.

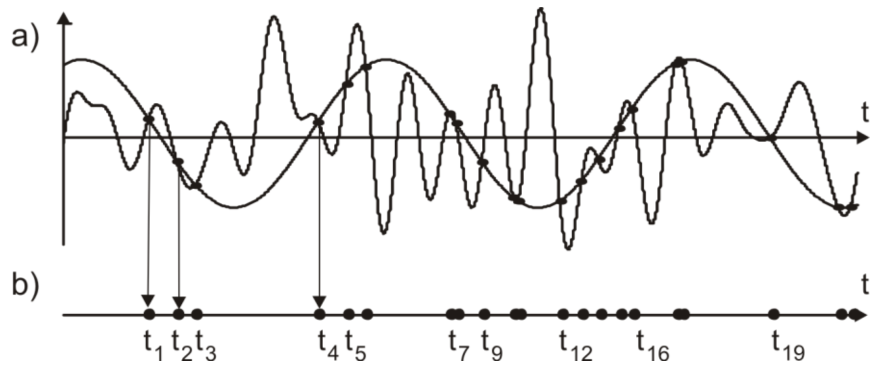

Figure 5.7 Digital signal (b) in the case where a signal crosses a low frequency reference function as shown in (a).

There are some considerations that might be taken into account. In general, at low reference frequencies the relative resolution with which the crossing events are fixed in time is better than at high reference frequencies. From that point of view, low reference frequency seems to be preferable. On the other hand, at low reference frequencies, the crossings typically occur as it is shown in Figure 5.7 (a). Then the crossing point pattern in time basically depends on the signal frequency content as the signal typically crosses the reference function a number of times during each period of the reference and the sampling point process then is characterized by relatively high values of the ratio σ/μ as it is rather irregular. Consequently, distortions of the sampled signal processing due to the cross-interference phenomenon might be expected then.

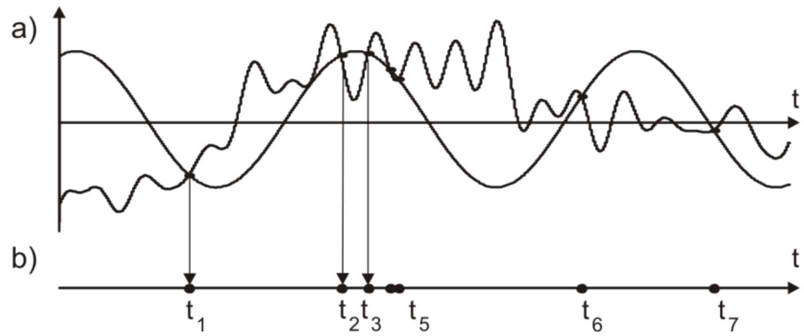

Figure 5.8 Illustration of a sampling case where the reference sinusoid is not crossing the signal within relatively large signal segments. (a) crossings of the signal and the reference function; (b) obtained digital signal.

Another drawback typical for the cases where low frequency reference functions are used is illustrated in Figure 5.8. As can be seen, there are relatively large gaps between the detected crossing points. In result, essential information is lost during these time intervals. The formed digital signal, namely, the sampling (crossing) point process, given in Figure 5.8 (b), again is nonuniform and it is characterized by large values of the ratio σ/μ.

The digital signal, obtained in the cases where relatively high frequency reference function is used, typically is more regular as the reference function basically imposes the crossings. A typical sampling process of this kind is given in Figure 5.9. As can be seen, the formed digital signal indeed is more regular in this case.

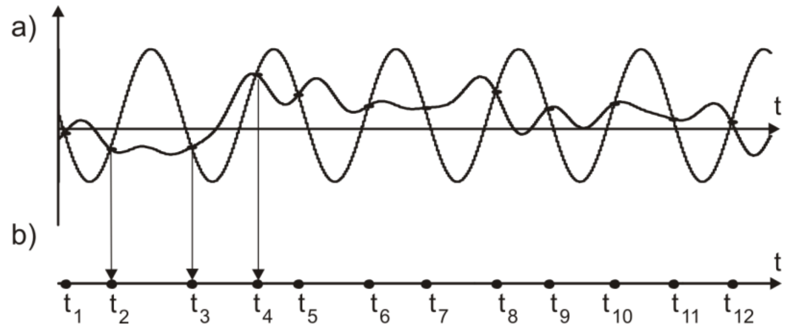

Figure 5.9 Illustration of the digital signal forming in the case where relatively high frequent reference function is used: (a) sampling process; (b) formed digital signal.

As the given illustrations show, usually it is preferable to use reference sinusoids at relatively high frequencies. However even then the irregularities of the obtained digital signal might lead to significant distortions of the signal processing results. These distortions are typical for any kind of NU sampling and they are caused by the cross-interference between the nonuniformly sampled signal spectral components. While more often than not it is desirable to work at higher reference frequencies, increasing of the reference frequency is limited. And the consideration of the time-resolution basically is the dominating factor setting up this limit. Therefore the mean sampling rate, directly depending on the reference frequency, often has to be traded-off against the achievable time-resolution.

5.4 SWC sampled signal properties in the frequency domain

This Section reveals the particularities of SWC sampled signals in the frequencies domain.

5.4.1 SWC sampled signals spectrum particularities

The digital signals discussed in this paper clearly are highly specific and, in this sense, unusual. First of all, their definition differs from the classical and traditionally used one. Timed sampling event sequences or, in other words, sampling point processes in time are considered as digital representations of the respective analog input signals rather than sequences of signal sample values as usual. Next, the sampling time instants under these conditions are signal-dependent and time intervals between them are nonuniform. On the other hand, these sampling intervals not necessarily are random. As they are related to the input signals, there might be periodicities present in the digital signals representing the original analog signals. Therefore overlapping of frequencies or aliasing might be expected. There may be also cross-interference between signal components typical for NU sampled signals. Actually the specific properties of the digital signals of this kind are not pre-determined, they strongly depend on the input signal and the used reference function.

Hence the considered digital signals indeed are highly specific and they have features unparalleled by other digital signals. It still has to be learned how to effectively process them under varying conditions. However there is a factor that draws attention and stimulates interest to this sampling approach. The point is that the digital signals obtained in the mentioned way have an outstanding positive feature. The envelope of the digital signal instantaneous value sequences, in the case of this kind of analog-to-digital conversions, remains constant no matter what is the spectral content of the respective analog signals. This fact represents a powerful advantage of the considered type of signal sampling as the constant envelope of various digital signals obtained under the mentioned conditions leads to various options in processing them. Some of these options, including complexity-reduced spectrum analysis and massive data acquisition, are briefly discussed in [1, 22]. Specific properties of the constant envelope digital signals, obtained in the case of SWC sampling, are studied and described here. The features of the digital signals obtained then are essentially specific. The feature of special interest is overlapping of frequencies or aliasing observed in the cases where sampling is performed in the mentioned way and the digital signal itself is a sampling point process or, in other words, a sequence of timed sampling events. Consideration of aliasing issues characterizing this type of digital signals follows.

5.4.2. Aliasing of SWC sampled signals

To observe how frequencies are overlapping in the considered signal digitizing case and how aliasing does impact processing of the obtained digital, DFT of a signal, containing only three components at frequencies f_1, f_2 and f_3, was performed. The sampling-specific complexity-reduced algorithm and the following equations (5.3), discussed in [1, 22], were used for calculations of the Fourier coefficient estimates at the frequency f_i.

Evidently no multiplications of the signal and filtering function digital values have to be carried out in this case. This is a significant advantage of the discussed sampling approach as DFT based on calculations carried out according to these equations is exclusively applicable only for spectrum analysis of the digital signals obtained in result of sampling based on the reference sine-wave crossings.

The spectrogram obtained in this way is given in Figure 5.10. As can be seen, there are many other peaks in this spectrogram in addition to the peaks that might be considered as spurious noise. Actually the most pronounced additional peaks appear in the spectrogram in connection with the frequency overlapping or aliasing effect. In this specific sampling case, positions of the peaks related to aliasing depend on the frequencies related to the periodicity in the sampling point stream. This means that both the reference frequency and the mean sampling frequency play some role in that and are to be considered in this light.

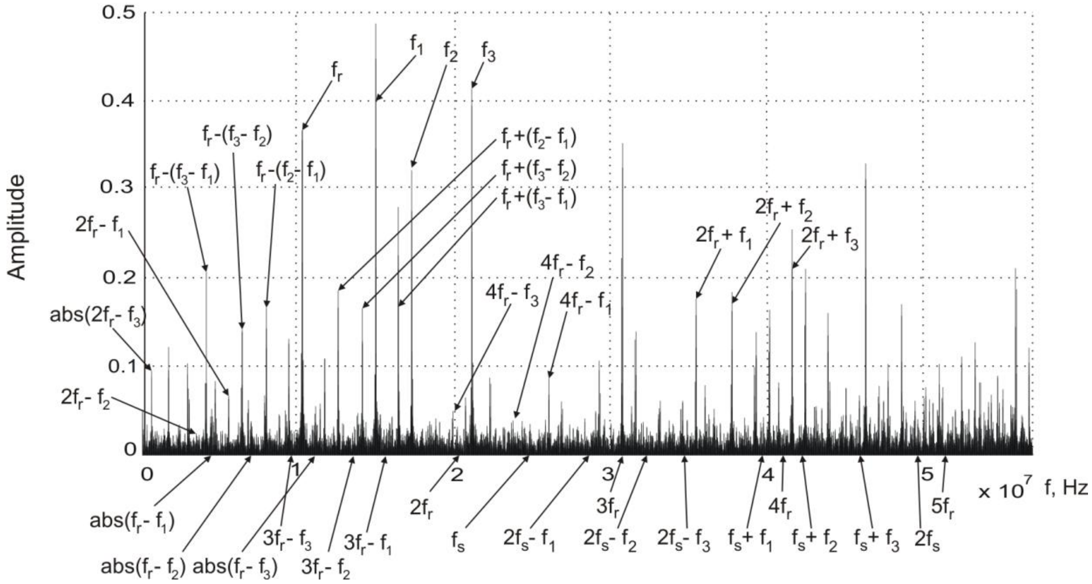

Figure 5.10 Illustration of the aliasing frequency pattern.

Consider the spectrogram given in Figure 5.10. The frequencies f_i and f_n of the signal components, along with other typical frequencies such as the reference frequency f_r and the mean sampling rate f_s, are indicated in the spectrogram. Note that the frequencies of the reference function together with the mean sampling frequency define the positions of the aliasing frequencies displayed in it. The pattern of the peak positions on the frequency axis helps to reveal the essence of the mentioned relationships defining the aliasing conditions. Actually there are three rows of the expected aliasing frequencies. They are:

$$
\begin{array}{ll}
f_i;\ f_r \pm f_i;\ 2f_r \pm f_i;\ 3f_r \pm f_i;\ \ldots; & i=1, 2, 3, \ldots \\
f_s \pm f_i;\ 2f_s \pm f_i;\ 3f_s \pm f_i;\ \ldots; & i=1, 2, 3, \ldots \\
f_r \pm (f_i \pm f_n);\ 2f_r \pm (f_i \pm f_n);\ 3f_r \pm (f_i \pm f_n);\ \ldots; & \text{for } i \neq n \text{ and } i=1, 2, 3, \ldots;\ n=1, 2, 3\ldots
\end{array}
\quad (5.4)
$$

Where f_i and f_n are frequencies of a signal components, f_r is the reference frequency and f_s is the mean sampling rate.

Peaks due to aliasing might be found at any frequency given in (5.4). Their magnitude depends on the specific conditions under which the crossings of the signal and the reference function occur. In general, the relationships defining the aliasing conditions in this case are more complicated than in the cases where the sampling process is pre-determined and does not depend on the signal. First, as can be seen from this spectrogram, there are more aliases than in the case of the conventional periodic sampling. Second, the aliasing process is suppressed. The peaks at frequencies of true signal components are much stronger then the aliases. That is due to the fact that the sampling process is both periodic and nonuniform. The nonuniformities of the sampling intervals lead to this effect of alias suppression. The fact that the aliases are to some extent suppressed is significant. This helps to separate them from the signal components. Third, the aliases related to the indicated in row (5.4) three frequency rows might be not equally strong. For instance, while the aliases related to the mean sampling rate f_s are rather weak in the case illustrated by Figure 5.10, they are well pronounced in the diagram shown in Figure 5.11. This difference in aliasing can be traced to the differences in signal sampling conditions. Fourth, aliasing illustrated by Figure 5.11 occurs also at frequencies related to the reference frequency and signal component differences/sums $(f_i \pm f_n)$; *…;* for $i \neq n$ and $i=1, 2, 3, \ldots; n=1, 2, 3\ldots$ That is unusual.

Actually the question is arguable whether the aliasing effect does take place in the discussed case at all. Indeed, it is clear that there is no full-scale frequency overlapping. While peaks appear in the spectrogram at frequencies belonging to the row (5.4), they are significantly suppressed. This type of aliasing is considered as so-called fuzzy aliasing [22]. It seems that in this specific case it might be even assumed that there are cross-interference effects rather than aliasing while these effects are amplified at the indicated in (5.4) frequencies.

It is possible to check if this assumption is right. If the peaks in question do appear in result of the cross-interference due to the sampling irregularities, then it should be possible to take them out by adapting signal processing to the specific sampling nonuniformities. That was checked and the discussion of the obtained result follows in the next Section.

5.4.3 Cross-interference between signal components

The considered sampling process is nonuniform and, consequently, some distortions of signal spectrograms due to the cross-interference between NU sampled signals are to be expected [22]. There are two aspects of this impact. There is a background noise with spurious frequency peaks and the mentioned interference actually distorts more or less the whole spectrogram. The spurious frequencies, reflecting the impact of the cross-interference between the signal components and present in the spectrogram, confirm this expectation. These spurious frequencies are not very noticeable in the particular spectrogram of Figure 5.10. They are more powerful in the spectrogram given in Figure 5.11. Under certain sampling conditions providing for small sampling point irregularities this kind of spectrum distortions might be negligible as it is shown in [1]. In other cases special signal processing procedures for adapting the sampled signal to the sampling nonuniformities has to be carried out in a way described in [22].

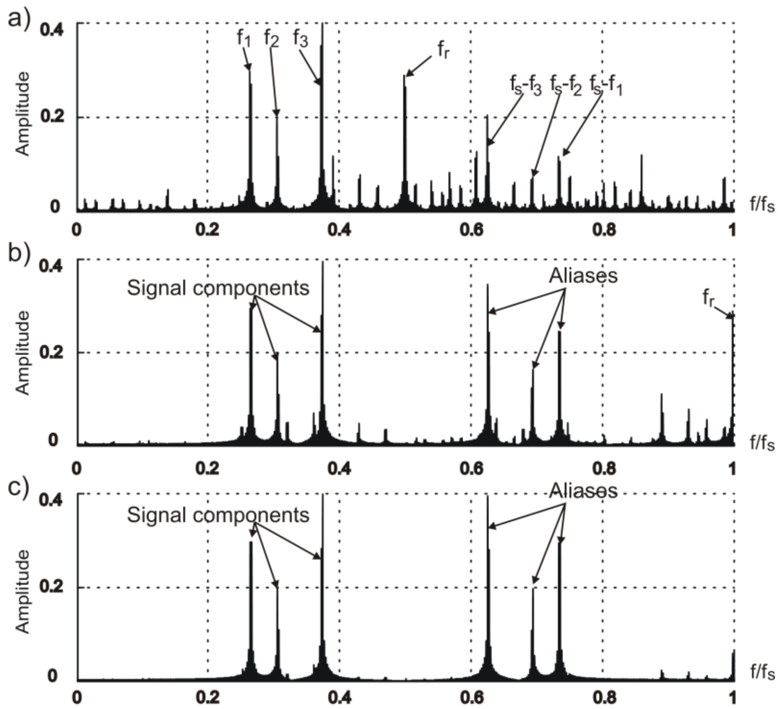

Figure 5.11 Impact of sampling regularization on the aliasing conditions.

The impact of this cross-interference on the signal spectrograms directly depends on the signal sampling conditions. The spectrograms displayed in Figure 5.11 illustrate this. The signal in this particular case has only three components and the sampling conditions are varied. In result, the peaks in the spectrogram indicating the aliases and the power of the spurious frequencies vary as well. While all signal and the reference crossing events are taken into account in the first case illustrated by the spectrogram in Figure 5.11 (a), the sampling operation is enabled only during each sixth half-period of the reference function in the second case (Figure 5.11 (b)) and during each tenth half-period in the third case (Figure 5.11 (c)). As can be seen, this approach to sampling significantly impacts the features of the obtained digital signal. Introduction of the enabling function actually has the effect of sampling regularization. Increasing the interval during which the sampling operation is blocked results in smaller power of the introduced element of the randomness and that in turn leads to reduction of the effects induced by the cross-interference and to increasing of the peaks in the spectrogram due to aliasing.

5.4.4 Evolution of anti-aliasing capabilities

The problem of alias elimination usually comes up when periodic sampling could not be performed at sufficiently high frequencies. This typically happens either when the upper frequency of the input signal in a single input channel case exceeds the sampling frequency or there are many input channels and the rate of signal sample value taking depends on the number of channels and the achievable channel-switching rate. An effective technique for massive data acquisition providing protection against aliasing in the latter case is randomization of enabling for remote sampling at sine-wave crossing instants. Figure 5.12 illustrates this approach.

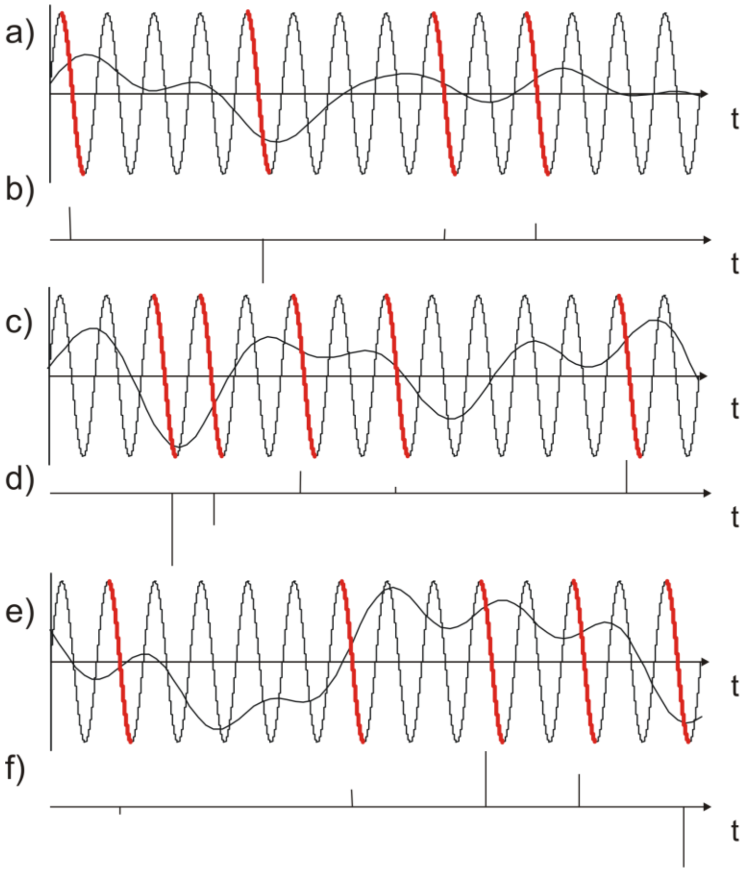

Figure 5.12 Pseudo-randomized enabling of the sampling operation to be carried out in three particular input channels.

Sequential enabling of a number of samplers fulfils the functions typically performed by multiplexers. In both cases analog-digital conversions of a multitude of input signals is carried out by connecting the converter to each of the signal sources repeatedly for a short time period. If this switching is performed periodically, as it is in the typical case, then the number of the signal sources limits the frequency range where signals could be processed without distortions due to aliasing. To avoid aliasing in a much wider frequency range, multiplexer switching and sequential enabling of samplers should be pseudo-randomized. Achieving of the anti-aliasing effect in both cases apparently is based on the same principles. They are discussed in [2, 14, 22] relative to pseudo-randomized switching of a multiplexer. Pay attention to the fact that taking signal sample values at time instants with unequal distances between them, while it is a necessary anti-aliasing condition, does not guarantee obtaining of high quality signal processing results. To achieve high precision at signal processing, the nonuniformly taken signal sample values have to be processed in a proper way with the sampling irregularities taken into account. Algorithms for processing NU sampled signals adapted to the sampling nonuniformities should be used for that as it is described in [22]. The achievable improvement is signal processing achievable in this way is illustrated in [14].

To achieve the capability of suppressing signal aliases, sampling based on the sine-wave crossings has to be enabled at random or pseudo-random half-periods of the reference function. The smallest digit of the sampling time interval then is equal to the period of the reference function. While it is possible to realize various sampling modes in that way, it is actually senseless to use additive sampling in this case as there is no obstacles preventing taking of the sample values occasionally also at successive reference periods. If the sampling operation is enabled at each period of the reference function with an equal probability, then there is no secondary aliasing. Consequently, the cross-interference taking place whenever the sampling operation is randomized then does not have high peaks at some frequencies typically observed whenever the secondary aliasing takes place.

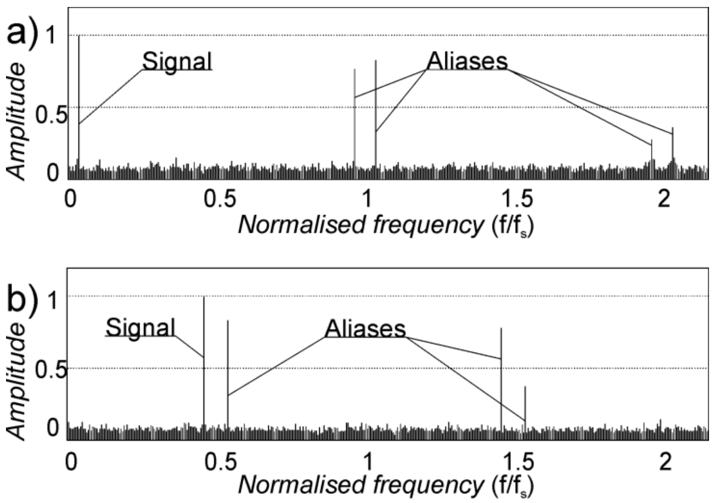

Figure 5.13 Spectrogram of a single tone signal obtained in the case where the sampling operation is enabled randomly.

The spectrogram characterizing sampling of this kind is given in Figure 5.13. It has been obtained for the case where the sampling operation was enabled at each second half-period of the reference sine wave with constant probability equal to 0.1. The spectrogram in Figure 5.13 confirms the fact that suppressing of aliasing is much more pronounced when the sampling operation is enabled randomly.

5.5 Data acquisition based on SWC sampling

5.5.1 Timed signal and reference crossings as information carriers

The sampling based on signal and sine-wave crossings also called SWC sampling is a special case of signal-reference sampling class, where the choose of reference lays on the sine-wave function:

$$r(t_k) = A_r \sin(2\pi f_r t_k + \varphi_r),\ k=1,\ 2,\ 3\ldots \qquad (5.5)$$

Where $r(t_k)$ - reference signal, t_k - time instants, when the equation is true, A_r, f_r and φ_r are the amplitude, frequency and phase angle of the reference sinusoid respectively.

Signal sample value taking at the time instants $\{t_k\}$, satisfying equation (5.5), represents the basic model of the considered sampling process. Figure 5.18 illustrates it.

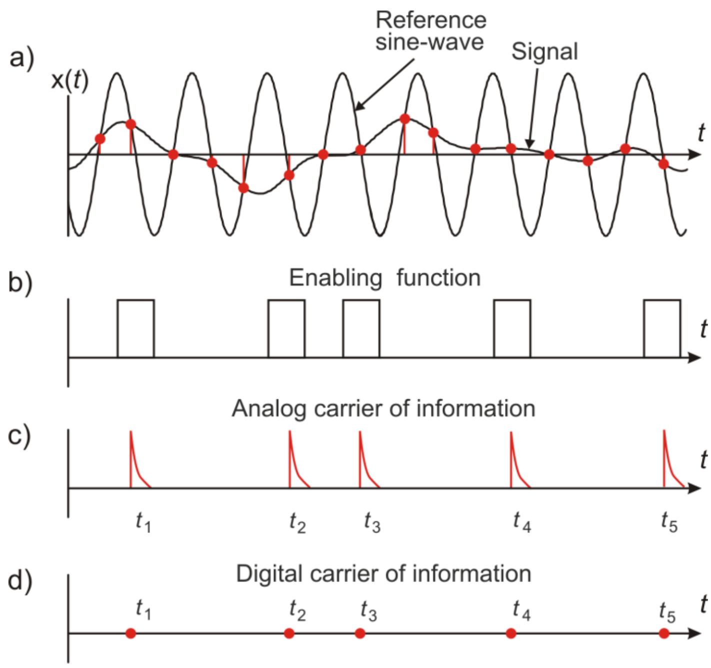

Figure 5.14 Time diagrams illustrating specific two types of input signal representation in the digital domain. (a) sampling based on signal and the reference function crossings; (b) enabling function; (c) analog carrier of information; (d) digital carrier of information.

Digitally timed events, defined as crossings of an input signal and a reference function, is used in this case for representation of analog signals in the digital domain. The most responsible elements of this system apparently are the comparators used for detection of the time instants t_k at which the signal *x(t)* intersects the reference function *r(t)* that is given as a sine wave at frequency f_r. It has constant amplitude A_r. The physical output *y(t)* of the comparator is formed as a pulse whenever the sampler is enabled by a function *z(t)* (Figure 5.14 (b)) and a crossing of the input signal *x(t)* and the reference function *r(t)* takes place. These pulses *y(t)* at the sampler output are formed so that they carry the timing information indicating the exact crossing instants t_k of the signal and the reference function. It is assumed that the output pulses, having sharp front edges are formed with a constant delay after each signal and the reference sine-wave crossings. Thus the sampler output signal is carrying the original information encoded as the sequence $\{t_k\}$ of the sine-wave crossing instants. It is transferred over some shorter or longer distance to the host computer. Note that this sequence fully represents the respective input signal. It means that the crossing instant sequence might be used either for recovery of the input signal sample values and reconstruction of the signal or the input data processing might be based on direct processing of these crossing instants as it is explained below [8].

While the sequence of the signal and reference function crossing instants represents in this case the input analog signal in the digital domain, either an analog or a digital carrier may be used for transmitting this information, as it is shown in Figure 4c and 4d. A train of position-modulated short pulses (Figure 5.14 (c)) is used as an analog information carrier and a sequence of digital crossing instant values $\{t_k\}$ (Figure 5.14 (d)). The analog carrier is used primarily for gathering and transmission of data from the cluster of remote samplers to the master part of the distributed ADC (Figure 5.15). The digital carrier is used at the stages of data reconstruction and/or their pre-processing and data transfer to computers (Figure 5.15).

5.5.2 Reconstruction of signal sample values from SWC timing instants

The instantaneous values of the reference function $r(t_k) = A_r \sin(2\pi f_r t_k + \varphi_r),$ corresponding to the time instants $\{t_k\}$, obviously defines the sequence $x(t_k)$ of the instantaneous values of the input signal. Therefore recovery of the input signal sample values basically is a straightforward operation. In Figure 5.3, it is illustrated as a quantizing procedure. While various techniques might be used for the recovery of the input signal sample values, basically a replica of the reference function waveform is sampled and quantized for that. Note that this copy of the reference function could be given either in analog or digital format. The signal sample values, of course, might be recovered and presented digitally in both cases.

The recovery of the input signal sample values concludes the analog-digital conversion of the signal. The digital signal obtained in result of this conversion then has to be processed in one or other way and that has to be done with the specifics of the digital signal taken into account. The problem is that the recovered sample values are placed on the time axis non-uniformly. In addition, the information about their positions $\{t_k\}$, provided by the sampler, is given in an analog form. While this is true, recovery of the digital quantized signal sample values actually leads also to the possibility of recovering the signal sampling instants in digital form. Indeed, each of the signal sample values is equal to the corresponding reference function value $u(t_k)$ fixed in time. Therefore, knowing the value $r(t_k)$ makes it possible to calculate the value of t_k. It gives a chance to express time instants t_k as:

$$t_k = kT_r + \frac{T_r}{2\pi} \arcsin \frac{u_r(t_k)}{A_r}, \tag{5.6}$$

where T_r is the period of the reference sine-wave and $k=0, 1, 2,\ldots$ is the number of the sampling event taking place within the k-th period of the reference sine-wave.

The formula (5.6) can be divided into two parts where kT_r is fully deterministic. Therefore the time instants $\{t_k\}$ could be described only with $\frac{T_r}{2\pi}\arcsin\frac{u_r(t_k)}{A_r}$. That reduces the length of the words carrying information about $\{t_k\}$.

This (5.6) expression is valid in the case where the comparator is enabled during the descending-value half-waves of the reference function. Therefore if the enabling conditions are different, this expression has to be modified. There should not be problems with that. However, is it necessary to carry out these calculations or not, that is another question. The point is that the digital values of the sampling instants quite often simply are not needed for resolving a given signal processing task. This issue is discussed in some detail below.

The mentioned fact that different digital signals of the considered kind have invariable envelope also means that the sampling point processes actually fully describes the respective sampled signals as the envelopes of the sample value sequences are invariable and pre-determined. Indeed, if a sampling time instant t_k is given, the equation (5.5) provides for recovery of the respective signal sample value $x(t_k)$. Therefore this type of point processes actually could be considered as digital signals fully representing the respective original analog signals in the digital domain.

5.5.3 Architecture of an energy-efficient system for multichannel data acquisition.

The suggested hardware architecture for simultaneous multichannel data acquisition is shown in Figure 5.15. Reduction of power consumption to a large extent is due to the method used for sampling. Application of it not only leads to the simplicity of the front-end design of this system. Remote samplers that can be placed directly at the locations of the sensors then are used rather than ADCs. This approach is well suited for remote signal sampling applications and for building the shown architecture of the system that actually is a distributed ADC. As can be seen, the sampling and quantising operations, in this structure, are distanced. This approach makes it possible to use many remote samplers at the front-end of it and to gather data from them in a rational way.

So far we have discussed functioning of a sampler performing signal sampling functions according to the sampling method based on detection of the signal and the reference function crossing instants. Relatively many of such samplers are used in the system shown in Figure 5.15. To ensure proper performance of them in parallel, specific enabling control functions are introduced and used. Only those crossings are taken into account that happen during the time intervals when the respective comparator is enabled by a specially generated enabling function (see Figure 5.14 (b)). This enabling function is exploited also for executing the input multiplexing. The analog input signal switching could be avoided then and that certainly is a significant positive fact. Another role the enabling function is playing is taking part in forming the digital information carrier. It is essential that the distribution of the time intervals between successive digital values of this signal is characterized by a relatively small standard deviation. Sequential enabling of the remote samplers and enabling of them during half-waves of the reference function helps in achieving this.

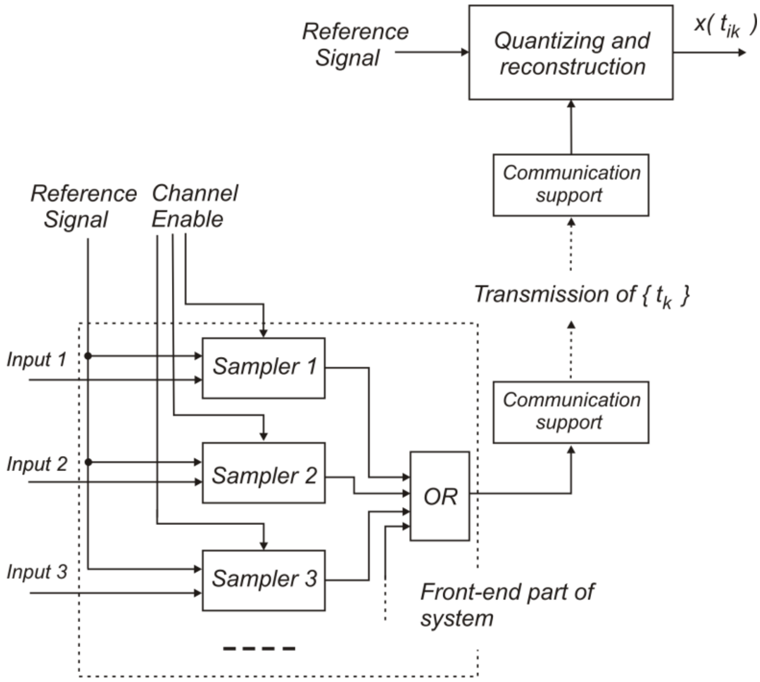

Figure 5.15 Architecture of the considered energy-efficient system fulfilling simultaneous data acquisition functions based on SWC sampling.

While this type of signal digital representations is specific and successful using of it requires some skills, it leads to obtaining of significant benefits summarized in Table 5.1.

The channel count of such a DAQ system shown in Figure 5.15 is limited with some factors discussed further. In general, the mean sampling rate f_s of a signal connected to one channel of this type data acquisition depends on the reference function shape and parameters. Also it depends on the number m of the input channels. In the case that reference is sine-wave function the important parameter is its frequency f_r. Although only one of the reference sine-wave half-periods is enabled for sampling in each separate channel, different half-periods are used in various channels. This means that sampling occurs in the system twice during each period of the reference function. Therefore the mean sampling rate $f_s=2f_r/m$ and the number of inputs $m=2f_r/f_s$. Thus the maximal number of the inputs is proportional to the ratio of the reference and sampling frequencies. They in turn depend on various conditions, including the perfection of microelectronic designs, current technological level of microelectronic product manufacturing, conditions and requirements for processing the digitized signals. The upper limit of the reference sine-wave frequency depends on the required resolution of quantizing.

At the current technological level, this limit is approximately 25 *MHz* for 8 to 10 bit quantizing. It is not so easy to achieve it. More realistic figures are 5–10 *MHz* with the quantization rate up to 12 bits. This leads to the maximal number of channels equal to 1000 for the mean sampling frequency equal to 20 *KHz*. Then the input signal could be processed in the alias-free way within the bandwidth 0–10 *KHz*. More often than not the required input numbers are smaller. Then the input signal bandwidth could be proportionally widened.

5.5.4 Achieving the applicability of standard DSP algorithms

To avoid SWC sampling nonuniformities, regularization of SWC sampling results is considered. A very simple method for this regularization has been developed and is suggested. It has remarkable advantages in comparison with other reconstruction methods where burdensome signal processing is involved. The suggested signal regularization does not require any additional computation power at all. Of course, the results may be acceptable for end-users only under certain conditions.

Regularization of SWC sampling leads to obtaining the possibility of using standard DSP algorithms for processing SWC sampled signals. Whenever this type of regularization is carried out, the wealth of existing DSP algorithms can be used for processing the signal sample values obtained in result of SWC sampling. This method can be implemented with help of the enabling function.

Treating signal sample values obtained with usage of SWC sampling as a traditionally equidistantly sampled values leads to error (according to regularization the signal samples are placed on time grid in regular manner). The mechanism of this error is explained in Figure 5.16. This regularization error ignorance may emerge as distortions and insufficient quality of results after signal deliberated processing.

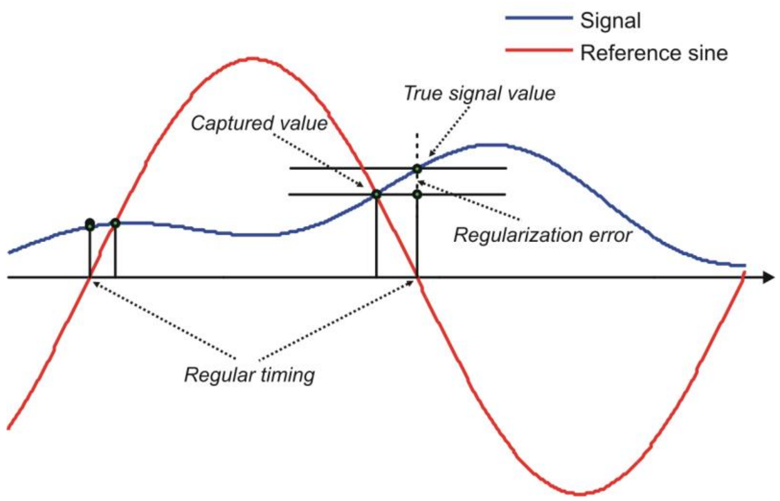

Figure 5.16 Regularization of SWC sampling samples.

The given curves in Figure 5.17 have been obtained varying signal sampling frequency and keeping constant reference frequency. The reference frequency, with the enabling decimation factor *n* varying, was changed according to $f_s = f_r / n$. Then with *n* growing, the sampling conditions are becoming closer to regular until it reaches the point at which the sampling mode could be considered as regular and all DSP algorithms can be directly applicable. Unfortunately the regularization process proportionally decreases the signal sampling frequency.

The estimated SNR for some signals is shown in Figure 5.17 and the parameters of these signals are given in Table 5.2.

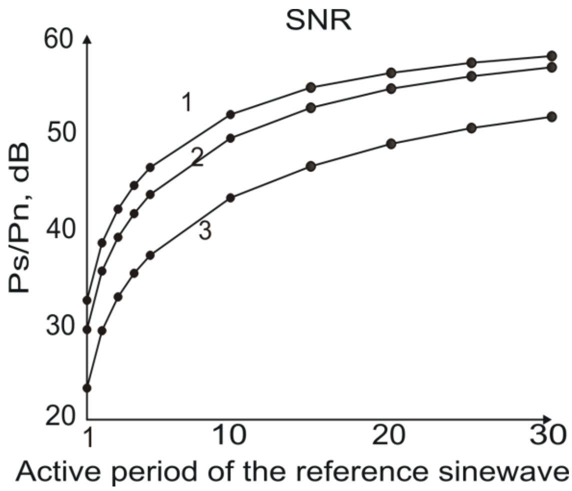

Figure 5.17 Signal-to-noise ratio SNR versus decimation coefficient n of the activated reference function periods for three various signals.

How it can be seen from Figure 5.17 the SNR is acceptable starting to 20-th activated sine-wave half period. Actually it greatly depends on particular application.

Table 5.2 Parameters of test signal discrete components used in Figure 5.17.

f_i/f_s	Signal 1		Signal 2		Signal 3	
	a_i	b_i	a_i	b_i	a_i	b_i
0.025	0.1214	0.0882	0.1214	0.0882	-	-
0.036	0.0278	0.0856	0.0278	0.0856	-	-
0.055	0.2092	0.068	0.178	0.1293	-	-
0.144	0.0324	0.0235	0.0124	0.038	0.1942	0.1411
0.156	0.16	0	0.16	0	0.0494	0.1522
0.188	-	-	0.1	0	0.1537	0.1117
0.231	-	-	0.0243	0.0176	0.0764	0.1052
0.255	-	-	0.0556	0.1712	0.18	0

Apparently this regularization approach, whenever it is applicable, is of high application value as the wealth of the existing classical DSP algorithms and computer programs then is applicable for processing signals sampled on the basis of sine-wave crossings. Especially valuable is the possibility of using the fast algorithms, especially FFT. To illustrate this, a real-life signal has been sampled in according to SWC sampling and reconstructed by using FFT and inverse DFT. A speech signal was used for that.

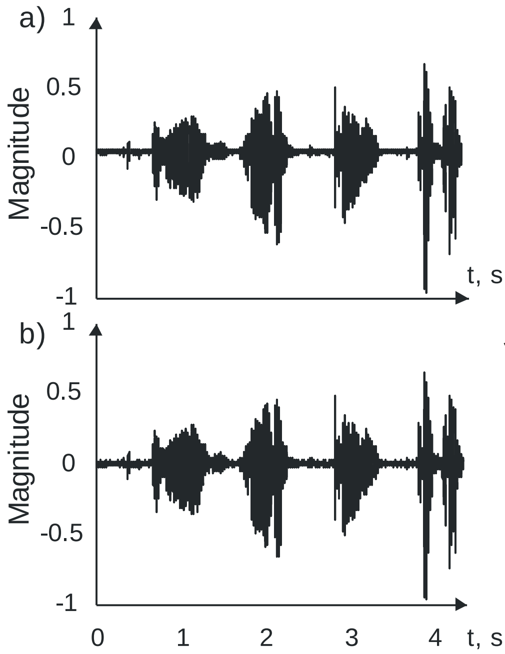

Figure 5.18 Waveform of a speech signal sampled at sine-wave crossing instants and reconstructed on the basis of Fourier Transform by applying the described sampling regularization approach.

The reconstructed speech signal waveform is given in Figure 5.18. It is very close to the original waveform. Figure 5.19 illustrates the recovered signal sample values in comparison with the original signal. As can be seen, these sample values actually overlap the original waveform.

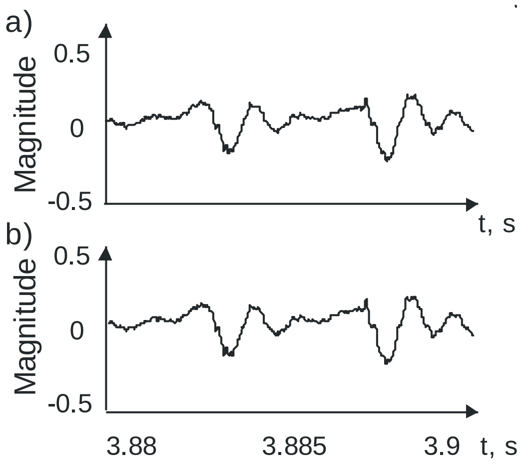

Figure 5.19 Zoomed up original speech signal and the sample values of the reconstructed waveform.

The given example simply demonstrates the feasibility of using standard DSP software tools for processing the sampled signals obtained by using the discussed sampling techniques. Of course, it is not suggested that these techniques should be exploited for processing of speech signals. There are a wide selection of excellent methods and algorithms for doing that. It was simply convenient to use this real-life signal for demonstration the applicability of DSP algorithms under the conditions of the considered specific NU sampling. Versatile processing of biomedical signals might be mentioned as a field where this regularization approach to processing signals sampled according to the sine-wave crossing method should prove to be of high application value.

5.6 Conclusion

A specific approach to signal sampling, based on detection of signal and sine-wave function crossings (so-called SWC signal sampling method), is considered in this Chapter. It is shown that under certain conditions it is possible to represent analog signals with timed sequences of events without loss of information. A comprehensive comparison of the classical signal sampling method and suggested method for SWC sampling is given in Table 5.1. The analysis is done in a number of relevant aspects and from different points of view essential for data acquisition.

The discussed specific signal digitizing method, based on signal sample value taking at the time instants when the signal crosses a sinusoidal reference function, is analyzed in the time and frequency domains. It certainly has unusual positive and some not so positive features.

The following points can be extracted after SWC sampling analysis in this Chapter:

- Algorithms and signal processing. Signals sampled according to the SWC method has constant envelope not depending on the original analog signal frequency content. That makes it possible to develop algorithms for processing them without massive multiplication of multi-digit numbers.
- A new signal filtering algorithms, exploiting the constant envelope property, have been developed is described in [6].
- DFT without massive multiplication operation is possible.
- Applicability of traditional DSP algorithms under certain conditions has been achieved. This applicability of classical DSP algorithms can be obtained by using regularization process of SWC sampled signals.
- To gain from of the constant envelope sampling, it has to be learned how to effectively cope with the drawbacks related to the nonuniformity of the obtained digital signals. The signal regularization using the enabling function is recommended

as effective tools for controlling signal sampling conditions. However it reduces the mean signal sampling rate for each DAS channel depending on particular application.

- Sampling properties. The SWC sampling properties are evaluated in the time domain and as well as in the frequency domain. Trading-off the mean sampling rate against the time resolution has to be done to provide for proper quality sampling. It is considered how the particularities of this type of signal spectra differ from spectra of the traditionally sampled signals.
- DAQ system architecture. Application of SWC sampling leads to simpler and more energy efficient hardware architectures of data acquisition systems as the signal sampling operation can be performed on the basis of a single comparator instead of ADC.

The main conclusion is that SWC signal sampling method is well suited to simultaneous multi-channel data acquisition from a large number of relatively low-frequency signal sources.

6. FPGA based implementation of the considered DAQ methods

As it is shown in Subsection 6.1, execution of DAQ functions could be based on DASP sampling and quantizing methods and this leads to various nontraditional DAQ techniques. To evaluate the expected benefits obtainable by using these research results, specifics of FPGA based implementation of the considered DAQ methods have been considered.

In this Subsection the performance of real logic structures is estimated. All structures are defined and implemented into FPGA by using hardware description language VHDL. *Altera Quartus 10 Web Edition* software is used for comparison and estimation of the required resources.

6.1 Pin-to-pin delays for various types of FPGA logic structures

The pin-to-pin delays are essential parameters closely related to performance of all types of systems. The pin-to-pin delay is the delay in propagation of a signal through a particular logic. Small delays allow using of high clock frequency for the system and that improves the operational speed of the systems performance. Therefore this parameter to some extent reveals the efficiency of a considered design. In other words, comparison of various design efficiency can be based on measurements of this parameter.

Cascades of two types of logic structures are considered for experimental comparison. Specifically, the first is a cascade of adders and the second is a cascade of embedded multipliers. In general, these delays more or less depend on the word bit number.

The pin-to-pin delays in a FPGA chip are calculated by using *Altera Quartus 10 Web Edition Classic Timing Analyzer* and *Altera Cyclone II EP2C70F672C6N* chip model. *Altera Cyclone II EP2C70F672C6N* chip model is used as it is specially designed for applications of digital signal processing. Nevertheless all other FPGAs could be used as well. General structure of the experimental FPGA setup is given in Figure 6.1.

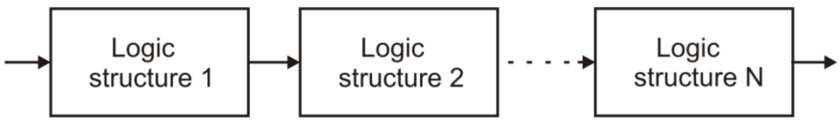

Figure 6.1 General structure of the experimental FPGA setup.

All obtained measurement results of the pin-to-pin delays for 6 bit and 12 bit words are summarized in Table 6.1.

Table 6.1 Pin-to-pin delay within cascades of typical logic structures

Count of cascade elements	6 bit adders in cascade*	6 bit embedded multipliers in cascade	6 bit multipliers in cascade*
1	12.137 ns	13.582 ns	16.532 ns
4	14.250 ns	26.656 ns	45.087 ns
8	18.048 ns	37.855 ns	81.329 ns
16	28.096 ns	71.360 ns	147.463 ns
32	45.595 ns	131.520 ns	300.351 ns
64	72.513 ns	246.407 ns	599.806 ns
Count of cascade elements	**12 bit adders in cascade***	**12 bit embedded multipliers in cascade**	**12 bit multipliers in cascade***
1	10.978 ns	14.175 ns	29.789 ns
4	15.443 ns	28.070 ns	87.247 ns
8	22.482 ns	44.619 ns	163.152 ns
16	29.486 ns	80.333 ns	321.059 ns
30	42.056 ns	143.897 ns	602.468 ns

* Built from available *Altera Cyclone II EP2C70F672C6N* Logic Elements

Given tables shows the time delay after which the right result appears at the output of system. Nevertheless if the triggers are involved at system design process (the design is pipelined) then the clock frequency appears and has meaning. In such a case the number of clock frequency cycles determines delay after which the right result appears at the output of system. In such a way the design performance can be improved.

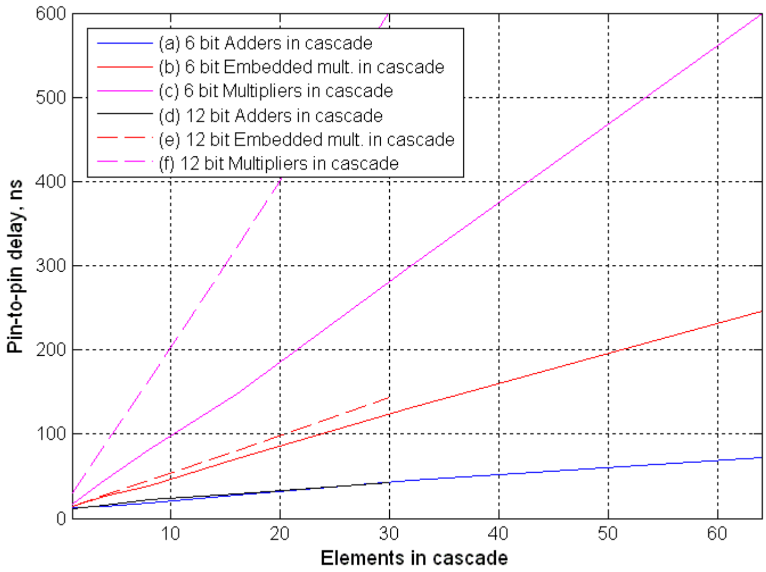

Figure 6.2 Worst case Pin-to-pin delay for 6 bit and 12 bit cascades of typical logic structures.

Obviously, as it can be seen from Table 6.1 and Figure 6.2, the pin-to-pin delay for the cascade of adders is significantly smaller than in the case of a cascade of multipliers. These results reveal what can be expected from replacement of massive multiplication operations by massive addition operations. The impact of twice longer words also is shown. While execution of multiplication operations are sensitive to additional bit in words, addition operation delays practically are not impacted by that.

6.2 Averaging large quantities of signal value multiplications with coefficients

Various approaches to FPGA based FIR filter implementation have been chosen as the platform for evaluation of the typical data pre-processing procedures. Indeed, averaging of a large quantity of signal sample value multiplications with filter coefficients is a typical operation widely used at resolution of various DAQ preprocessing tasks. Such averaging function actually is generic. Indeed, it covers a wide variety of signal processing tasks performed both in time and frequency domains, including convolution, correlation functions and all types of digital filtering, performed on the basis of filter banks or DFT. Therefore studies of FPGA implementation of such averaging function reveals relationships essential for FPGA implementations of data pre-processing.

Typical FIR filter structures with parallel multipliers and a shared multiplier are shown in Figure 6.3. The filter performance and the required FPGA resources needed for filter implementation are estimated.

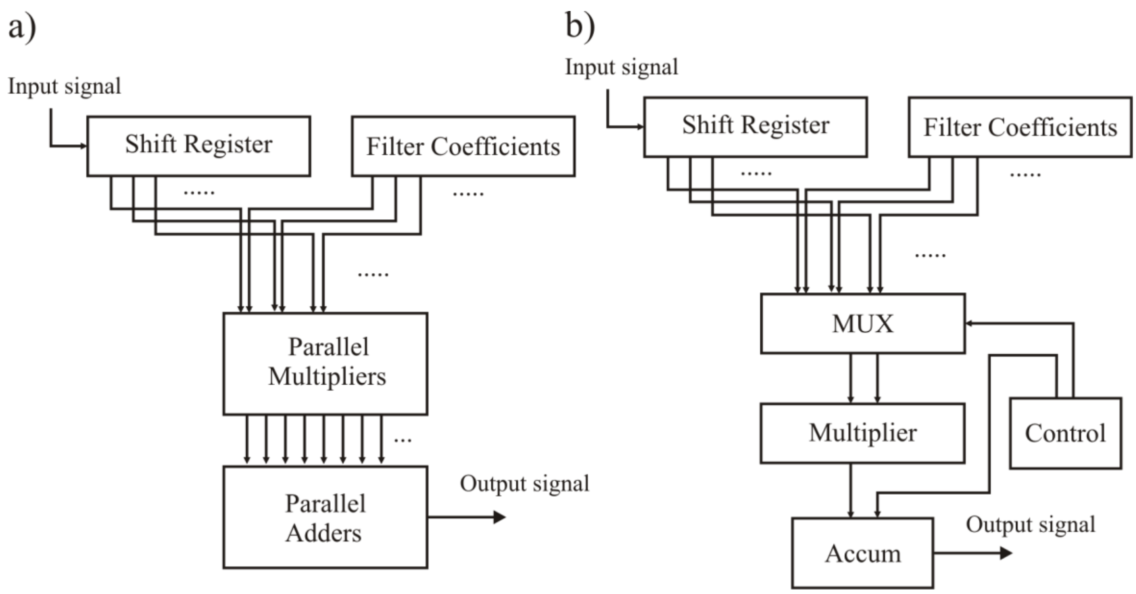

Figure 6.3 (a) Typical FIR filter structure with parallel multipliers and (b) FIR filter structure with a shared multiplier.

Important parameters for filter performance characterization are the system clock frequency (this parameter is closely tied to with input signal bandwidth) and the system delay that shows how much time it will take for a signal to propagate through the system logic. It is also important to know the requirements for the FPGA resources (in terms of logic gate count etc.) needed for implementation of the respective logic structures. In the case of FIR filters, these required resources are summarized in Appendix 6 and Figures 6.4. For comprehensive comparison of the two FPGA chip models, different architecture filters having various numbers of coefficients (with one shared and many parallel multipliers) are considered.

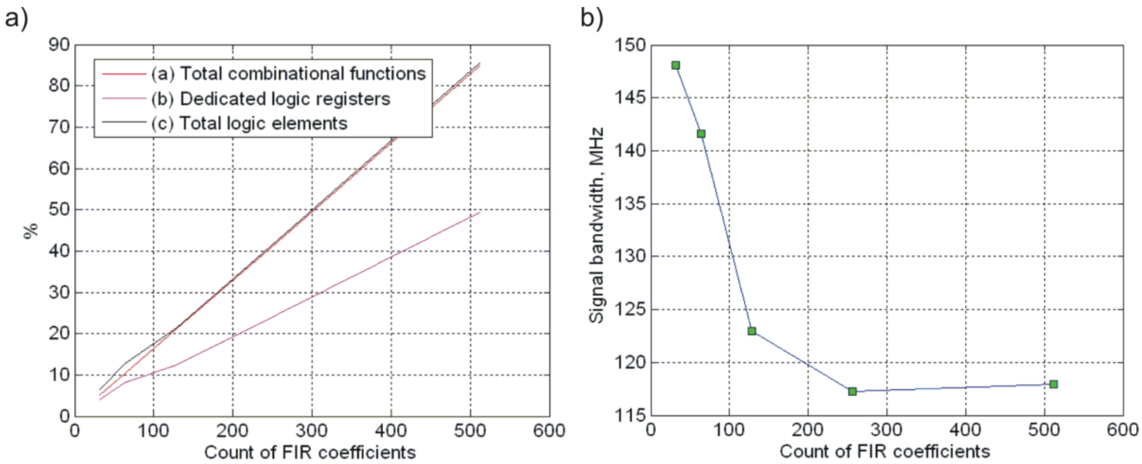

Figure 6.4 (a) Required FPGA resources (in percents) depending on the number of FIR filter coefficients in the case of the typical FIR filter structure based on parallel multipliers and (b) Dependence of the input signal bandwidth on the number of FIR filter coefficients for digital filters based on parallel multipliers.

Note that the filter clock frequency is directly related to the filter input signal bandwidth. If the FIR filter with parallel multipliers is considered then the bandwidth of the filter input signal might be half of filter clock frequency (according to Nyquist criteria). In the case of the filter with one shared multiplier the signal bandwidth has to be divided also by the number of filter coefficients.

Proposed alternative [6] is to use digital filters with a structure given in Figure 6.4 (b). The advantage of filters with this structure is that they operate without multipliers. This operation is avoided by using specific signal encoding on the basis of timing information, studied and described in Chapter 5.

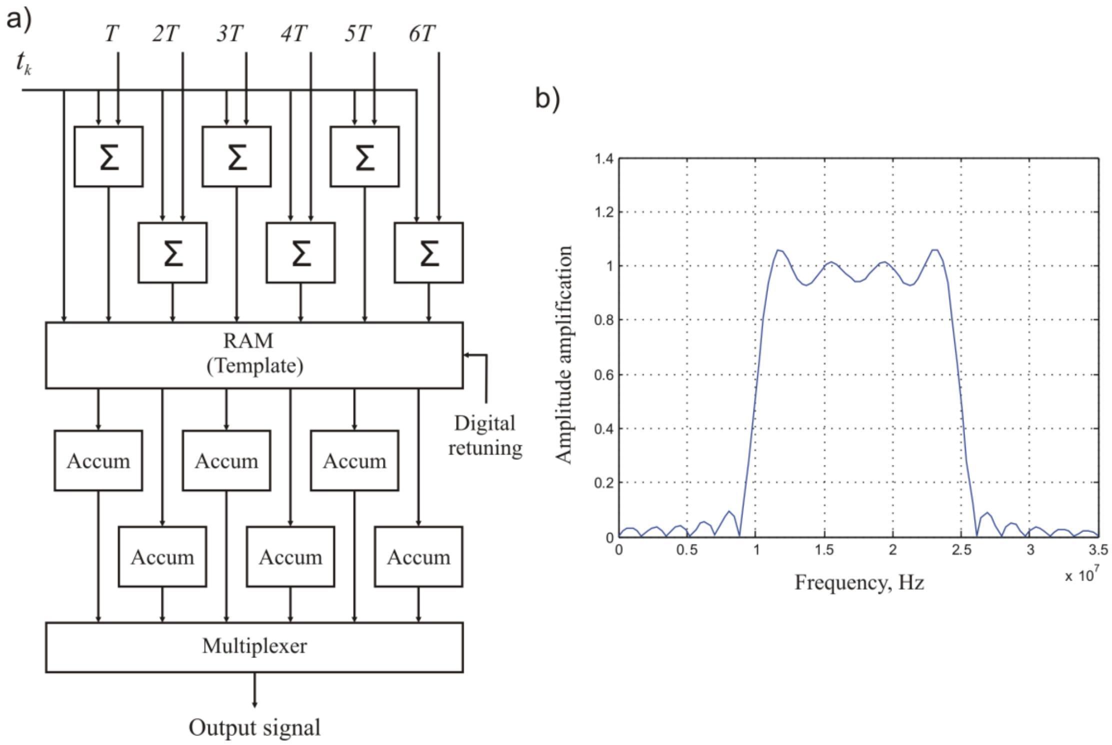

Figure 6.5 (a) Nontraditional multiplier-less structure of FIR filter and (b) Amplitude-Frequency characteristic of a 32-tap band-pass multiplier-less FIR filter.

An example of a possible filter Amplitude-Frequency characteristic of a band-pass filter is given in Figure 6.5 (b).

Results of comparison various FIR filters, specifically, their performance and required resources, are displayed in Figure 6.4 and given in Appendix 6 (in terms of combinational functions and registers). The given parameters show what could be expected at implementation of particular filters or other similar functional blocks on the basis of FPGA chips.

6.3 FPGA based implementation of fast DFT for data pre-processing

FPGA based implementation of a specific DFT multiplier-less structure for fast pre-processing of data has been developed and FPGA implementation specifics studied. This type of FPGA is applicable for designs of various application-specific systems fulfilling digital signal pre-processing related to data time-frequency representation, data compression/reconstruction, spectrum analysis, filtering, parameter estimation and demodulation.

Experimental system has been programmed and tested on the basis of *Altera Cyclone II EP2C70F672C6N* chip model. The basic structure of the Fast DFT Processor implemented is given in Figure 6.6. The core of it is represented by a multiplier-less Adder-Subtractor Matrix. In addition to this Matrix, there are data input and output subsystems. Designs of these subsystems depend on specifics and requirements of various applications. Therefore the data input and output version shown in Figure 6.6 is just one of the possible modifications. Real-time DFT and batch processing of data for DFT are two of the most often needed types of data pre-processing that can be performed on the basis of the developed FPGA chip.

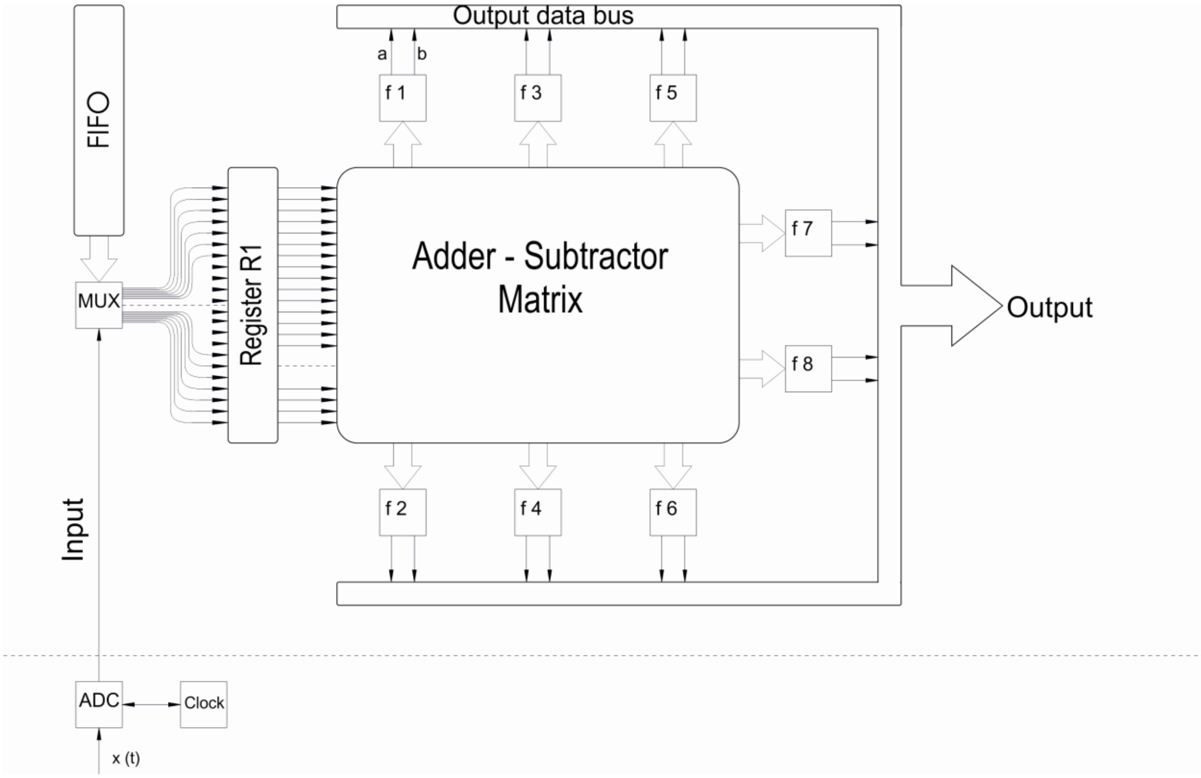

Figure 6.6 Block diagram of the Fast DFT Processor implemented as a FPGA chip.

Requirements dictated by a specific bioimpedance measurement system were taken into account at definition of the parameters of DFT for the specification of this FPGA chip. These parameters are the following: Fourier coefficients have to be calculated simultaneously at frequencies f0 (data mean value), f1, f2, f4, f8, f16, f32 and f64 by processing N=256 real signal sample values. The absolute values of these frequencies depend only on the parameters of data acquisition, in particular, on the specifics of the signal source and the used ADC. Thus the considered processor can perform DFT in a wide frequency range from KHz up to GHz.

The most important parameter that has to be experimentally measured is the achieved pin-to-pin delays characterizing the Matrix, as this parameter actually defines the upper repetition rate of DFT operation or system clock frequency. Printout of so-called Clock setup, showing pin-to-pin delays for the involved data flows at the specified frequencies, follows.

Clock Setup: 'clk'

	Slack	Actual fmax (period)	From	To
1	N/A	101.49 MHz (period = 9.853 ns)	req[231][7]	f8c7[0]
2	N/A	101.79 MHz (period = 9.824 ns)	req[231][7]	f16c1_2[0]
3	N/A	101.82 MHz (period = 9.821 ns)	req[109][6]	f16c3_1[0]
4	N/A	101.94 MHz (period = 9.810 ns)	req[109][8]	f16c3_1[0]
5	N/A	102.06 MHz (period = 9.798 ns)	req[248][7]	f32c2_1[0]
6	N/A	102.21 MHz (period = 9.784 ns)	req[237][8]	f16c3_1[0]
7	N/A	102.26 MHz (period = 9.779 ns)	req[136][6]	f32c2_1[0]
8	N/A	102.29 MHz (period = 9.776 ns)	req[231][7]	f8c7[1]
9	N/A	102.45 MHz (period = 9.761 ns)	req[147][6]	f16c3_1[0]
10	N/A	102.45 MHz (period = 9.761 ns)	req[87][8]	f8c7[0]
11	N/A	102.53 MHz (period = 9.753 ns)	req[231][7]	f16c1_2[1]
12	N/A	102.56 MHz (period = 9.750 ns)	req[109][6]	f16c3_1[1]
13	N/A	102.67 MHz (period = 9.740 ns)	req[109][7]	f16c3_1[0]
14	N/A	102.67 MHz (period = 9.740 ns)	req[173][6]	f16c3_1[0]
15	N/A	102.68 MHz (period = 9.739 ns)	req[109][8]	f16c3_1[1]
16	N/A	102.70 MHz (period = 9.737 ns)	req[87][8]	f16c1_2[0]
17	N/A	102.72 MHz (period = 9.735 ns)	req[147][8]	f16c3_1[0]

Figure 6.7 Printout showing test results of the F-DFT processor measured by *Quartus* software. Achievable clock frequencies for various data flow routes and the related pin-to-pin delays are names are given for the indicated addresses.

As can be seen in Figure 6.7, the worst case is for the data flow in the Matrix from register reg[231][7] to the output f8c7[0]. According to the Figure 6.7, the achievable clock frequency of the F-DFT processor the under described conditions is 101.49 MHz and the worst-case pin-to-pin delay is 9.853 ns. Required resources for the F-DFT processor design are given in the printout of Figure 6.8.

Flow Summary

Flow Status	Successful - Tue Sep 06 14:05:21 2011
Quartus II Version	10.0 Build 262 08/18/2010 SP 1 SJ Web Edition
Revision Name	f_dft_processor
Top-level Entity Name	f_dft_processor
Family	Cyclone II
Device	EP2C70F672C6
Timing Models	Final
Met timing requirements	Yes
Total logic elements	14,108 / 68,416 (21 %)
Total combinational functions	11,640 / 68,416 (17 %)
Dedicated logic registers	7,498 / 68,416 (11 %)
Total registers	7498
Total pins	26 / 422 (6 %)
Total virtual pins	0
Total memory bits	0 / 1,152,000 (0 %)
Embedded Multiplier 9-bit elements	0 / 300 (0 %)
Total PLLs	0 / 4 (0 %)

Figure 6.8 Required resources of the designed F-DFT processor (*Altera Quartus* snapshot).

To compare both, the following points have to be taken into account: (1) the considered particular F-DFT processor calculates simultaneously outputs of 15 filters (1 filter for f0 and two filters for each other 7 frequencies) in parallel; (2) the structure of the considered single FIR filter is pipelined, therefore the indicated clock frequency for it depends on the delay of only a single filter stage.

For the explained reasons, the performance of both devices cannot be directly compared. As to the resources, the requirements of F-DFT are significantly reduced.

Table 6.2 Summary of required resources and parameters of the F-DFT processor and particular digital FIR filter.

Cyclone II Device EP2C70F672C6	F-DFT data block 256	Pipelined FIR on 256 coefficients with 256 multipliers
Clock frequency	101.49 MHz	117.25 MHz
Total combinational functions	11,640 / 68,416 (17 %)	28,785 / 68,416 (42 %)
Dedicated logic registers	7,498 / 68,416 (11 %)	16,807 / 68,416 (25 %)
Total logic elements	14,108 / 68,416 (21 %)	29,115 / 68,416 (43 %)
Total pins	26 / 422 (7 %)	30 / 422 (7 %)
Embedded Multiplier 9-bit elements	0 / 300 (0 %)	0 / 300 (0 %)

6.4 Application potential of the developed DAQ methods

The application range for the DAQ methods, developed in result of the obtained research results, is wide. Basically they could be used for obtaining data from various biomedical and industrial objects and transferring them to computers. These DAQ methods, in general, are specific. That is especially true for the DAQ methods based on the DASP concept of the Distributed Remote Sampling Analog-to-Digital conversions and the algorithms for alias-free processing of nonuniform data streams. This approach makes it possible to obtain a number of application benefits. Specifically:

- This type of multi-channel data acquisition systems is flexible and applicable for simultaneous data acquisition from many signal sources (up to 250 or even more);
- The upper frequencies of the input signal spectra not necessarily depend on the quantity of the input channels;
- Input signals are sampled directly at their sources by front-end devices;
- Input front-end devices are much simpler than the traditionally used ADCs;
- Reduced power consumption of these front-end devices.

On the other hand, DASP technology is specific. Therefore special hardware and software tools are needed to implement this approach DAQ. Streams of digitally timed sampling events are used as digital signals representing the acquired data. Massive data acquisition is based on pseudo-randomised time-sharing, analog-to-event and time-to-digital conversions.

While the existing microelectronic components can be used to some extent, development and using of special elements would provide much better results. Using the FPGA technology partly solves this problem. However ASICs also are needed for effective implementation of the signal encoding by timing information.

Original fast multiplier-less algorithms for pre-processing of data, represented by the streams of digitally timed sampling events, have been developed and their FPGA implementation specifics studied. They are applicable for digital signal pre-processing related to signal reconstruction, spectrum analysis, filtering, parameter estimation and demodulation.

Experimental systems have been designed, made and tested specifically for data acquisition from wideband, event timing and large distributed clusters of signal sources. Modular system design has been used for achieving versatility in customizing the data acquisition systems.

If the power consumption of the front-end devices is not considered to be of primary importance, reference frequency 30 MHz might be used. Under this condition and if the number of input channels is up to 1000, the mean sampling rate of inputs then evidently is equal to 30 KHz and the upper frequency of the inputs signals is limited at 15 KHz. If data has to be acquired also from wideband signal sources, then the upper frequencies of the input signals would be limited at 15 MHz. However processing of the data gathered from the outputs of these modules then will be more complicated.

As the USB throughput and USB drivers of the development software impose the limitation on the data transmission rate, other interface options might be also used if needed. On the other hand, the number of inputs needed for many applications does not exceed 250. The data transmission rate of 3 MHz for this quantity of inputs would support the mean sampling rate 12 KHz.

In the cases where massive data acquisition has to be performed under conditions requiring very low power consumption at remote sampling, the reference frequency usually has to be decreased. If the required input signal bandwidth is given as well, then there might be some limitations imposed on the achievable number of inputs. Using of NU sampling then might be considered for reducing these limitations, as the input signal bandwidth then does not directly depend on the numbers of the inputs.

Apparently, to achieve significantly higher performance level, the considered multi-channel data acquisition approach has to be implemented on the basis of special ASICs.

7. Obtained research results

7.1 Current situation in the field of DAQ

Overview of the specifics related to development and production of currently available DAQ systems, made in Chapter 2, reveals the basic tendencies characterizing the situation in this field. While about 300 industrial companies are active in this area and seemingly many various DAQ systems are offered, actually progress there is relatively slow. As it is shown in Chapter 2, the basic limiting factor there is the dependency of DAQ methods on the classical theory of DSP, especially on the dominating theoretical principles of periodic sampling. Indeed, the classical DSP theory is currently used in this field almost exclusively. Consequently, progress in development of new and better DAQ systems currently depends on achievements of the technologies for microelectronic element production. In particular, the quantity of the information sources from which data could be acquired simultaneously is directly tied (for the given highest frequency in the signal spectra) to the achievable highest sampling rate. This restriction is typical for DAQ systems based on multiplexing. The number of input channels is inversely proportional to the sampling frequency. To avoid this restriction, separate ADCs are used in every input channel. However then DAQ systems are significantly more complicated and their power consumption level is relatively high.

The mentioned overview and analysis of the current situation in the area of DAQ, shows that the most effective way how to significantly improve DAQ characteristics should be based on reconsideration and improvement of the DAQ theoretical basis. It should be upgraded by using the latest theoretical principles of DSP developed relatively recently. Specifically, theory of randomized and alias-free signal processing is rather well suited for DAQ applications. This fact has been taken into account and the undertaken research activities of these doctoral studies are based on and exploit a number of essential results of the Digital Alias-free Signal Processing theory. That concerns mostly non-traditional methods for signal sampling and quantizing performed in the process of digitizing the input signals used at data acquisition. The digital data obtained in result of these conversions have specific features and special algorithms are to be used for their processing. The point is that signal digitizing performed in this way is rather flexible and can be adjusted to the needs of various DAQ applications. The approach to DAQ explored in the Thesis is based on these considerations. Summary of the obtained research results follows.

7.2 Summary of the obtained research results

Description of the research activities and discussions of various problems and obtained results are given in the Chapters 3, 4, 5 and 6. Specifically:

1. Chapter 3 is dedicated to exploration of the potential of NU sampling for DAQ. The obtained results, given in conclusion of this chapter, show that NU sampling is widely applicable for improving DAQ procedures. That leads to the possibilities of gaining significant improvements of DAQ systems on this basis, specifically:
   - Data acquisition at several times higher frequencies and within a wider dynamic range than it is achievable at similar digitizing performed on the basis of periodic sampling.
   - Simultaneous data acquisition in parallel from significantly increased number of signal sources.
   - Asymmetric data compression/reconstruction.
   - Data fault tolerance.
   - Very fast image data asymmetric (in the sense that most of the computational burden is put on the reconstruction stage) compression/reconstruction. Methods and algorithms for that have been developed and explored. Experimental complexity-reduced hardware/software system based on this method has been developed, made and tested. Image data compression up to 5 times has been achieved and the compressed image reconstruction quality is demonstrated by processing various images, including color and standard images.
   - Spectrum analysis of data obtained in result of NU sampling, in particular, bioimpedance data demodulation done by using DFT. Various approaches to DFT coefficient estimation are considered, analyzed and described.
2. Chapter 4 is dedicated to DAQ based on the deterministic, randomized and pseudo-randomized quantizing methods. They are discussed and compared. Obtained results:
   - Impact of pseudo-randomized signal quantizing on precision of spectrum analysis of data is explored and clarified.
   - Methods for spectrum analysis of data, based on pseudo-randomized signal quantizing, have been developed. It is shown that application of them leads to significantly improved precision of spectral estimations.
   - Performing of DFT on the basis of rectangular functions has been suggested. This approach provides for significantly simpler bioimpedance data demodulation.
   - Comparison of all three quantizing versions shows that pseudo-randomized quantizing usually outperforms two other quantizing options.

3. Chapter 5 covers work done on development of a new approach to DAQ based on acquiring timing information. The obtained results are:
    - A method for signal sampling, based on detection of signal and sine-wave crossing instants (SWC sampling), has been computer-simulated and extensively explored. It is shown that this sampling method provides a number of advantages, which are well suited to the specifics of DAQ system designs.
    - The most significant advantage of SWC based DAQ systems probably is their capability of data gathering from a very large quantity of signal sources distributed over an object of technical or biomedical origin.
    - And there are other advantages. In particular, SWC sampling provides for simple and energy saving architecture for DAQ system hardware. According to this sampling concept, ADCs in input channels can be replaced by much simpler devices, by comparators. The data from system front-end to the data collecting point then are transmitted using sequence of short pulses. It makes such DAQ systems much simpler and less energy consuming.
    - SWC sampled signal regularization can be performed to ensure the applicability of standard DSP algorithms.
    - This regularization decreases the signal sampling frequency, but increases signal quality, as the regularization error and the comparator element delay diminish at the same time. This approach is applicable when the signals have relatively low-frequency bandwidth, in particular, for biomedical data acquisition.
    - Special signal processing methods applicable in the case of SWC sampling have been developed for complexity-reduced design of digital filters and multiplier-less structures for DFT. The further research activities in this direction are very desirable.
4. Chapter 6 contains description of experimental activities and obtained research results. The novel logical structure for DFT coefficients estimation without massive multiplication has been implemented into FPGA and its performance evaluated. The comparison with equal purpose FIR digital filter reveals that considered F-DFT processor structure requires approximately 2 times less count of logical elements. The development of F-DFT processor has to continue.

Computer simulations of the explored DAQ methods have been performed on the basis of the developed and used MATLAB programs.

8. Conclusions

The goal of this work, discovering innovative methods for efficient massive data acquisition from real life objects and supplying computers with this information, has been reached and the planned tasks have been fulfilled. The developed and investigated innovative methods for complexity-reduced DAQ and energy-efficient pre-processing of the data are based on the theory, concepts and methods of the non-traditional digital signal processing DASP. The obtained research results show: (1) how that can be done and (2) what can be gained at computer system linking to the real world technical and biological objects by using the developed DAQ methods. The basic benefits that can be obtained in this way, specifically, are the following:

1. The developed methods for multi-channel data acquisition systems are flexible and applicable for simultaneous data acquisition from many signal sources.

2. Simultaneous data acquisition from many signal sources is performed in parallel under conditions where the upper frequencies of the input signal spectra do not depend on the quantity of the input channels.

3. Input signals can be sampled directly at their sources by front-end devices that are much simpler than the traditionally used ADCs.

4. Consequently, the power consumption of these front-end devices might be significantly lower.

However DASP technology is specific. Therefore hardware and software implementing DAQ based on this technology are specific as well. MATLAB based software tools have been developed and they could be used to implement the chosen approach. Streams of digitally timed sampling events are used as digital signals representing the acquired data. Massive data acquisition is based on pseudo-randomised time-sharing, analog-to-event and time-to-digital conversions.

Experimental investigations of the developed DAQ methods were carried out by using hardware tools that have been developed in the Laboratory 2.2.of Institute of Electronics and Computer Science in the framework of ERAF Project Nr. VDP1/ERAF/CFLA/05/APK/2.5.1/000024/012 “Development of multi-channel systems for acquisitions of data from biomedical, ecological and industrial systems and transferring them to computerized systems”, co-sponsored by the European Union. Author of this research work participated in this project as a member of the team.

Tests and experimental evaluation of the developed DAQ systems show that:

1. Experiments confirm the results obtained theoretically.

2. The existing microelectronic components, including FPGA chips and their programming technology, basically are suitable and can be used for implementation of gathered data specific pre-processing.

3. Potential of FPGA usage for specific data pre-processing is demonstrated by performance of the developed Fast DFT Processor (see Protocol of F-DFT Processor international evaluation results given in Attachment).

4. Attempts to use the existing microelectronic components for implementation of the front-end operations at DAQ show that this approach basically does not lead to sufficiently high results.

5. To fully gain from the research results obtained in the framework of this work, implementation of the front-end DAQ procedures, defined by the developed DAQ methods, should be based on developed new specific ASICs (Application Specific Integrated Circuits).

List of Publications

[1] Bilinskis I., Sudars K., “Processing of signals sampled at sine-wave crossing instants”, Proceedings of the “2007 Workshop on Digital Alias-free Signal Processing” (WDASP’07), London, UK, 17 April 2007, pp. 45-50.

[2] Sudars K., Ziemelis Z., “Expected performance of the sine-wave crossing data acquisition systems”, Proceedings of DASP Workshop, London, UK, 17 April 2007.

[3] Bilinskis I., Sudars K., “Digital representation of analog signals by timed sequences of events”, “Electronics and Electrical Engineering”, No. 3(83), March, 2008, Presented in International Conference “Electronics 2008”, Kauna, Lithuania, 20-22 May 2008.

[4] Bilinskis I., Sudars K., “Specifics of constant envelope digital signals”, “Electronics and Electrical Engineering”, No. 4(84), April, 2008, Presented in International Conference “Electronics 2008”, Kauna, Lithuania, 20-22 May 2008.

[5] Artyukh Yu., Bilinskis I., Sudars K., Vedin V., “Multi-channel data acquisition from sensor systems”. Proceedings of the 10th International Conference “Digital Signal Processing and its Applications” (DSPA'2008), Moscow, Russia, 2008, Vol.X-1, pp.117-119.

[6] Artyukh Y., Bilinskis I., Sudars K., European Patent Application No. EP2075912 A1, *Method for complexity-reduced digital filtering and parameter estimation of analog signals*, Assignee: Institute of Electronics and Computer Science of Latvia, European patent Bulletin, January 7, 2009.

[7] Bilinskis I., Sudars K., Min M., Annus P., “Advantages and limitations of an approach to bioimpedance data acquisition and processing relying on fast low bit rate ADCs”, Baltic Electronic Conference BEC 2010, Tallinn, Estonia, 4.-6. October 2010.

[8] Artyukh Y., Bilinskis I., Roga S., Sudars K., “Digital Representation of Analog Signals leading to their Energy-efficient Processing”, Green Information Technology (GREEN IT 2010), Singapore, 25.-26. October 2010.

[9] Sudars K., “Data Acquisition Based on Nonuniform Sampling: Achievable Advantages and Involved Problems”, “Automatic Control and Computer Science” Magazine, Allerton Press, 2010, Vol. 44, No. 4, pp. 199-207.

[10] Bilinskis I., Skageris A., Sudars K. “Method for fast and complexity-reduced asymmetric image compression”, “Electronics and Electrical Engineering”, No. 4(110), May, 2011, Presented in International Conference “Electronics 2011”, Kauna, Lithuania, 17-19 May 2011.

[11] Artyukh Y., Bilinskis I., Rybakov A., Sudars K., Vedin V., “Modular Multi-channel Data Acquisition Systems”, “Automatic Control and Computer Sciences” Magazine, Allerton Press, 2008, Vol. 42, No. 3, pp. 113–119.

References

[12] Artyukh Y., Bilinskis I., Boole E., Rybakov A., Vedin V., “Wideband RF signal digititizing for high purity spectral analysis,” Proceedings of the 2005 International Workshop on Spectral Methods and Multirate Signal Processing, (SMMSP 2005) June 20-22, 2005, Riga, Latvia. pp. 123-128.

[13] Artyukh Y., Bilinskis I., Greitans M., Mednieks I., Rybakov A., “DASP-Lab System – a demonstrator of the new DSP technology”, Automatic Control and Computer Science, Allerton Press, 2000, No. 6, pp. 3-21.

[14] Artyukh Y., Bilinskis I., Rybakov A., Stepin V., “Pseudo-randomization of multiplexer-based data acquisition from multiple signal sources,” Proceeding of DASP Workshop, London, UK, 17 April 2007.

[15] Balakrishnan A. V., “On the problem of time-jitter in sampling”, IRE Trans. Theory, IT-8 (4), pp. 226-36.

[16] Beutler F.J., “Alias-free randomly timed sampling of stochastic processes”, IEEE Trans. Inf. Theory, IT-16 (2), pp. 147-52, 1970

[17] Beutler F.J., “Error-free recovery of signals from irregularly spaced samples”, SIAM Rev., 8 (3) 328-35.

[18] Beutler F.J., “Recovery of randomly sampled signals by simple interpolators”, Inf. Control, 26 (4), pp. 312-40, 1974

[19] Beutler F.J., Leneman O.A., “The spectral analysis of impulse processes”, Inf. Control, 12 (3), pp. 236-58, 1968

[20] Beutler F.J., Leneman O.A., “The theory of stationary point processes”, Acta Math., 116, pp. 159-97, 1966

[21] Beutler F.J., Leneman, O.A., “Random sampling of random processes: stationary point processes”, Inf. Control, 9 (4), pp. 325-46, 1966

[22] Bilinskis I., *Digital Alias-free Signal Processing*, Wiley, 2007, ISBN: 978-0-470-02738-7

[23] Bilinskis I., Mikelsons A., *Randomized Signal Processing*, Prentice Hall, 1992, ISBN: 0-13-751074-8

[24] Bilinskis I., Rybakov A., “Iterative spectrum analysis of nonuniformly undersampled wideband signals,” Electronics and Electrical Engineering, 2006, vol. 4(68), pp. 5-8.

[25] Blackledge J. M., Burge R. E., Barratt N. R., “Phase imaging by real-zero conversion and its applications to synthetic aperture radar”, Journal of Physics D: Applied Physics, Volume 20, Issue 11, November 14, 1987

[26] Borokhovych Y., Gustat H., “4-bit, 15 GS/s ADC in SiGe,” NORCHIP 2008, 16-17 Nov. 2008, Tallinn, Estonia, pp. 268-271.

[27] Candès E. J., Wakin M. B., "An Introduction to Compressive Sampling", IEEE Signals Processing Magazine, March 2008

[28] Contadini F., "Oversampling with averaging to increase ADC resolution", *Intertnet resource*: http://www.embedded.com/design/223000385, 1 March 2010

[29] Daria V. R., Saloma C., "High-accuracy Fourier transform interferometry, without oversampling, with a 1-bit analog-to-digital converter", Applied Optics, Volume 39, Issue 1, January 1, 2000, pp. 108-113

[30] Eng F., *Non-Uniform Sampling in Statistical Signal Processing*, Dissertation at Linköpings Universitet, Sweden, 2007, ISBN: 978-91-85715-49-7

[31] *Internet resource:* http://en.wikipedia.org/wiki/Data_acquisition

[32] *Internet resource:* http://www.datatranslation.com/docs/whitepapers/benefits_simulataneous_daq.pdf

[33] *Internet resource:* http://www.radiolocman.com/news/new.html?di=64921

[34] Koch P., Prasad R., "The Universal Handset," IEEE Spectrum, vol. 46, pp. 32-37, April 2009.

[35] Kumaresan R., Wang Y., "On representing signals using only timing information", The Journal of the Acoustical Society of America, Volume 110, Issue 5, November 2001, pp. 2421-2439

[36] Leneman O.A., "On error bounds for jittered sampling", IEEE Trans. Autom. Control, AC-11 (1), pp. 150, 1966

[37] Leneman O.A., "Random sampling of random processes: impulse sampling", Inf. Control, 9 (4), pp. 347-63, 1966

[38] Leneman O.A., "Random sampling of random processes: optimum linear interpolation", J. Franklin Inst., 281 (4), pp. 302-14, 1966

[39] Leneman O.A., Lewis J.B., "On mean-square reconstruction error", IEEE Trans. Autom. Control, AC-11 (2), pp. 324-5, 1966

[40] Leneman O.A., Lewis J.B., "Random sampling of random processes: mean-square comparison of various interpolators", IEEE Trans. Aurora. Control, AC-11 (3), pp. 396-403, 1966

[41] Lim M., Saloma C., "Direct signal recovery from threshold crossings", Physical Review E (Statistical Physics, Plasmas, Fluids, and Related Interdisciplinary Topics), Volume 58, Issue 5, November 1998, pp. 6759-6765

[42] Logan Jr. B. F., "Information in the zero crossings of bandpass signals", Bell System Technical Journal, Volume 56, April 1977, pp. 487-510

[43] Marvasti F. (editor), *Nonuniform Sampling Theory and Practice*, Kluwer Academic/Plenum Publishers, 2001, ISBN: 0-306-46445-4

[44] Marvasti F., *A Unified Approach to Zero-crossings and Nonuniform Samplingof single and multidimensional signals and systems*, Illinois Institute of Technology, 1987, ISBN: 0-9618167-0-8

[45] Masry E., “Alias-free sampling: an alternative conceptualization and its applications”, IEEE Trans. Inf. Theory, IT-24 (3), pp. 317-24, 1978

[46] Masry E., “Poisson sampling and spectral estimation of continuous-time processes”, IEEE Trans. Inf. Theory, IT-24 (2), pp. 173- 83, 1978

[47] Masry E., “Random sampling and reconstruction of spectra”, Inf. Control, 19 (4), pp. 275-88, 1971

[48] Masry E., “Spectral estimation of continuous-time processes: performance comparison between periodic and Poisson sampling schemes”, IEEE Trans. Autom. Control, AC-23 (4), pp. 679- 85, 1978

[49] Masry E., Lui M.C., “Discrete-time spectral estimation of continuous-parameter processes: a new consistent estimate”, IEEE Trans. Inf. Theory, IT-22 (3), pp. 298-312, 1978

[50] Mikelsons A., “Alias-free spectral estimation of signals with components of arbitrary frequencies”, Adaptive Methods and Emergent Techniques for Signal Processing and Communications, Ljubljana, Slovenia, April 1994, pp. 105-8.

[51] Min M., Bilinskis I., Artyukh Y., Annus P., Land R., Märtens O., “Nonuniform Sampling and Demodulation for Wideband Multi-frequency Bioimpedance Measurements,” Proceedings of the Workshop on Digital Alias-free Signal Processing, London, 17 April 2007

[52] Nait-Ali A., Cavaro-Menard C. (editors), *Compression of Biomedical Images and Signals*, Wiley, 2008, ISBN: 978-1-84821-028-8

[53] Nazario M. A., Saloma C., “Signal recovery in sinusoid-crossing sampling by use of the minimum-negativity constrain”, Applied Optics, Volume 37, Issue 14, May 10, 1998

[54] Papenfus F., *Digital Signal Processing of Nonuniformly Sampled Signals*, Dissertation at Universität Rostock, Publisher: Shaker Verlag, 2008, ISBN: 978-3-8322-6895-4

[55] Raghavendra C. S., Sivalingam K. M., Znati T. (editors), *Wireless Sensor Networks*, Kluwer Academic, 2004, ISBN-13: 978-1402078835

[56] Rieke F., Warland D., R. R. van Steveninck, Bialek W., “Spikes: Exploring the Neural Code”, MIT Press, Cambridge, MA, 1997

[57] Sundstrom T., Alvandpour A., “A 2.5-GS/s 30-mW 4-bit Flash ADC in 90nm CMOS,” NORCHIP 2008, 16-17 Nov. 2008, Tallinn, Estonia, pp. 264-267.

[58] Zeevi Y. Y., Gavriely A., Shamai (Shitz) S., “Image representing by zero and sine-wave crossings”, Journal of the Optical Society of America A, pp. 2045-2060, 1987

Appendix 1 – Typical basic parameters of currently available DAQ systems

Table A1.1 Typical basic parameters of currently available DAQ systems (May 6, 2010)

Parameter	Value
System clock frequency	Up to 48 MHz
Sampling frequency	150 – 750 Ks/s per channel
Channel count	1-32
Resolution	12-24 bits
Analog input range	-10 to +10 V
PC interfaces	USB, ISA, PCI, PCI-Express

Simultaneous Series modules from "Data Translation" are shown in Figure A1.1.

Figure A1.1 Simultaneous Series DAQ modules from "Data Translation" illustrating technical complexity of currently produced DAQ systems.

As it is given in [26], the Simultaneous Series modules from *"Data Translation"*, built according to the structures shown in Figure 1.1 (a), provide a 16-bit ADC for each analog channel. This allows the user to correlate high-speed (up to 2 MHz) measurements of all input signals at the exactly same time instants. These modules are also designed with 500V galvanic isolation to maximize signal integrity and protect the PC. This series was developed for customers seeking to correlate highly accurate, high-speed measurements while eliminating phase noise from channel-to-channel data acquisition. A common clock and trigger are used for simultaneous and synchronous sampling of all inputs. This means that all functions of the data acquisition modules (ADC, DAC, DIO, Counter/Timers, and Quadrature Decoders) can be simultaneously triggered internally or externally. The data can then be clocked either internally or externally and streamed synchronously to host memory. The synchronous operation allows all I/O data to be processed and correlated for all inputs and outputs. This is very valuable in determining the response across a device-under-test to stimuli at the same exact instant.

Table A1.2 Significant parameters of currently available ADCs from companies *"Analog Devices"* and *"MAXIM"* (May 11, 2010)

Resolution [Bits]	**Sampling frequency [Msps]**	**Analog input range [MHz]**
6	800	400
8	2200	2800
10	300	700
12	400 (250)*	480 (780)*
14	150	650
16	125	650
18	2	50
24	2.5	1.35

* *Parameters of second better ADC.*

For some ADCs available channel count is up to 16. In these cases the ADCs sampling frequency will be proportionally smaller.

Table A1.3 Significant parameters of currently available multiplexers and switches from company *"Analog Devices"* (May 11, 2010)

Bandwidth [MHz]	**Transition time [ns]**	**Channel count**
350	4	2:1
700	10	4:1
800	1	4:1
1000	4	2:1

Appendix 2 – Typical sensor nodes

Few prominent companies and organizations in the field of developing and manufacturing wireless sensor networks for data acquisition are following:

- *Crossbow* (www.xbow.com) – *Crossbow* is supplier and developer of smart sensor technologies for more than a decade and has shipped hundreds of thousands of smart sensors to more than 4000 customers worldwide. Today, *Crossbow* is a leading supplier of wireless sensor technology and inertial MEMS sensors for navigation and control;
- *Ember* (www.ember.com) – *Ember* seeks to develop wireless sensor and control network technologies that enable dramatic energy efficiency improvements for businesses, homes and the utilities that serve them;
- *Microstrain* (www.microstrain.com) – *Microstrain* makes tiny sensors that are used in a wide range of applications, including knee implants, civil structures, advanced manufacturing, unmanned military vehicles and automobile engines. Company develops and produces innovative, smart, wireless, microminiature displacement, orientation and force sensors;
- *IMEC* (www.imec.be) – *Imec* is Europe’s largest independent research center in nanoelectronics and nano-technology. Its staff of more than 1750 people includes over 550 industrial residents and guest researchers. *Imec’s* research is applied in better healthcare, smart electronics, sustainable energy and safer transport.

Appendix 3 – Experimental setups of the developed DAQ systems

Figure A3.1 Novel multi-channel data acquisition system prototype. The system's front-end part is based on SWC sampling principles, involving data transmission with timing instants.

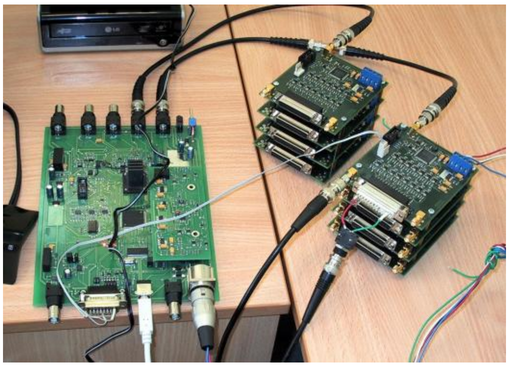

Figure A3.2 Developed multi-channel DAQ system.

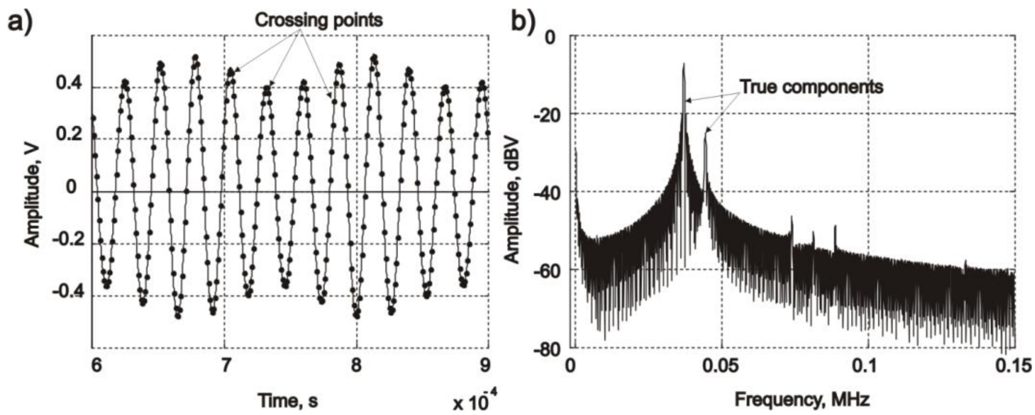

Figure A3.3 Typical experimental measurement and analysis of front-end part and timing event decoder of the multi-channel DAQ pilot system: (a) The acquired test signal with the multi-channel DAQ system and (b) its spectrum.

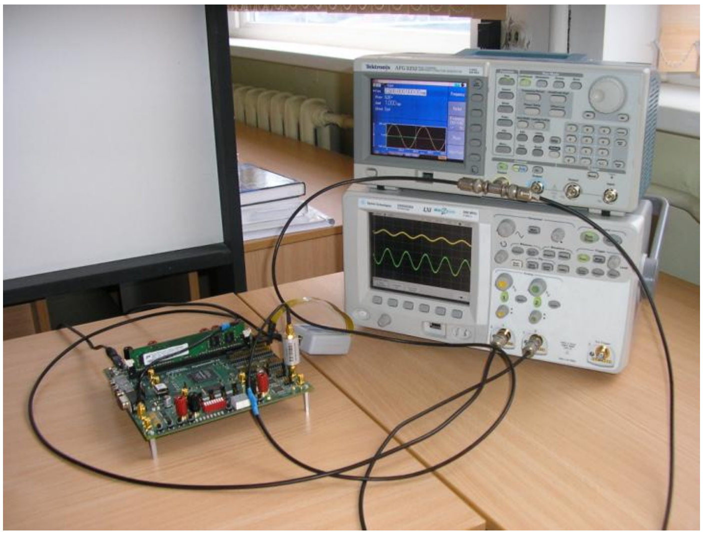

Figure A3.5 Work place (consists of oscilloscope, signal source and FPGA development board) for DSP digital structure FPGA development and testing. In this particular case the selective digital FIR filter on 1024 coefficients is implemented into FPGA.

Appendix 4 – Examples of VHDL defined structures

The VHDL programming is carried out to define logic structures for their comparison and find out the real numbers of required resources for their implementation.

VHDL code for multiplier cascade

```
-- EMBEDDED MULT.
-- 9 standard MULT in cascade
library ieee;
use ieee.std_logic_1164.all;
use ieee.std_logic_arith.all;
use ieee.std_logic_unsigned.all;
entity p2p_delay_mult is
port(
ie1, ie2, ie3, ie4, ie5, ie6, ie7, ie8, ie9, ie10 : in std_logic_vector (8 downto 1);
iz : out std_logic_vector (16 downto 1)
);
end entity;
architecture arch of p2p_delay_mult is
signal tmp1, tmp2, tmp3, tmp4, tmp5, tmp6, tmp7, pop : std_logic_vector (16 downto 1);
begin
-- Mult 1
tmp1 <= ie1*ie2;
-- Mult 2
tmp2 <= tmp1(8 downto 1) * ie3;
-- Mult 3
  tmp3 <= tmp2(8 downto 1) * ie4; --"10110011";
  -- Mult 4
  tmp4 <= tmp3(8 downto 1) * ie5; --"11101011";
 -- Mult 5
 tmp5 <= tmp4(8 downto 1) * ie6; --"00101011";
  -- Mult 6
  tmp6 <= tmp5(8 downto 1) * ie7; --"10110010";
  -- Mult 7
  tmp7 <= tmp6(8 downto 1) * ie8; --"11100010";
-- Mult 8
  tmp8 <= tmp7(8 downto 1) * ie9; --"10110011";
-- Mult 9
  iz <= tmp8(8 downto 1) * ie10; --"01011010";
end architecture;
```

VHDL code for adder cascade

```
-- 9 Adders in cascade
library ieee;
use ieee.std_logic_1164.all;
use ieee.std_logic_arith.all;
use ieee.std_logic_unsigned.all;
entity p2p_delay_measuring is
port(
ie1, ie2, ie3, ie4, ie5, ie6, ie7, ie8, ie9, ie10 : in std_logic_vector (8 downto 1);
iz : out std_logic_vector (8 downto 1)
```

```
);
end entity;
architecture arch of p2p_delay_measuring is
signal tmp1, tmp2, tmp3, tmp4, tmp5, tmp6, tmp7, tmp8 : std_logic_vector (8 downto 1);
begin
-- Cascade summing
-- Adding 1
tmp1 <= ie1+ie2;
-- Adding 2
tmp2 <= tmp1 + ie3;
-- Adding 3
  tmp3 <= tmp2 + ie4;
-- Adding 4
  tmp4 <= tmp3 + ie5;
 -- Adding 5
 tmp5 <= tmp4 + ie6;
  -- Adding 6
  tmp6 <= tmp5 + ie7;
  -- Adding 7
  tmp7 <= tmp6 + ie8;
-- Adding 8
  tmp8 <= tmp7 + ie9;
-- Adding 9
iz <= tmp8 + ie10;
end architecture;
```

Appendix 5 – Used *Altera Quartus*, *ModelSim* and *Matlab* tools

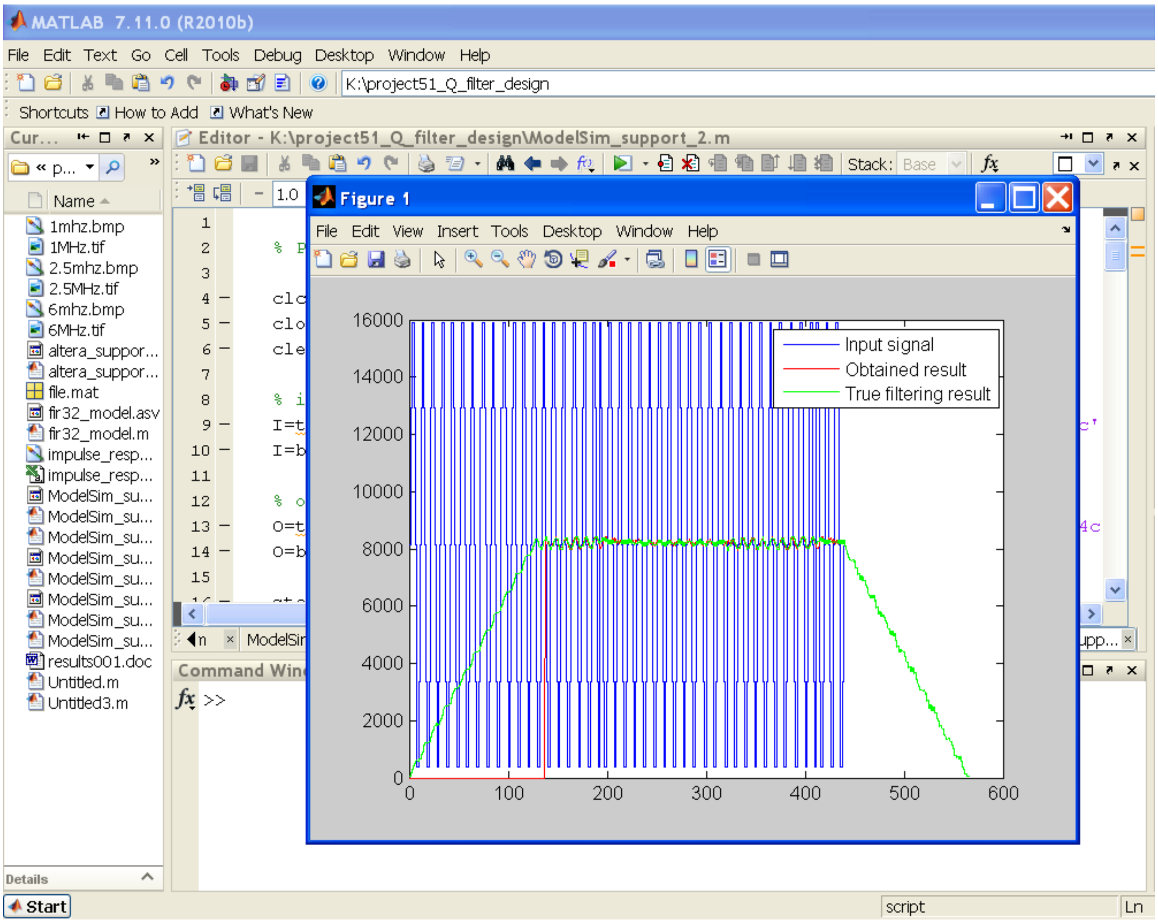

Figure A5.1 MATLAB simulation environment used for FIR filter model development and testing. It was used in addition for testing the behaviour of created logic structures and VHDL code.

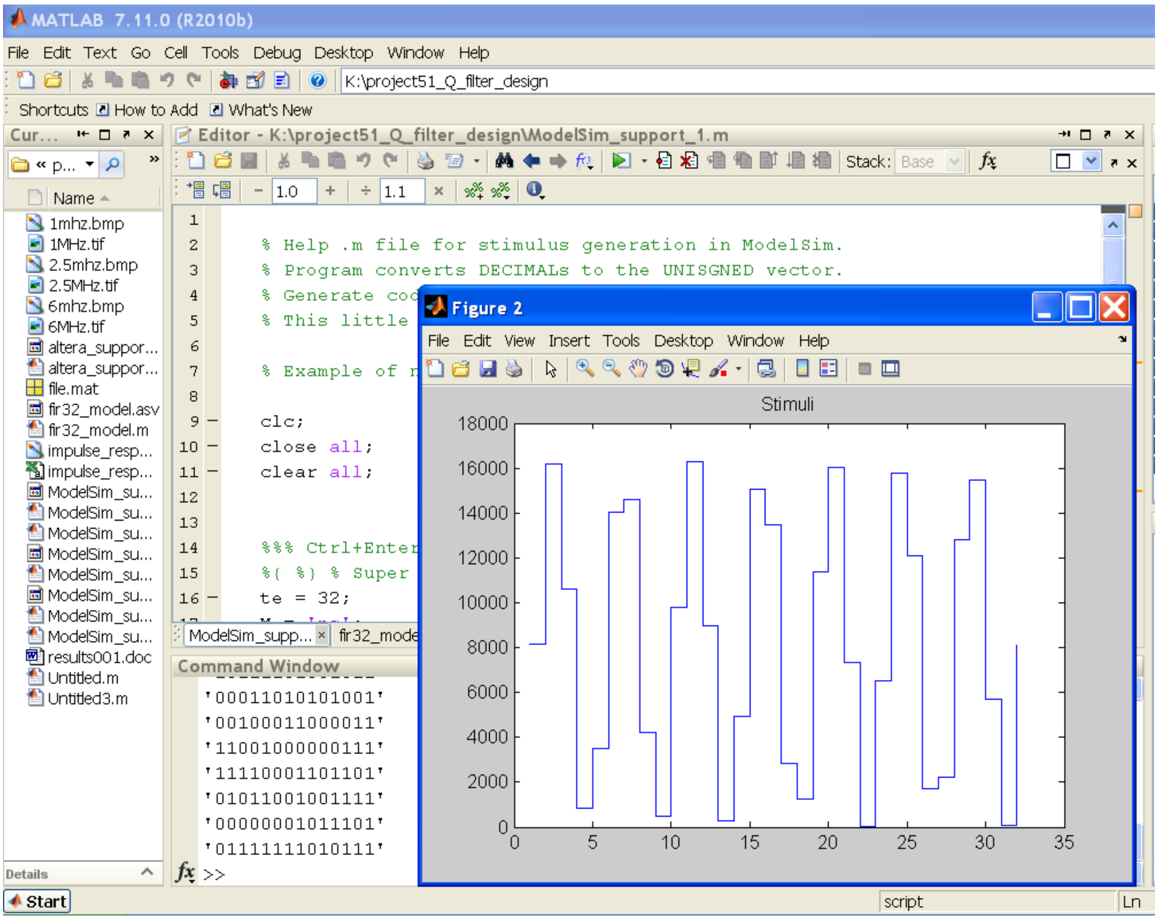

Figure A5.2 Virtual test signal and part of code generated in MATLAB for the *ModelSim* VHDL code development and testing environment.

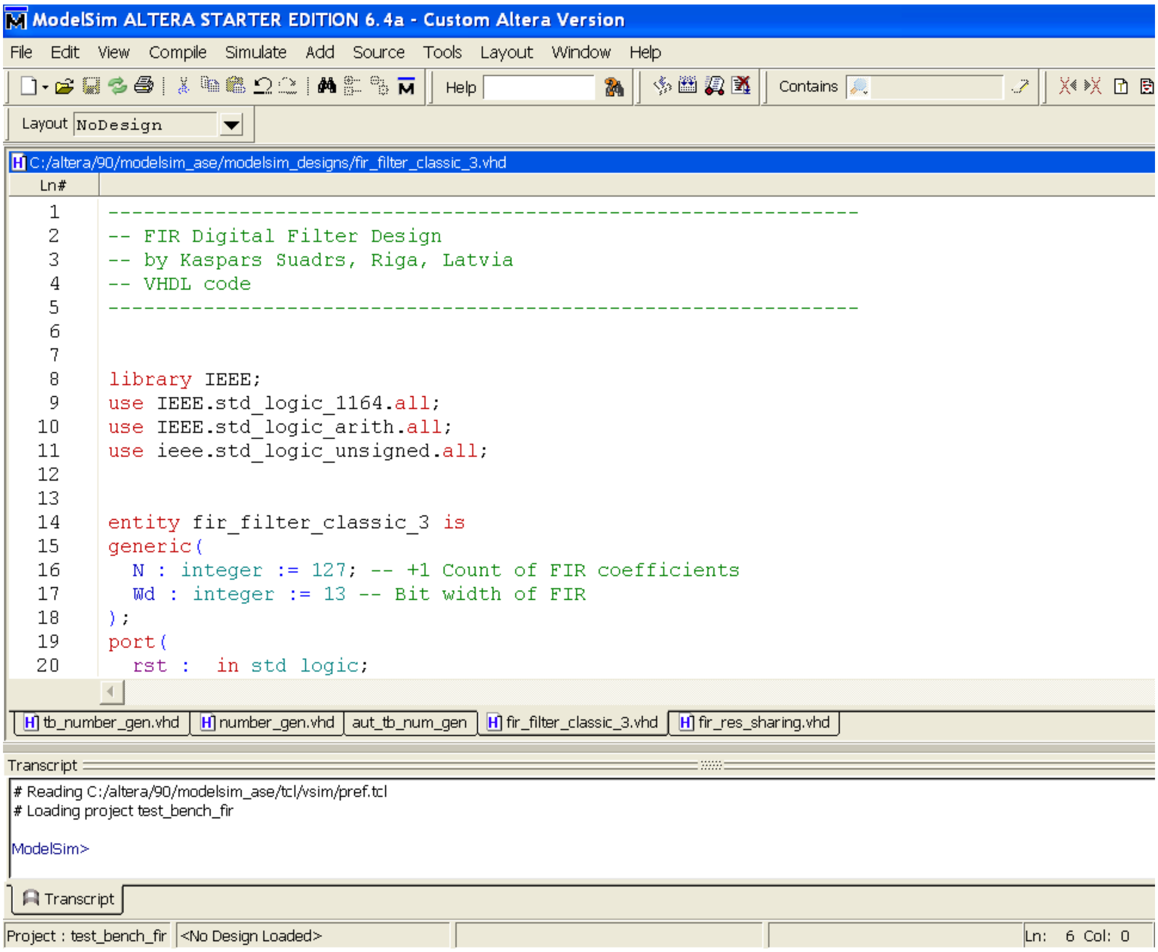

Figure A5.3 *ModelSim* environment. It was used for logic structure description by VHDL code and for debugging and functionality tests (writing test benches).

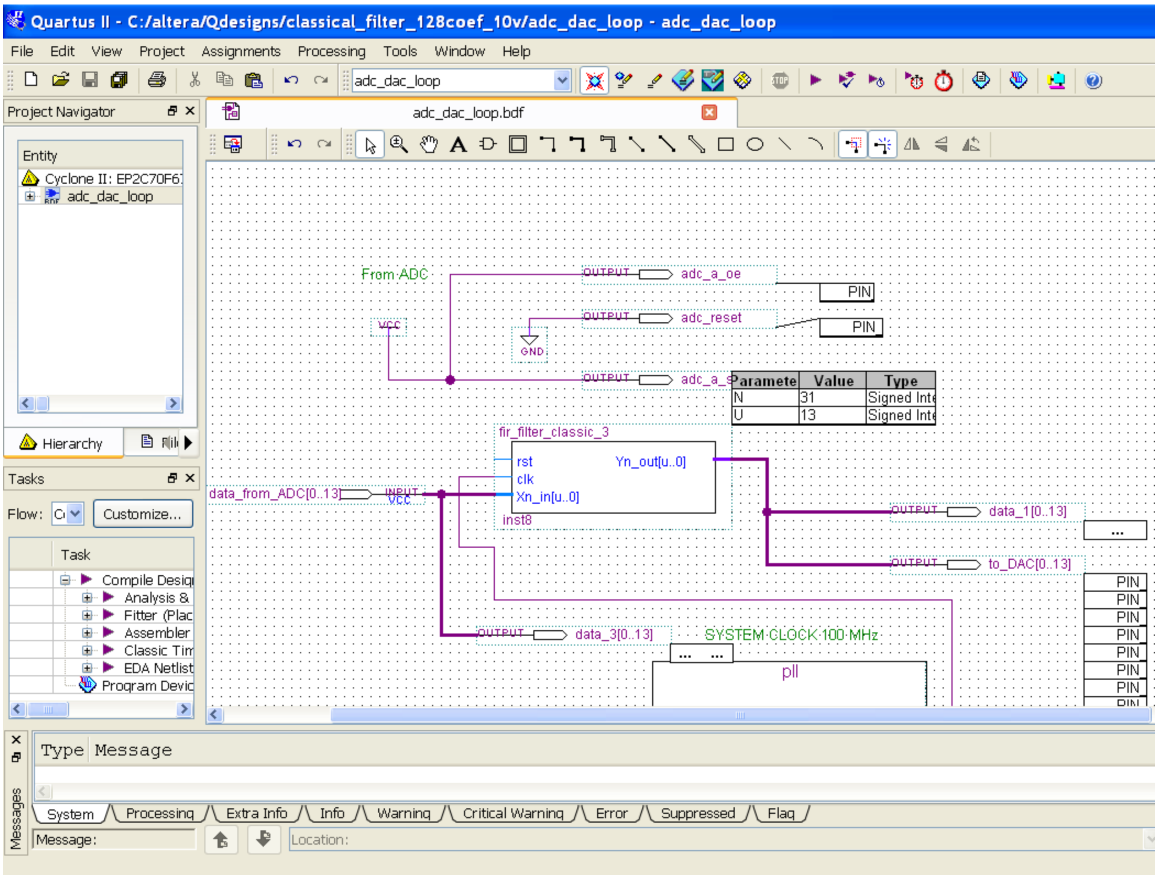

Figure A5.4 *Altera Quartus* software used for programming *Cyclone* FPGA located on *Altera* DSP development board used for estimating required resources for logic structure implementation into FPGA.

Appendix 6 – Estimated FIR filter performance and required resources for the developed experimental models

Cyclone II Device EP2C70F672C6	FIR on 32 coefficients with 1 shared multiplier	FIR on 32 coefficients with 32 parallel multipliers	FIR on 64 coefficients with 64 multipliers
Signal bandwidth	4.3494 MHz	148.08 MHz	141.64 MHz
Total combinational functions	2,108 / 68,416 (3 %)	3,570 / 68,416 (5 %)	7,174 / 68,416 (10 %)
Dedicated logic registers	1,349 / 68,416 (2 %)	2,803 / 68,416 (4 %)	5,650 / 68,416 (8 %)
Total logic elements	2,780 / 68,416 (4 %)	4,367 / 68,416 (6 %)	8,759 / 68,416 (13 %)
Total pins	30 / 422 (7 %)	30 / 422 (7 %)	30 / 422 (7 %)
Embedded Multiplier 9-bit elements	2 / 300 (< 1 %)	0 / 300 (0 %)	0 / 300 (0 %)

Cyclone II Device EP2C70F672C6	FIR on 128 coefficients with 128 multipliers	FIR on 256 coefficients with 256 multipliers	FIR on 512 coefficients with 512 multipliers
Signal bandwidth	122.94 MHz	117.25 MHz	117.98 MHz
Total combinational functions	14,396 / 68,416 (21 %)	28,785 / 68,416 (42 %)	58,012 / 68,416 (85 %)
Dedicated logic registers	8,447 / 68,416 (12 %)	16,807 / 68,416 (25 %)	33,828 / 68,416 (49 %)
Total logic elements	14,534 / 68,416 (21 %)	29,115 / 68,416 (43 %)	58,466 / 68,416 (85 %)
Total pins	30 / 422 (7 %)	30 / 422 (7 %)	30 / 422 (7 %)
Embedded Multiplier 9-bit elements	0 / 300 (0 %)	0 / 300 (0 %)	0 / 300 (0 %)

Cyclone III Device EP3C120F780	FIR on 32 coefficients with 1 shared multiplier	FIR on 32 coefficients with 32 parallel multipliers	FIR on 64 coefficients with 64 multipliers
Signal bandwidth	4.095 MHz	128.16 MHz	127.88 MHz
Total combinational functions	2,108 / 119,088 (2 %)	3,570 / 119,088 (3 %)	7,174 / 119,088 (6 %)
Dedicated logic registers	1,349 / 119,088 (1 %)	2,803 / 119,088 (2 %)	5,650 / 119,088 (5 %)
Total logic elements	2,780 / 119,088 (2 %)	4,367 / 119,088 (4 %)	8,756 / 119,088 (7 %)
Total pins	30 / 532 (6 %)	30 / 532 (6 %)	30 / 532 (6 %)
Embedded Multiplier 9-bit elements	2 / 576 (< 1 %)	0 / 576 (0 %)	0 / 576 (0 %)

Cyclone III Device EP3C120F780	FIR on 128 coefficients with 128 multipliers	FIR on 256 coefficients with 256 multipliers	FIR on 512 coefficients with 512 multipliers
Signal bandwidth	121.62 MHz	118.81 MHz	118.55 MHz
Total combinational functions	14,396 / 119,088 (12 %)	28,785 / 119,088 (24 %)	58,012 / 119,088 (49 %)
Dedicated logic registers	8,447 / 119,088 (7 %)	16,807 / 119,088 (14 %)	33,828 / 119,088 (28 %)
Total logic elements	14,531 / 119,088 (12 %)	29,095 / 119,088 (24 %)	58,467 / 119,088 (49 %)
Total pins	30 / 532 (6 %)	30 / 532 (6 %)	30 / 532 (6 %)
Embedded Multiplier 9-bit elements	0 / 576 (0 %)	0 / 576 (0 %)	0 / 576 (0 %)

Appendix 7 – Results of asymmetric colour image compression and reconstruction

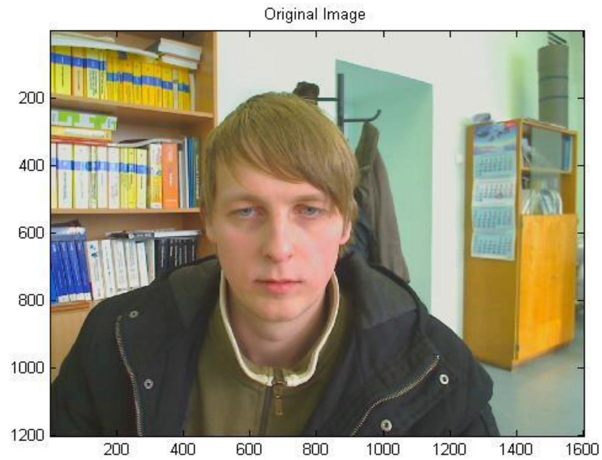

Figure A7.1 Original image 1200×1600 pixels.

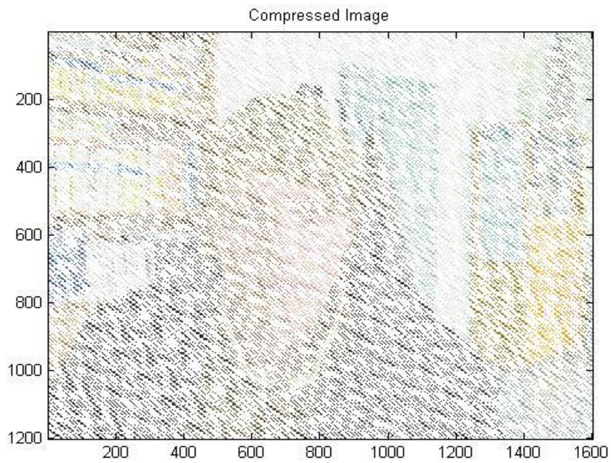

Figure A7.2 Compressed image with 80% of all pixels taken out.

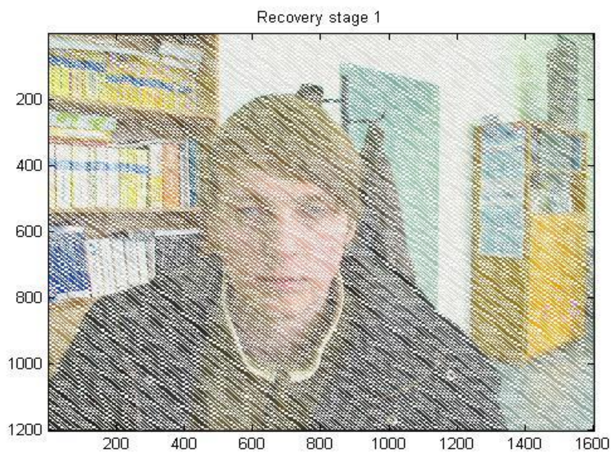

Figure A7.3 Image after recovery stage 1.

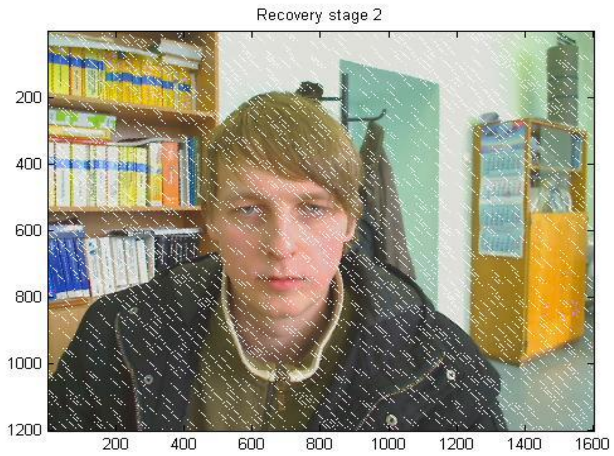

Figure A7.4 Image after recovery stage 2.

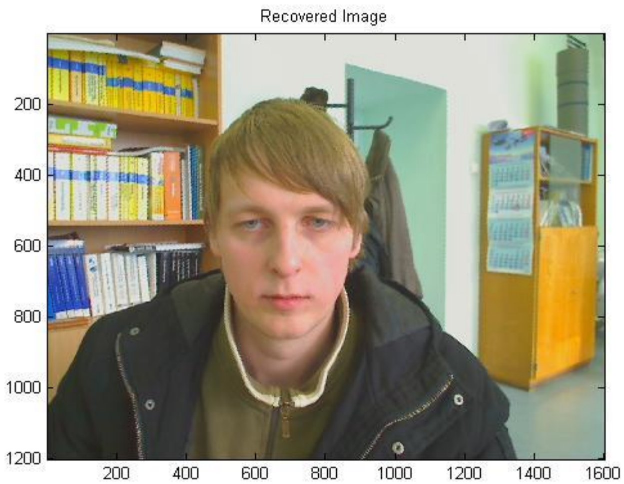

Figure A7.5 Compressed image is reconstructed with the average relative error 0.1648 %.

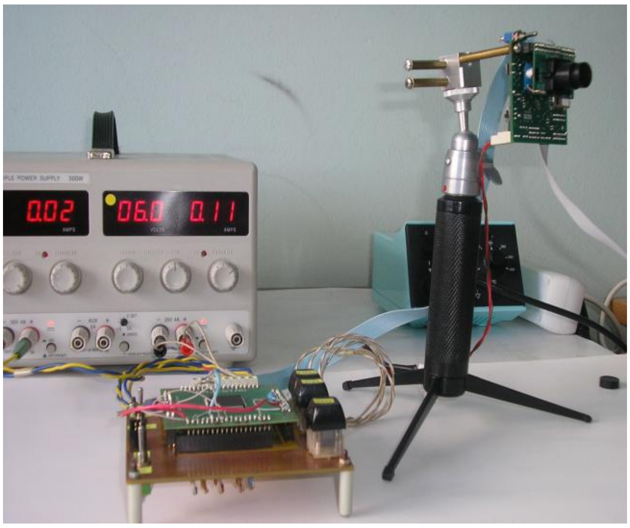

Figure A7.6 The developed asymmetric data capturing device.